



McGill

**Therapeutic potential of targeting eukaryotic translation initiation factor
(eIF2B) in mutant KRAS lung cancer**

By

Laleh Ebrahimi Ghahnavieh

Experimental Medicine

McGill University, Montreal

April 2024

A thesis submitted to McGill University in partial fulfillment of the requirements of the
degree of

Master of Science

Table of Contents

Acknowledgements	4
Abstract	5
Résumé	7
Preface	9
List of figures	11
List of tables	12
List of Abbreviations	13
Chapter 1: Introduction	15
1. Cancer	16
1.2 Lung cancer	17
1.3 Mitogen-activated protein kinase (MAPK) pathway overview	17
1.3.1 Targeting mutant KRAS	20
1.3.2 Resistance to Drugs Targeting mutant KRAS.....	22
1.4 mRNA translational initiation.....	23
1.4.1 The Integrated Stress Response (ISR) in translational control	28
1.4.2 Translation Alteration in ISR.....	30
1.4.3 ISR Termination	31
1.4.4 The role of translation initiation in the context of cancer	32
1.4.5 Targeting ISR by eIF2B	34
1.5 eIF2B dysregulation in human cancer	37
1.5.1 Unleashing the Potential of PROTACs to Target eIF2B for Novel Therapeutic Strategies	38
1.6 Rational, study design and hypothesis.....	40
1.6.1 Rational.....	40
1.6.2 Hypothesis	41
1.6.3 Specific aims	41
1.6.4 Study design	42
Chapter 2: Material and Methods	44
2.1 Computational Structural Biology analysis	45
2.1.1 Blind Protein-Protein Docking of existing structures of KRAS/SOS1 and eIF2B	45
2.1.2 Assessing Clinical relation of mutant KRAS in patients Lung tumors	46
2.2 Cell culture and impairing eIF2B	47

2.2.1 Cell culture.....	47
2.2.2 Knocking down eIF2B5 by shRNA.....	47
2.2.3 Knocking down eIF2B5 by si-RNA.....	47
2.3 RNA-seq data analysis.....	49
2.3.1 Data analysis for common genes in mKRAS cell lines	50
2.4 Develop strategies to impair eIF2B for the treatment of mutant KRAS cancers	50
2.4.1 Developing ISRIB-PROTACs Structures.....	50
2.4.2 Evaluation of ISRIB-PROTACs function in cell culture	52
2.5 Immunoblotting (western blot)	53
2.6 Statistical analysis of patient data	54
Chapter 3: Results	56
3.1 KRAS(G12C) bonded SOS1-eIF2B Protein Interaction evaluation via Blind docking.....	57
3.2 eIF2B somatic mutations in LUAD patients.....	59
3.3 Identify signaling pathways orchestrated by eIF2B specifically in mutant KRAS tumor cells.....	62
3.3.1 Analysis of gene expression as a result of eIF2B function in mutant KRAS cells.....	63
3.3.2. Gene Ontology (GO) and KEGG pathway enrichment analysis	69
3.3.3 Analysis of eIF2B-dependent genes in mutant KRAS cells	70
3.4 Probing PROTAC Efficacy: Characterizing its Function in Targeting eIF2B.....	76
Chapter 4: Discussion and Conclusion	86
4.1 Discussion and Contribution to original knowledge	87
4.2 Conclusion.....	103
Appendices	104
References	115

Acknowledgements

I am filled with immense gratitude for the progress I have made during my MSc studies, and I owe it all to the invaluable help and support of many remarkable individuals. I would like to take a moment to express my deepest appreciation to Prof. Antonis E. Koromilas, my supervisor, for his unwavering mentorship, technical expertise, and encouragement. I cannot thank him enough for his guidance and support throughout my research journey.

My advisory committee members, Prof. Volker Blank and Prof. Maria Hatzoglou, also deserve a special mention for their expert opinions and guidance at various stages of my research. I am truly grateful for their valuable insights and contributions that have helped shape my research project.

I would also like to acknowledge my advisor, Prof. Raquel Aloyz, whose invaluable support and advice have been instrumental in every step of my studies. Her unwavering encouragement and guidance during difficult times have been a source of strength and inspiration, and I am deeply grateful for her mentorship.

Financial support from McGill University, particularly through the McGill Experimental Medicine Graduate Studies scholarship, has been a huge help, and I extend my heartfelt thanks to the university for this opportunity.

Special thanks to Dr. Philip Lumb and his Ph.D. student Carlos Razziel Azpilcueta Nicolas, for providing the PROTACs compounds for my project. I am grateful for their contribution to my research.

I would also like to express my deepest appreciation to all my friends at the Lady Davis Institute for their assistance, friendship, and advice.

My deepest appreciation goes to my beloved parents and sister for their love, inspiration, and sacrifices. Without their unconditional love and affection, my success would not have been possible.

Special mention to Dr. Sofiane Berrazouane for his encouragement and revision of the French format of this thesis abstract.

Abstract:

KRAS mutations are highly prevalent in colorectal, lung, and pancreatic cancers, leading to continuous cell proliferation and cancer progression. Mutant KRAS (mKRAS) exposes cells to oncogenic forms of stress (i.e., genotoxic, metabolic, and proteostatic stress), which disrupt proliferation and tissue homeostasis. To cope with stress, cells engage at the level of mRNA translation and involve the functional interplay between the translation initiator factors eIF2 and eIF2B. Phosphorylated eIF2 antagonizes the guanine exchange function (GEF) of eIF2B to mediate translational and transcriptional reprogramming to promote adaptation under stress. We examine how mutant KRAS interacts with translation initiation factor B, leading to the activation of the RAF-MAPK pathway in tumor cells. We hypothesize the connection between mKRAS and eIF2B, presenting a potential therapeutic vulnerability to overcome drug resistance and tumor development in mKRAS cancer.

We investigate the importance of interacted subunits of the eIF2B protein with the SOS1-mKRAS (G12C) *in-silico* docking model, which is related to somatic mutations in eIF2B subunits in KRAS G12 mutation lung adenocarcinoma (LUAD) patients, suggesting an impact of mKRAS/eIF2B interaction on mRNA translation, KRAS downstream signaling pathways, and tumor progression. We assessed the regulated genes by bulk RNA sequencing in impaired eIF2B in mutant KRAS lung and colon cancer, which impact Wnt interaction in lipid metabolism and immune response, Jak-STAT, and cholesterol metabolism activity. Moreover, eIF2B knockdown in mKRAS cell lines showed alterations in ERK1/2 and MEK1/2 phosphorylation, indicating the regulation of the MAPK signaling pathway. However, this effect was not observed in wild-type KRAS at the protein level.

Furthermore, the ISR inhibitor (ISRIB) substantially stabilizes the eIF2B protein complex, and its modification to PROTACs (Proteolysis-Targeting Chimera) is an innovative approach to selectively degrading disease-causing proteins, including eIF2B, within cells. A PROTAC brings the eIF2B target protein and the E3 ligase together, leading to the transfer of ubiquitin and subsequent degradation of the eIF2B and its interacted proteins by the proteasome. The library of ISRIB-PROTACs with different E3 ligase ligands (VHL and CRBN) with various linker lengths has been tested. The results have the potential to be used in various diseases, as

treatment showed concentration-dependent MAPK pathway regulation. Research in this field is ongoing to optimize designs for efficient function on these targets.

To summarize, eIF2B plays a regulatory role in cancer pathways, making it a potential treatment target for mKRAS lung cancer.

Résumé:

Les mutations du gène KRAS sont très répandues dans les cancers colorectaux, pulmonaires et pancréatiques, entraînant ainsi une prolifération cellulaire continue et la progression du cancer. Le gène KRAS mutant (mKRAS) expose les cellules à des formes de stress oncogènes (c'est-à-dire génotoxiques, métaboliques et protéostatiques), qui perturbent la prolifération et l'homéostasie tissulaire. Pour faire face au stress, les cellules s'engagent au niveau de la traduction de l'ARNm et impliquent l'interaction fonctionnelle entre les facteurs initiateurs de la traduction eIF2 et eIF2B. L'eIF2 phosphorylé antagonise la fonction d'échange de guanine (GEF) de l'eIF2B afin d'enclencher la reprogrammation traductionnelle et transcriptionnelle pour favoriser l'adaptation au stress. Nous examinons comment KRAS mutant interagit avec le facteur B d'initiation de la traduction, conduisant à l'activation de la voie RAF-MAPK dans les cellules tumorales. Nous émettons l'hypothèse d'un lien entre mKRAS et eIF2B, présentant une cible thérapeutique potentielle pour surmonter la résistance aux médicaments et le développement de tumeurs dans le cancer mKRAS.

Nous étudions l'importance des sous-unités de la protéine eIF2B qui interagissent avec le modèle d'ancrage in silico SOS1-mKRAS (G12C), qui sont liées aux mutations somatiques des sous-unités eIF2B chez les patients atteints d'adénocarcinome pulmonaire à mutation KRAS G12 (LUAD), ce qui suggère un impact de l'interaction mKRAS/eIF2B sur la traduction de l'ARNm, les voies de signalisation sous-jacentes de KRAS et la progression de la tumeur.

Nous avons évalué les gènes régulés par séquençage de l'ARN en vrac dans les cancers du poumon et du colon KRAS mutants, qui ont un impact sur l'interaction Wnt dans le métabolisme des lipides et la réponse immunitaire, aussi sur la voie de signalisation Jak-STAT et sur l'activité du métabolisme du cholestérol. De plus, le knockdown de l'eIF2B dans les lignées cellulaires mKRAS a montré des altérations dans la phosphorylation de ERK1/2 et MEK1/2, indiquant ainsi la régulation de la voie de signalisation MAPK. Toutefois, cet effet n'a pas été observé au niveau des protéines dans les cellules KRAS de type sauvage.

En outre, l'inhibiteur de l'ISR (ISRIB) stabilise considérablement le complexe protéique eIF2B, et sa modification en PROTAC (Proteolysis-Targeting Chimera) constitue une approche innovante pour dégrader sélectivement les protéines pathogènes, y compris l'eIF2B, à

l'intérieur des cellules. Une PROTAC réunit la protéine cible eIF2B et la ligase E3, ce qui conduit au transfert de l'ubiquitine et à la dégradation ultérieure de l'eIF2B et des protéines en interaction par le protéasome. La bibliothèque d'ISRIB-PROTACs avec différents ligands E3 ligase (VHL et CRBN) et avec diverses longueurs de liens a été testée. Les résultats ont le potentiel d'être utilisés dans diverses maladies car le traitement a montré une régulation de la voie MAPK dépendante de la concentration. De plus, la recherche dans ce domaine est en cours pour optimiser les conceptions afin d'obtenir une fonction efficace sur ces cibles. En résumé, eIF2B joue un rôle régulateur dans les voies du cancer, ce qui représente une cible thérapeutique potentielle pour le cancer du poumon mKRAS.

Preface

This thesis is presented in the traditional format following the National Library of Canada guidelines. The data presented in this thesis is the candidate's original work and will be used in a manuscript in preparation.

1. Kim, H., Ghaddar, N., **Ghahnavieh, L. E.**, Wang, S., Cho, K. J., Sasaki, A., & Koromilas, A. E. (2023). Abstract A022: Translation initiation factor 2B (eIF2B) stimulates mutant KRAS function in cancer. *Molecular Cancer Research*, 21(5_Supplement), A022-A022.

Author Contributions

In Chapter 2 (Materials and Methods), I conducted the experimental work concerning tissue culture treatments, siRNA knockdown assays, and immunoblotting analysis of cells. Additionally, I performed RNA and protein extractions for RNA-seq and ISRIB-PROTAC treatments of cultured cells. I also generated all plots and immunoblotting data in Chapter 3 (Results). The data were discussed with Dr. Antonis E. Koromilas and presented at lab meetings.

I conducted all bioinformatics analyses, including structural analysis and docking, variant calling for somatic mutations from TCGA database patients, and bulk RNA-seq analysis. I am responsible for the interpretation of this data.

The work of the graduate student Hyungdong Kim on eIF2B and KRAS shaped the idea of this project. The H358 cell line expressing eIF2B shRNA was generated by Hyungdong Kim. ISRIB-PROTACs were synthesized and provided by Dr. Jean-Philip Lumb's lab. I wrote the original version of the Thesis, with revision edits from Dr. Antonis E. Koromilas. I revised the final form following the recommendations of the external reviewer, Dr. George Simos.

The work in the Thesis was supported by an Innovation Grant from the Canadian Cancer Society Research Institute (CCSRI) to Dr. Antonis Koromilas.

List of figures

Figure 1.1 Active form of KRAS bounded GTP regulates different downstream signaling pathways.

Figure 1.2 The canonical pathway of eukaryotic translation initiation.

Figure 1.3 Schematic overview of the canonical eukaryotic translation initiation pathway.

Figure 1.4 The Integrated Stress Response (ISR) as an important regulator of translation initiation.

Figure 1.5 Effects of ISR on uORF mRNA with ribosome interactions.

Figure 1.6 Human eIF2B complex bound to ISRIB.

Figure 1.7 Modulation illustration of eIF2B activity.

Figure 1.8 Schematic illustration of PROTAC mechanisms of action.

Figure 1.9 Plot of relative FP signal from samples of fluorescein-ISRIB interacted with purified eIF2B

Figure 3.1 3D ribbons representation for the crystal structure of protein complexes 7L70 and 6EPL,

Figure 3.2 Ribbons representation of the eIF2B interacted with SOS1-KRAS G12C complex based on model 7

Figure 3.3 Estimation of eIF2B5 knockdown efficiency and MAPK pathway regulation in protein level.

Figure 3.4 eIF2B regulates important genes involved in tumorigenesis in mutant and wildtype KRAS

Figure 3.5 Top GO enrichment pathways in BP to illustrate up and down regulated pathways

Figure 3.6 Shared genes regulated by eIF2B in mutant KRAS cells.

Figure 3.7 Survival analysis of LUAD TCGA database for common genes regulated by eIF2B.

Figure 3.8 Survival Rate analysis of all eIF2B subunits expression in Lung and colon adenocarcinoma.

Figure 3.9 ISR inhibition by ISRIB antagonizes eIF2B function in mutant KRAS lung tumor cells.

Figure 3.10 Immunoblotting of H358 cells treated with biotinylated ISRIB and ISRIB-linkers (PEG 4-6) to dysregulate ATF4 in mutant KRAS lung tumor cells.

Figure 3.11 Immunoblotting of HEK293T cells treated with the first generation of ISRIB-PROTAC (ISRIB-CRBN-PEG2) with fixed concentration (20uM) and different time points.

Figure 3.12 Immunoblotting of H358 cells treated with second generation of ISRIB-PROTAC.

Figure 3.13 ISRIB-PROTACs with CRBN ligand and different linker lengths affect ISR in the presence of thapsigargin via ATF4 expression

Figure 3.14 The PROTAC-PEG6 dysregulates ATF4 levels in H358 cells with mKRAS G12C.

Figure Supplementary 1. PCA plot.

List of tables

Table 2.1. Sequences of shRNA and siRNA of the corresponding target genes

Table 2.2. Summary of the chemical structures and properties of ISIRB-PROTACs.

Table 2.3 List of antibodies used in the study.

Table 3.1 Model scores for the balanced coefficient set when docking the eIF2B to SOS1 interacted with KRAS G12C.

Table 3.2 Somatic mutation in eIF2B subunits in mutant KRAS LUAD patients in TCGA.

Table 3.3 Annotated function of common down-regulated and up-regulated genes by eIF2B in mutant KRAS cell lines

Table Supplementary 1. List of eIF2B upregulated GO enrichment signature identified in BP analyses.

Table supplementary 2. List of eIF2B downregulated GO enrichment signature identified in BP analyses.

Table Supplementary 3. List of overlapped dysregulated genes by eIF2B transcriptional signature identified in different groups.

List of Abbreviations

4E-BP: eIF4E binding protein

ATP: adenosine tri-phosphate

AKT/PKB: Protein kinase B

AMPK: AMP activated protein Kinase

ATF: Activating transcription factor

CHOP/GADD153: C/EBP homology protein/growth arrest and DNA damage

ECM: extracellular matrix

EGF: epidermal growth factor

ER: Endoplasmic reticulum

eIF: eukaryotic initiation factor

GADD34: growth and DNA-damage-inducible protein

GAP: Guanine activating protein

GCN2: General control non-derepressing kinase-2

GDP: guanosine diphosphate

GEF: Guanine exchange factor

GPCR: G-protein coupled receptor

GTP: guanosine triphosphate

HIF: Hypoxia induced factor

HRI: Heme regulated inhibitor

IFN: Interferon

IRE-1: Inositol-requiring enzyme -1

ISR: Integrated stress response

ISRIB: Integrated stress response inhibitor

m7G: 7-methyl-guanosine

MAPK: Mitogen-activated protein kinase

mTOR: mammalian target of rapamycin

NF- κ B: Nuclear factor kappa-light-chain-enhancer of activated B cells

ORF: Open reading frame

PABP: poly-A binding protein

PERK: PKR like endoplasmic reticulum (ER) kinase
PKR: Protein kinase activated by dsRNA
PIC: Pre-initiation complex
PP1: Protein phosphatase 1
PROTAC: proteolysis-targeting chimeras
PTEN: Phosphate and tensin homolog deleted of chromosome 10
UPR: Unfolded Protein Response
uORF: upstream open reading frame
UTR: Untranslated region
JNK: c-Jun-N-terminal kinase
TC: Ternary complex
ROS: Reactive oxygen species
RTK: Receptor tyrosine kinase

Chapter 1

Introduction

1. Cancer

Cancer is a complex and devastating disease characterized by the abnormal proliferation of various cells that, under certain circumstances, can infiltrate and metastasize to other parts of the body (1). Understanding the mechanisms underpinning cancer development has been a critical pursuit in oncology. Previous studies portrayed the six hallmarks of cancer, providing a conceptual framework that has greatly enriched our comprehension of this multifaceted disease. These hallmarks encompass evading cell death, self-sufficiency in growth signals, insensitivity to anti-growth signals, limitless replicative potential, sustained angiogenesis, and activation of tissue invasion and metastasis (2). The accumulation of genetic changes in oncogenes and tumor suppressor genes accompanies cancer development. An oncogene can govern cell proliferation, differentiation, and survival, as it can potentially trigger cell transformation (2).

Cancer can result from alterations in specific genes called oncogenes that can control cell proliferation, differentiation and survival as they can induce cell transformation. In normal cells, cell division and growth are controlled by genes called "proto-oncogenes." Proto-oncogenes encode proteins, stimulating cell division, making it essential for human development. Proto-oncogenes can become oncogenes when mutated, permanently activating the gene and leading to increased cell proliferation. Eventually, the increased cell proliferation leads the normal cells to become cancerous (3). Several genes encode for cell surface receptors found on the plasma membrane. The cell surface receptors act as a bridge to communicate between the extracellular environment and the inside of the cell. Receptor tyrosine kinases like epidermal growth factor receptor (EGFR), responsible for growth factor signaling, are one of the most common oncogenes altered in cancer (4). Tumor suppressor genes can also inhibit oncogenes to prevent the oncogenic activity to halt cancer development. Thus, studying cancer to understand better the development of different mutations is vital, as understanding the mechanism results in improved therapeutic approaches.

1.2 Lung cancer

Lung cancer is the most frequently prevalent and diagnosed type of cancer, a leading cause of cancer-related death worldwide. Based on reports, cigarette smoking is thought to cause about 80-90% of lung cancers. The average survival rate for lung cancer is 15% (5), and exposure to cigarette smoking as second-hand is also a risk factor for developing lung cancer. High mortality rates of this disease can be explained by late-stage diagnosis (6). There is still a long way to go to better treat and manage this disease.

Subtypes and histological classifications of lung cancer are categorized into small-cell lung cancer (SCLC) or non-small cell lung cancer (NSCLC). SCLC is highly metastatic and accounts for 15% of lung cancers. NSCLC corresponds to 85% of lung cancer cases and contains further subtypes such as lung adenocarcinoma (LUAD), squamous cell carcinoma (SCC), and large cell carcinoma (LCC) (6, 7). Adenocarcinomas are the most common type of NSCLC and tend to metastasize early. They can grow quite large before they are detected. Squamous cell carcinoma develops in the center of the lung and generally metastasizes late in the disease, but symptoms tend to have an early onset. Large cell carcinoma is less common but will grow rapidly and also cause late symptoms (8).

Driver oncogenes can be activated by missense, insertion, and in-frame deletion mutations and representative examples in NSCLCs include epidermal growth factor receptor (EGFR) (9, 10), Kirsten rat sarcoma viral oncogene (KRAS) (11), B-Raf proto-oncogene, serine/threonine kinase (BRAF) (12) and human epidermal growth factor receptor 2 (ERBB2) (13).

Lung Adenocarcinoma (LUAD) is the most common subtype of NSCLC and the leading cause of lung cancer death worldwide (14) and it has been shown that about 75% of lung adenocarcinomas emerge from gene mutations in the MAPK pathway, specifically *RAS* and *BRAF* (6).

1.3 Mitogen-activated protein kinase (MAPK) pathway overview

The intracellular mitogen-activated protein kinase (MAPK) pathway is a crucial intracellular pathway promoting cellular proliferation (15). Its components serve as a second messenger transporting signals from activated membrane receptors to various downstream proteins that lead to the regulation of nuclear transcriptions. Several different MAPK pathways have been

identified, of which the one that is commonly described is the RAS-RAF-MEK-ERK Pathway (16).

In the 1960s, during research on retroviruses in mice with sarcomas, Harvey (17), Kirsten, and Mayer (18) discovered RAS oncogenes. Identifying Kirsten rat sarcoma viral oncogene homolog (KRAS) was a crucial breakthrough, as subsequent studies revealed that these viral oncogenes originated from normal cellular genes. Landmark articles by Stehelin *et al.*, Scolnick and colleagues, and others characterized the structure and function of the RAS family proteins, including their corresponding mutant forms in human cancer (19-21).

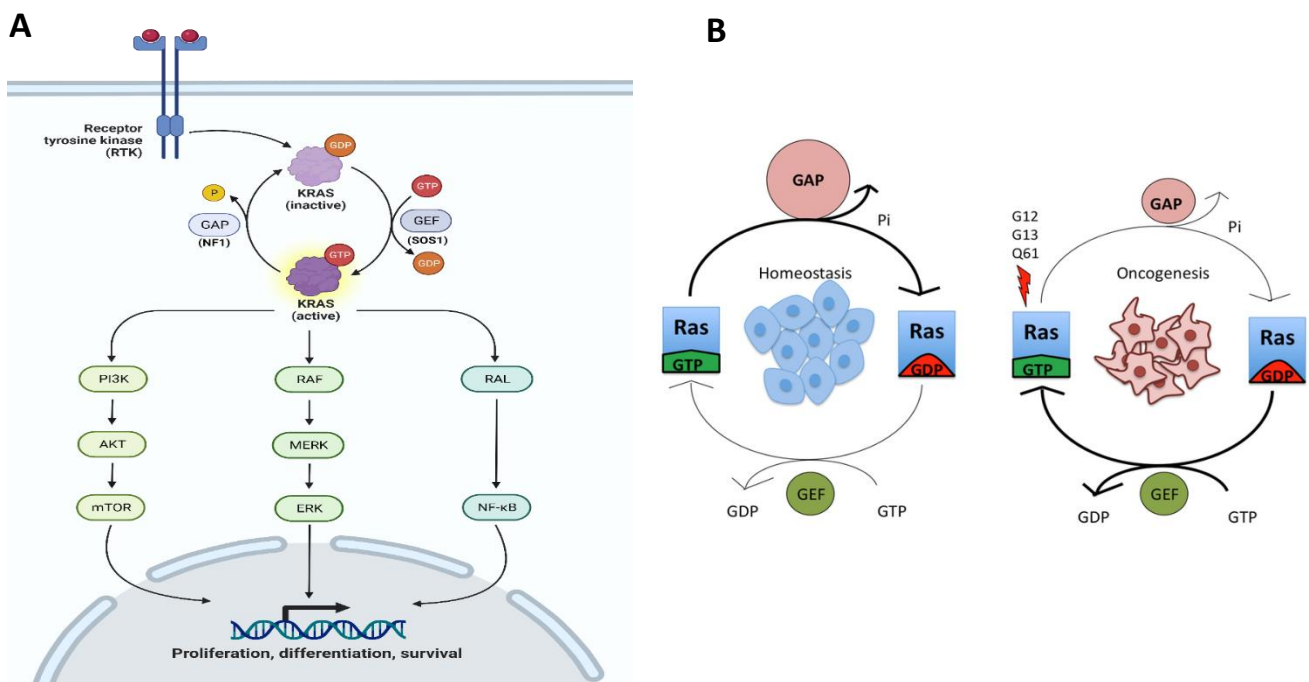


Figure 1.1 Active form of KRAS bound to GTP regulates different downstream signaling pathways. (A) KRAS, as a protein with GTPase function, cycles between an active GTP-bound state by GEFs and an inactive GDP-bound state by GAPs, controls proliferation and survival via MAPK and PI3K pathways, respectively. (B) The KRAS gene's most common mutations occur at codons 12, 13, and 61, which activate RAS signaling by impairing the GTPase or altering KRAS to become insensitive to GTPase-activating proteins. Lung cancer driver mutations in KRAS are mostly G12X and G13X. Adapted from biorender.com for (A) and from (22) for (B).

Today, we know that KRAS, with about 189 amino acids, is a member of the GTPase family, a large group of proteins that bind to the nucleotide guanosine triphosphate (GTP) and hydrolyze it to guanosine diphosphate (GDP). KRAS is a plasma membrane-bound protein that cycles between the on (GTP) and off (GDP) states, serving as a molecular switch for downstream signal transduction (23). KRAS is activated by guanine nucleotide exchange factors or GEFs (e.g., SOS1 and SOS2) and inactivated by GTPase-activating proteins (e.g., NF1), and it also has slow intrinsic GTPase activity. KRAS is positioned downstream of receptor tyrosine kinases (RTKs; e.g., EGFR) and interacts with effectors of the MAPK (RAF → MEK → ERK) and PI3K (AKT → mTOR) pathways to promote cell growth and survival, respectively (24). RAS is a GTPase that detects signals from G-coupled membrane receptors and activates RAF. Subsequently, RAF activation leads to MEK phosphorylation (p-MEK), which activates ERK by phosphorylation (p-ERK). Activated (phosphorylated) ERK then translocates into the nucleus. It activates two transcription factors, c-Jun and c-Fos, which increase the expression of several genes implicated in cellular proliferation (Figure 1.1). Similar other MAPK pathways use a similar linear scheme where a GTPase protein activates a MAPK kinase kinase (MAPK3K), which in turn activates a MAPK kinase kinase (MAPK2K). Ultimately, it activates the MAPK protein that directly phosphorylates proteins involved with cellular processes (25). Mutant KRAS is continuously in the active state, a GTP-bound. Wild-type KRAS cycles between an active, GTP-bound and an inactive, GDP-bound state, and it exists mainly in an inactive form in non-dividing cells. Toward growth factor stimulation, normal KRAS is activated by RAS guanine nucleotide exchange factors (RASGEFs), which facilitate the binding of GTP to KRAS. KRAS-GTP then binds downstream effectors. This signaling is attenuated due to the action of RAS GTPase-activating proteins (RASGAPs), which promote the hydrolysis of the bound GTP to GDP and, hence, the formation of inactive KRAS-GDP. The arrow thickness and relative size of the symbols for GEFs and GAPs indicate the level of signaling (Figure 1.1-B)(22).

Identifying and characterizing RAS family proteins, namely NRAS, HRAS, and KRAS, has been a significant scientific achievement. The journey leading to the development of targeted therapy for KRAS-mutated lung cancer has been a culmination of decades of persistent and iterative scientific investigations. Researchers have made breakthrough insights along the basic-to-clinical, bench-to-bedside, academia-to-industry continuum. RAS alterations are

among the most common activating lesions in human cancers, such as colon, lung, and pancreatic cancer (26). KRAS is the most common oncogene-driven form of non-small cell lung cancer (NSCLC), accounting for a quarter of these cancers. The prognosis for advanced mutant KRAS (mKRAS) lung cancers has been bleak, with a median survival of 1.2 years (27). mKRAS lung cancers are a specific type of NSCLC that possess unique clinical and biological features, distinguished by KRAS driver mutations, prevalent early and widespread in the evolution of the disease (28). They are often linked to smoking, have a high tumor mutation burden, and have a genetic signature that reflects exposure to tobacco smoke (29).

The KRAS gene is often affected by oncogenic missense mutations at codons 12, 13, and 61 (G12X, G13X, and Q61X, respectively), which constitutively activates KRAS by preventing the formation of van der Waals interactions between RAS and RAS-GAPs and interfering with the position of a water molecule necessary for GTP hydrolysis, respectively. These mutations modify KRAS in a way that activates RAS signaling, either by damaging the intrinsic GTPase or by altering the structure of KRAS to make it insensitive to GTPase-activating proteins. This ultimately results in an overall shift towards a KRAS on the state. In lung cancer, driver alterations in KRAS are mainly G12X (with G12C, G12V, and G12D being the most common mutations) and G13X (24, 30).

1.3.1 Targeting mutant KRAS

Targeting oncogenic KRAS directly poses several challenges, as its gene is essential for development and is highly conserved across species. Consequently, targeting the wild-type RAS could potentially lead to substantial toxicity. Efforts to develop competitive inhibitors, such as those that target ATP-binding proteins, have been hindered by the picomolar binding affinity of KRAS for GTP. Also, designing compounds to target an impaired enzymatic state is more challenging than inhibiting an active protein. These conditions have made it difficult to develop clinically direct KRAS inhibitors for decades, leading to the label "undruggable."

Indirect targeting of KRAS-driven lung cancers has not been successful. Approaches have focused on RAS post-translational modification and localization, upstream activation, and blockade of downstream effector pathways. KRAS proteins are modified post-translationally and localized to the plasma membrane through lipid anchors, such as palmitoyl and farnesyl

groups. Inhibition of these posttranslational modifications appeared to be a promising approach supported by preclinical experiments. As a result, selective and potent farnesyltransferase inhibitors were developed and entered clinical trials. Despite promising preclinical data, inhibition of farnesyl transferase to prevent post-translational modification necessary for membrane localization has been unsuccessful in KRAS-driven lung and other cancers because of alternative post-translational modification by other enzymes. Similarly, a RAS farnesylcysteine mimetic developed to prevent RAS membrane attachment was unsuccessful in clinical testing and had substantial adverse effects (31, 32).

Attempts to target specific signaling nodes downstream of KRAS have not resulted in meaningful clinical responses, primarily due to the rapid adaptation of compensatory signaling through alternative pathways. Clinical trials testing therapies that target MAPK and PI3K signaling pathways, such as MEK, RAF, and mTOR inhibitors, have either been ineffective (32) or have had limited efficacy due to toxicity concerns (33). Similarly, clinical studies of targets that were thought to lead to synthetic lethality, such as CDK and proteasome inhibitors and heat shock protein inhibitors, have not been successful (34-36). It was not until 2013 that a groundbreaking study by Ostrem *et al.* identified allele-specific covalent inhibitors of mKRAS G12C, which were the first direct inhibitors of oncogenic KRAS. Through structural biology and synthetic organic chemistry, researchers found a unique allosteric pocket in KRAS G12C, leading to the development of inhibitors that can lock KRAS in its inactive GDP-bound form. They also created a potent small molecule that binds to the mutant cysteine amino acid of mKRAS G12C, effectively locking it in the GDP-bound state. (37). This class of compounds has demonstrated the ability to shift the cellular preference for the KRAS off-state and directly limit KRAS interactions with downstream effectors.

Two direct inhibitors of KRAS-G12C were recently developed, namely sotorasib (also called AMG 510 or Lumakras) and adagrasib (also known as MRTX849). These inhibitors selectively form a covalent bond with cysteine 12 located within the unique pocket of KRAS-G12C protein to lock KRAS in the inactive state to arrest cell proliferation (38-40). JDQ443 is another promising mKRAS G12C inhibitor that may prevent resistance caused by gene mutations that disrupt inhibitor binding. It effectively inhibits mKRAS G12C cellular signaling and proliferation

in a mutant-selective manner. However, studies are ongoing to better understand resistance to this new class of therapies (41).

1.3.2 Resistance to Drugs Targeting mutant KRAS

The lack of response to mKRAS inhibitors in most patients with mKRAS G12C NSCLC and colorectal cancer highlights the need to identify mechanisms of intrinsic resistance. One such mechanism is signaling rebound and adaptive changes in signaling networks. mKRAS inhibitors suppress MAPK signaling for a short duration, but signaling rebound has been observed within 24 to 72 hours of treatment (42, 43). This is due to the compensatory activation of RTKs, which can spur SOS1-mediated nucleotide exchange and shift mKRAS from its GDP-bound inactive state to its GTP-bound active conformation (44-46). Other intrinsic resistance mechanisms include bypass signaling independent of the MAPK pathway driven through the PI3K-AKT-mTOR signaling axis and overexpression of wild-type RAS protein upon mKRAS inhibition (42, 43). Resistance can also be caused by tumor extrinsic mechanisms, such as cancer-associated fibroblasts, and immune-mediated mechanisms of tumor response may also play a role. The primary challenge is identifying these intrinsic resistance mechanisms and implementing patient enrichment schemes for effective combination strategies to maximize the therapeutic activity of mKRAS inhibitors.

Acquired resistance after a favorable initial response is a major hurdle in targeted cancer therapy. While DNA-based next-generation sequencing in tumor tissue is the gold-standard method for genomic alterations responsible for targeted agent resistance, serial biopsies for molecular profiling are often not feasible in the setting of resistance to systemic therapy (47). The resistance of mKRAS covalent inhibitors due to secondary mutations in the KRAS gene that restrict drug binding can also happen. In addition to clinically observed mutations, novel secondary mutations in KRAS that affect nucleotide exchange reaction have also been identified, which could result in resistance to mKRAS inhibition. Acquired secondary gene mutations along the RTK-RAS-MAPK-PI3K axis and oncogenic gene rearrangements are other genomic alterations identified in patients after Adagrasib treatment. This suggests that resistance could be overcome by targeting these oncogenic drivers. In addition to secondary mutations within KRAS and associated RTK and MAPK signaling molecules, acquired resistance to mKRAS inhibitors may arise from transcriptional remodeling within treated cancers. As

clinical studies reported, a NSCLC patient with a KRAS G12C mutation developed polyclonal acquired resistance to MRTX849. Additionally, the assessment illustrates a novel mutation in KRAS Y96D, which affects the G12C unique pocket targeted by inhibitors such as MRTX849 and other inactive-state inhibitors. These mutations interfere with protein-drug interactions, resulting in resistance to these inhibitors observed in both engineered and patient-derived mutant KRAS with G12C cancer models (48). Histologic transformation of adenocarcinoma to squamous cell carcinoma has been observed in patients who develop acquired resistance to mKRAS inhibitors, reminiscent of transformation from NSCLC to small-cell lung cancer observed in patients with acquired resistance to EGFR inhibitors. Finally, the activation of bypass signaling may depend on transcriptional as opposed to genomic alterations, which suggests that patients with acquired resistance to KRAS inhibitors may be good candidates for trials targeting epigenetic factors and mediators of cellular plasticity (33, 47, 49).

1.4 mRNA translational initiation

The process of mRNA translation is one of the most energy-intensive cellular activities and therefore, strictly controlled regulation of messenger RNA (mRNA) translation. This process involves the timely incorporation of translation factors, sufficient energy levels, and low mutation rates to produce a functional protein (54) by signaling pathways such as mTOR and MAPK. These pathways lead to quantitative and qualitative translation changes (50). Recent studies have shown that translation has a conserved role in regulating gene expression and plays a significant role in determining protein expression levels in mammalian cells (51). Measurements of oxygen consumption in rat thymocytes suggest that translation consumes around 20% of cellular ATP, making it the most energy-demanding cellular process. Consequently, translation dysregulation is implicated in various human diseases, including cancer (52, 53).

The proper functioning of genes requires Ribosomes to play a crucial role in facilitating efficient and accurate protein synthesis by identifying open reading frames (ORFs) within the mRNA and assembling polypeptides with amino acid sequences corresponding to the codon sequence on the mRNA. The production of a fully functional protein by mRNA translation is divided into three controlled steps: initiation, elongation, and termination (54). Each phase

has its own essential factors and tight regulation for successful protein production. In eukaryotes, translation initiation is the most crucial step, which is composed of a highly organized network of biomolecules working in coherence (Figure 1. 2). The scanning mechanism leads to the recognition of the AUG start codon in the mRNA, which involves an active 43S pre-initiation complex (PIC) composed of the methionyl initiator transfer RNA (Met-tRNA_i) bound to the small 40S ribosomal subunit (55). The recognition of the AUG start codon requires energy provided by guanosine triphosphate (GTP) carried by the eukaryotic initiation factor 2 (eIF2) and generates the ternary complex (TC) including the translation initiation factor eIF2, GTP and correct base pairing established with the initiator methionyl-tRNA (eIF2.GTP.tRNA_iMet), as illustrated in Figure 1.2; as soon as the mRNA leaves the nucleus to begin a round of translation, the TC is loaded onto an activated mRNA near the 5'-cap (56, 57).

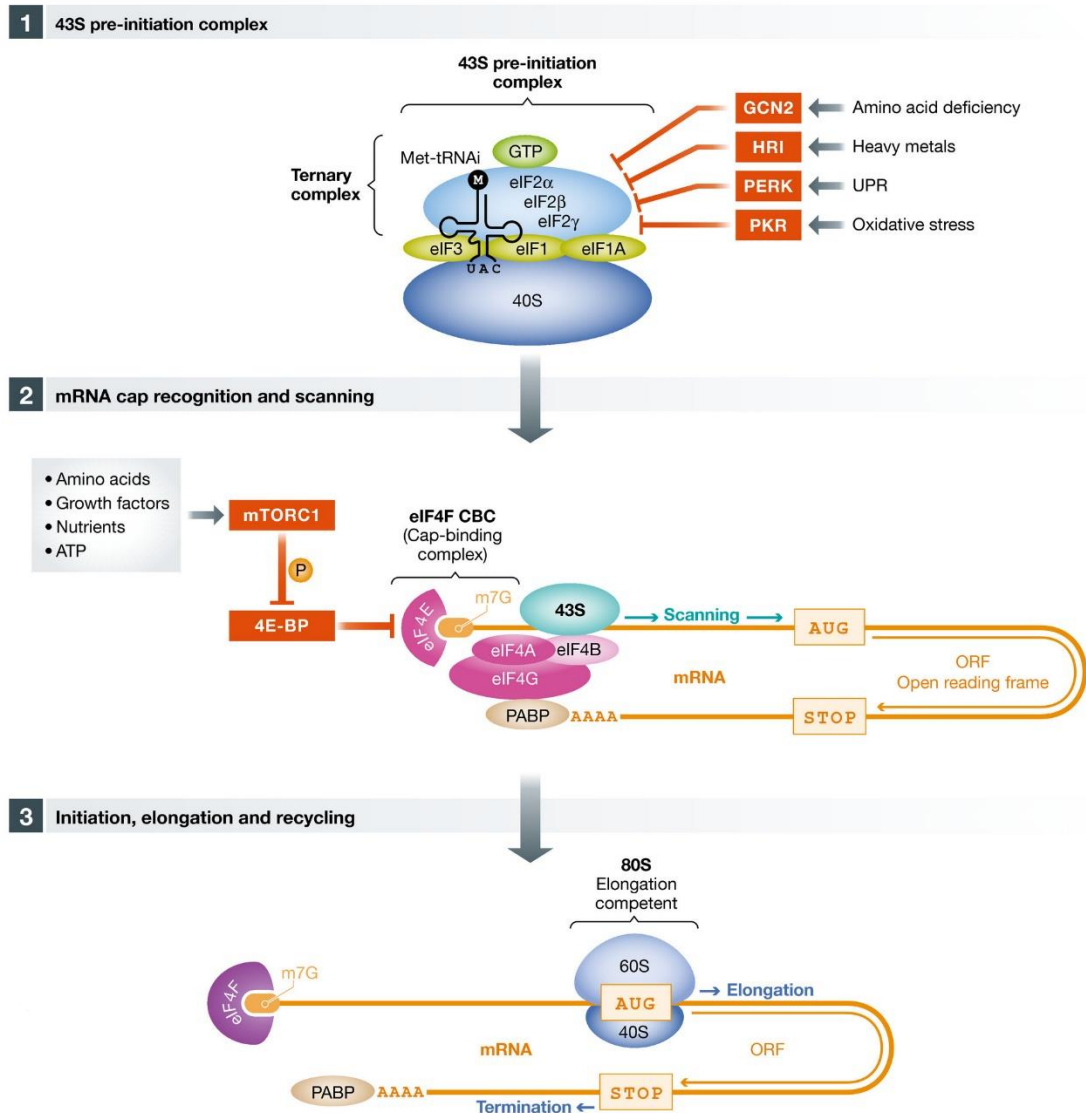


Figure 1. 2 The canonical pathway of eukaryotic translation initiation. The figure displays a schematic representation of the canonical pathway of eukaryotic translation initiation, including the canonical initiation factors and signaling pathways that regulate these initiation factors. Adapted from (58).

Furthermore, the process of attaching the m7G 5'-cap is made more accessible by the eIF4F complex, which consists of the cap-binding factor eIF4E, the scaffold protein eIF4G, and the ATP-dependent RNA helicase eIF4A. Due to the possibility of having secondary structures in the 5'-untranslated region (UTR), the eIF4A RNA helicase activity can resolve them, enhancing mRNA translation (59). The poly-A binding protein (PABP) attachment to the poly-A tail also

facilitates the translation process, which eventually forms a closed loop when joined with the 5'-cap, an essential step in translation initiation (Figure 1.3). The Pre-Initiation Complex (PIC) proceeds to scan the mRNA codon by codon, with the aid of GTP hydrolysis from the TC, until it detects the AUG codon that matches the complementary anticodon found on the Met-tRNA_i (60). Subsequently, the binding of the initiator tRNA to mRNA codons in the P site of the 40S ribosomes triggers the disassembly of the PIC. The dissociation of eIF1 highlights this process, the release of phosphate (Pi) from eIF2, and the conformational rearrangements of eIF5, 1A, -2 β , and -3c of the PIC⁷. Finally, GDP-eIF2 dissociates from the PIC, and eIF5B-GTP mediates the next step.

The target of rapamycin (TOR) and the mitogen-activated protein kinase (MAPK) pathways regulate the phosphorylation and function of many eIFs and associated factors. Another important signaling node in translation involves the eIF2 α kinases (61).

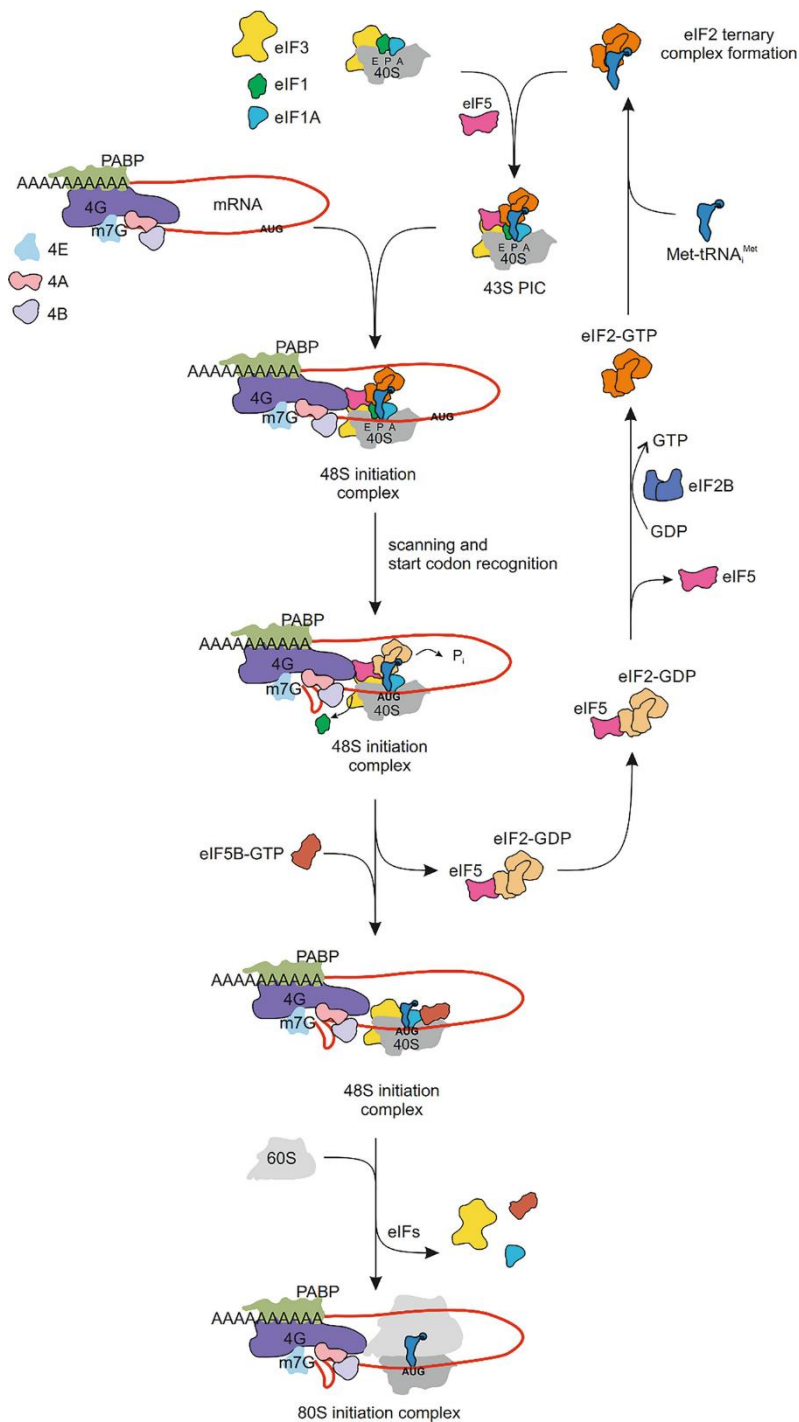


Figure 1.3 Schematic overview of the canonical eukaryotic translation initiation pathway.

eIF2-GTP-Met-tRNA^{Met} binds to 40S ribosomes to form the 43S pre-initiation complex (PIC) with eIF1, eIF1A, eIF3, and eIF5 to start protein synthesis. The eIF4F complex recruits mRNA to form the 48S PIC, and after scanning, the 60S subunit joins with the aid of eIF5B to make the 80S IC. Adapted from (62).

The released GDP-eIF2 is recycled to GTP-eIF2 by the guanine exchange factor (GEF) eIF2B for another round of initiation (63).

1.4.1 The Integrated Stress Response (ISR) in translational control

The integrated stress response (ISR) is governed by an additional step of regulation that highlights the importance of eIF2 in the initiation process (64, 65). Cells encounter different forms of stress during their lifecycle, such as metabolic, oxidative, hypoxic, proteotoxic, and genotoxic stress (66, 67). Under these conditions, p-eIF2 α impedes the GEF activity of eIF2B and hinders the recycling process and formation of the TC (65). This leads to the blockage of general translation initiation. However, translation of most mRNAs with uORFs occurs via cap-dependent translation via ribosome bypass of uORF or ribosome reinitiation (63), allowing for delayed reinitiation, which is essential to initiation and the Integrated Stress Response (ISR) (Figure 1.2) (59, 63-70).

During the lifespan of actively dividing healthy cells, they are frequently subjected to various types of stress. However, cells have several mechanisms that aid them in coping with stressful situations and restoring homeostasis. The Integrated Stress Response (ISR) is one such mechanism that operates at the mRNA translation initiation level. It comprises four kinases that possess similar kinase domains but distinct regulatory domains, enabling their activation in response to different types of stress (as illustrated in Figure 1.4)(54, 64, 65, 71).

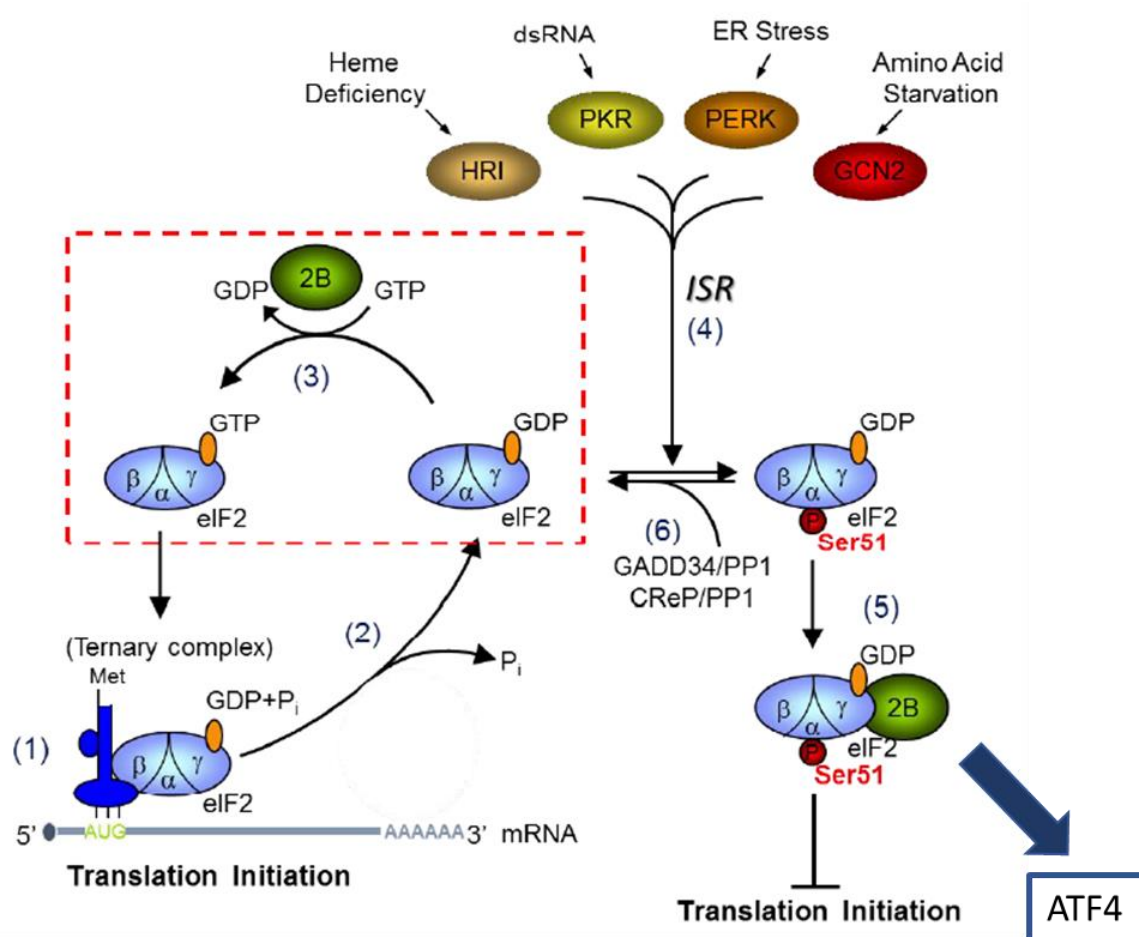


Figure 1.4 The Integrated Stress Response (ISR) as an important regulator of translation initiation. Activation of the four kinases, PKR, PERK, GCN2 and HRI in response to different forms of stress lead to phosphorylation at Serine 51 of the α subunit of eukaryotic initiation factor 2 (eIF2). The unphosphorylated GTP-bound form of eIF2 is essential for forming the ternary complex (TC) to initiate mRNA translation. However, the phosphorylated form in response to stress causes a global inhibition of mRNA translation except mRNAs with open reading frames (ORFs) in their 5'-untranslated regions such as ATF4. Adapted from (64).

When there is a lack of heme, HRI is triggered, halting the production of globin(72). Additionally, HRI safeguards erythroid precursors during iron deficiency, erythropoietic protoporphyria, and β -thalassemia (73, 74). On the other hand, PKR is activated by viral dsRNAs. This causes a reduction in mRNA translation and promotes apoptosis while also

facilitating the activation of a range of signaling pathways. PKR can also promote cell survival by activating NF- κ B and PI3K signaling pathways in specific cell types (75, 76).

The PKR-like ER kinase (PERK) is activated by endoplasmic reticulum (ER) stress as part of the unfolded protein response (UPR), which is crucial for maintaining proteostasis in the ER(76). PERK is normally associated with the chaperone protein BiP in its inactive state, but the accumulation of misfolded proteins leads to UPR activation and dissociation of BiP from PERK, resulting in its dimerization and activation(77). PERK is then phosphorylated at Thr980, which stabilizes the activation loop and the helix α G, allowing it to phosphorylate eIF2 α and inhibit new polypeptide synthesis, restoring ER homeostasis. Alternatively, PERK can be activated directly by binding to misfolded proteins. In addition to eIF2 α , PERK also activates the nuclear factor NRF2 and glycogen synthase kinase-3 β (77-80). Deacetylated His-tRNA primarily activates the general control non-derepressible 2 (GCN2) due to low amino acid content but can also be activated by other stressors such as UV light, viral infection, serum starvation, and oxidative stress. GCN2 autophosphorylates at Thr882 and Thr 887 and phosphorylates eIF2 α as its reported substrate is eIF2 α (63, 81-83). Recently, it was found that the ribosomal protein uL10 can also activate GCN2 (56, 71)(Figure 1.4).

1.4.2 Translation Alteration in ISR

Eukaryotic initiation factor 2 (eIF2) is a heterotrimeric complex composed of three subunits, α , β , and γ , crucial in regulating protein synthesis. Upon activation of any of the mentioned kinases, the α subunit of eIF2 gets phosphorylated at Serine 52 (p-eIF2 α), inhibiting the guanine nucleotide exchange factor eIF2B. The ϵ subunit of eIF2B catalyzes the exchange of GDP and GTP, which is essential for forming the active ternary complex (TC). The interaction between the γ subunit of eIF2 and the ϵ subunits of eIF2B causes an open conformation of eIF2 γ , facilitating the exchange of nucleotides. However, phosphorylation of eIF2 α due to active ISR hinders eIF2 γ -eIF2B ϵ interactions, impeding the formation of an active TC. Although this event leads to global inhibition of mRNA initiation, the translation of select mRNAs is paradoxically promoted (Figure 1.4). For instance, ATF4 and ATF5 are mRNAs that contain upstream open reading frames (uORFs) in their 5'-UTR that prevent their translation under normal conditions. ATF4, the most well-characterized ISR effector, contains multiple uORFs in

its 5'-UTR that require the TC to re-initiate for proper translation. Under normal conditions, ribosomes scan the mRNA and encounter the first uORF, which inhibits the formation of the active TC and prevents translation of the main ORF. However, in stressed conditions where the availability of TC is limited, the ribosome continues scanning until it reaches the main ORF and forms a functional translation machinery with TC that results in increased translation of the mRNAs. The second inhibitory, uORF, also inhibits the translation of ATF4 under normal conditions (84-86). However, in stressed conditions, the scarcity of TC allows the ribosome to bypass the second uORF and translate the main ORF, leading to an increased translation of the mRNA, as depicted in Figure 1.5.

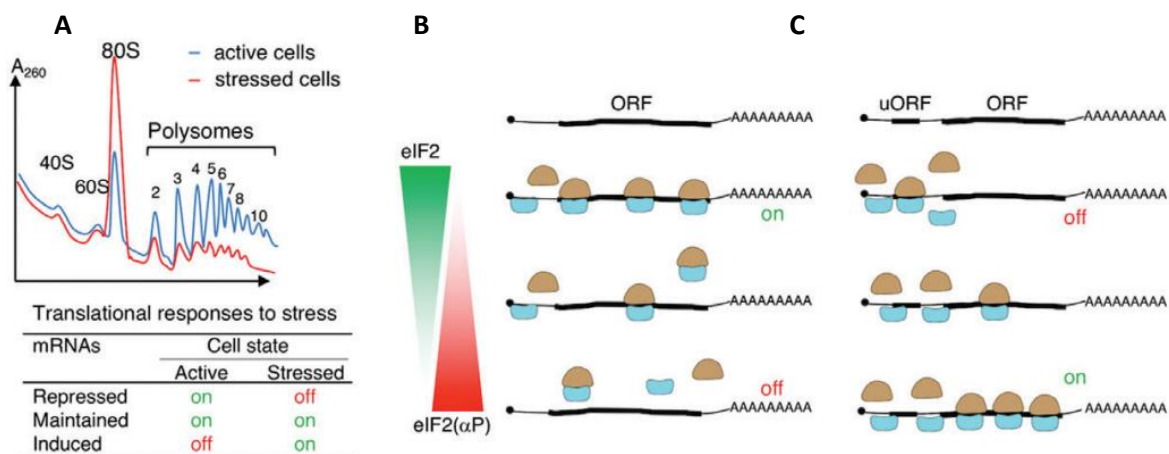


Figure 1.5 Effects of ISR on uORF mRNA with ribosome interactions. (A) Polysome profiles of A₂₆₀ active and stressed cells extracts on sedimentation of 15–50% sucrose gradients. Ribosomes interacted with (B) single ORF mRNA or (C) uORF-bearing mRNA depending on the phosphorylation of eIF2α. Adapted from (86).

1.4.3 ISR Termination

The termination of ISR holds significant importance in deciding the fate of cells and restoring homeostasis. The protein phosphatase 1 complex (PP1) comprises of a catalytic subunit (PP1c) and one of two regulatory subunits, PPP1R15A (GADD34) and PPP1R15B (CreP), activated by ATF4 (66, 87). While CreP maintains normal levels of eIF2αP under unstressed conditions, GADD34 dephosphorylates p-eIF2α under stressed conditions since it contains uORFs in its 5'-UTR and is directly upregulated by p-eIF2α. These two phosphatases are better

translated when eIF2 α is phosphorylated, which acts as a feedback mechanism to dephosphorylate p-eIF2 α and restore homeostasis. Additionally, GADD34 and CreP determine the pro-death or pro-survival fates of cells with active ISR (64, 88, 89) (Figure 1.4).

1.4.4 The role of translation initiation in the context of cancer

Cancer is a multifaceted disease that extends beyond cell proliferation and cell death resistance (90, 91). Cancer cells utilize mRNA translation regulation to facilitate their successful propagation (92-94). Specifically, the eIF4F complex is often disrupted in cancer, with its increased expression promoting the translation of mRNAs associated with survival and invasion. It is crucial to develop inhibitors that can target the components of the eIF4F complex, as elevated eIF4F levels are present in cells resistant to chemotherapy and targeted therapy (95, 96).

The eIF4F complex is frequently dysregulated in cancer, with eIF4E expression upregulated in many cancers. However, its overexpression does not seem to increase the translation rate (59, 95, 96). eIF4E-sensitive mRNA either possess long, highly structured 5'-UTRs, special elements in their 5'-UTR, or encode ribosomal proteins. eIF4E expression, as well as its phosphorylation, stimulates the expression of mRNAs with roles in survival (MCL) and invasion (e.g., Snail and MMP3)(59). However, variation in mRNA responsiveness across tumor types may occur. In nutrition and growth-factor-restricted cells, a tightly regulated process in cap-dependent translation initiation is blockage of eIF4F assembly by the 4E binding proteins, with 4E-BP1 being the most well-studied among the three isoforms (59, 97). Specifically, 4E-BP1 prevents the assembly of eIF4G to eIF4E. Two important signaling pathways mostly regulate eIF4E, namely the PI3K/AKT/mTOR and Ras/MAPK/MNK pathways (57, 98). These pathways often play a pro-tumorigenic function in cancer development. mTORC1 activation by various stimuli phosphorylates 4E-BP, causing eIF4E release to resume its initiation function (57, 99). On the other hand, MNK stimulates eIF4E phosphorylation at Ser 209 to initiate translation and plays an important role in tumor progression and metastasis (98). The oncogenic activity of eIF4F is critical, as highlighted by the development of inhibitors that target the components of the eIF4F complex, including targeting eIF4E function, eIF4E phosphorylation, and eIF4A activity. Additionally, eIF4F levels are elevated in cells resistant to

chemotherapy or targeted therapy, making it an attractive target for combination therapies (59, 95, 96).

The uncontrolled proliferation of cancer cells exposes them to multiple forms of stress, including ER stress, hypoxia, amino acid depletion, DNA damage, and reactive oxidative species (ROS)(67, 68, 100). As a result, the ISR is more readily triggered in cancer cells than normal cells, ending in the adaptation of cancer cells to the type of stress (100), which can either help in the survival and progression of the cancer cells or trigger pro-death signaling pathways (77, 101). The ISR has a dual nature based on its core function inhibiting most mRNAs while selectively upregulating specific mRNAs that play a role in cell adaptation to stress (102). Whether the ISR promotes cell survival or induces cell death in response to stress depends on the type of cancer, the nature of stress, and the oncogenic driver (103, 104). The pro-survival role of the ISR is highlighted in medulloblastoma, pancreatic cancer, BRAF-mutated melanoma, lung adenocarcinoma, and aggressive prostate cancer. Contrarily, the ISR can induce apoptosis in other types of cancer, such as glioblastoma multiforme (GBM), breast cancer, and Acute Myeloid Leukemia (AML) (100, 105-109). The pro-death or pro-survival function of the ISR is also activated in response to therapy to either confer resistance or contribute to cell death, respectively (104).

The ISR is a complex mechanism that utilizes kinases such as PERK and GCN2 to manage a range of stressors. In response to extreme hypoxic stress, basically anoxia which leads to endoplasmic reticulum (ER) disruptions, PERK is activated to enhance cell survival by inhibiting apoptosis (110-112), inducing pro-survival factors (such as miR-211, NFkB, and autophagy), and promoting tumor-related pathways like PI3K-Akt (68, 113, 114). On the other hand, when amino acid scarcity is detected, GCN2 is triggered to upregulate autophagy genes via ATF4, ensuring a pro-survival response by facilitating cellular component recycling and maintenance of ATP and amino acid levels (104).

However, it is important to note that persistent stress may shift ATF4 towards pro-apoptotic gene transcription. The PKR-p-eIF2 α pathway, while activating pro-survival mechanisms like NF-kB, may also trigger pro-death pathways involving FADD and PTEN. The ISR dynamically balances pro-survival and pro-apoptotic responses based on stress duration and context, thereby ensuring cellular homeostasis (115, 116).

The outcome would be the initiation of cell death by activating this pathway. Initially, the HRI kinase activity was believed to be confined to erythroid cells; however, recent findings also indicate its involvement in non-erythroid cells (116, 117).

1.4.5 Targeting ISR by eIF2B

For the treatment approach, specific inhibitors of eIF2 α phosphorylation are still unavailable; however, eIF2 α phosphorylation can be indirectly targeted by inhibiting upstream kinases, activating downstream phosphatases, or antagonizing its function in translational control. This therapeutic targeting of the ISR could be an effective anti-cancer regimen and sensitize cancer cells to chemotherapy or targeted therapies. Moreover, targeting the ISR could help gain a deeper understanding of the significance of this process in cancer biology and progression. Antagonizing the translational effects of p-eIF2 α by targeting eIF2B represents a promising therapeutic strategy (64).

The recently identified integrated stress response inhibitor (ISRIB) has been shown to rescue the inhibition of mRNA translation caused by eIF2 α phosphorylation by enhancing eIF2B GEF activity.

Mechanistically, ISRIB facilitates the binding of eIF2 to eIF2B by annealing together two tetrameric forms of eIF2B, which leads to an increased rate of eIF2B decameric assembly and a subsequent increase in GDP-GTP exchange on eIF2, resulting in more translation. This dampens the inhibitory effects of p-eIF2 α on translation. However, ISRIB's capacity to induce translation is highly dependent on the presence of p-eIF2 α , implying that ISRIB will only function in cells with an active eIF2 α phosphorylation. Therefore, the therapeutic efficacy of ISRIB is contingent upon cancer cells with highly activated eIF2 α phosphorylation. ISRIB has been employed as a singular agent in targeting lung adenocarcinoma and aggressive prostate cancer, with no toxic side effects observed in mice and prolonged survival observed in both models. In combination therapies, ISRIB has been shown to sensitize pancreatic cancer cells to Gemcitabine treatment and breast cancer cells to bortezomib (106, 118). Also, When administered to rodents, ISRIB enhances cognition and ameliorates cognitive deficits caused by traumatic brain injury and prion-induced neurodegeneration (119, 120). Furthermore, eIF2B activation rescues cognitive and motor function in mouse models of

leukoencephalopathy with vanishing white matter disease (VWMD), a fatal familial disorder associated with mutations spread over all eIF2B subunits (121) (Figure 1.6).

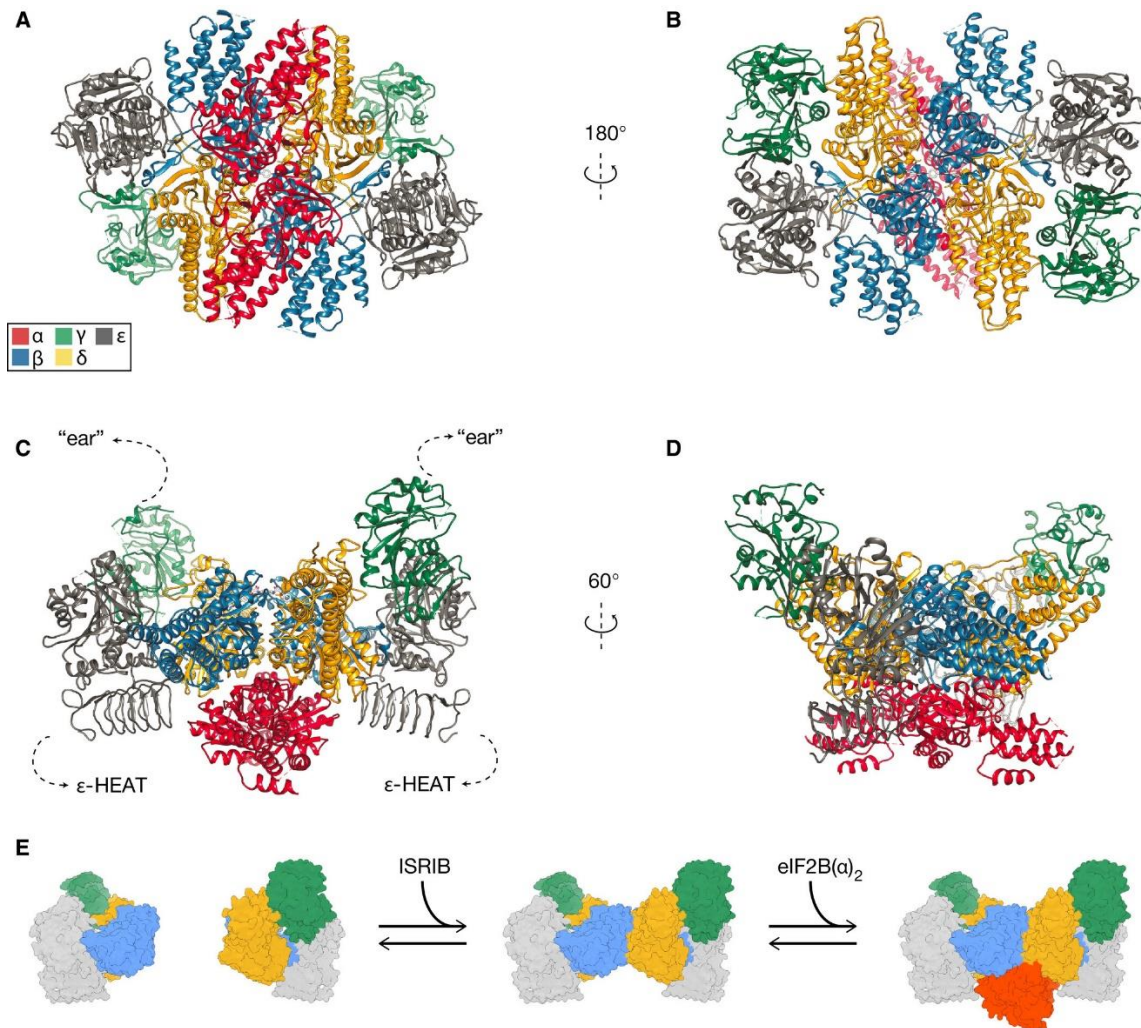


Figure 1.6. Human eIF2B complex bound to ISRIB. Four mirrors and distinct display of eIF2B (A-D), every subunit colored differently (α in red, β in blue, γ in green, δ in gold, ε in gray, and ISRIB in CPK coloring). Dotted lines (C) indicate a connection to the 'ear' domains of gamma and HEAT domain of epsilon for which density is not clearly defined. (E) Model for ISRIB's mechanism of action: eIF2B(βγδε) tetramers are dimerized upon ISRIB plus to form a stable octamer that can, in turn, bind the dimeric eIF2B(α₂) to assemble the active decamer. Adapted from (122, 123)

The regulation of the Integrated Stress Response (ISR) is dependent on the interaction between eIF2 and eIF2-P with eIF2B, a guanine nucleotide exchange factor enzyme that

enables eIF2's gamma subunit to bind to GTP. The eIF2B decamer is comprised of two eIF2B $\beta,\gamma,\delta,\epsilon$ tetramers and one eIF2B α_2 homodimer, which can easily assemble into stable subcomplexes (Figure 1.6). The eIF2B $\beta,\gamma,\delta,\epsilon$ tetramer has low basal GEF activity and only interacts with eIF2 through IF1-IF3 as initiation factors in prokaryotes (bacteria) that are involved in the initiation of protein synthesis in bacterial translation. The assembly of the eIF2B decamer is promoted by eIF2B α_2 , which drives the full GEF activity on eIF2 and inhibition by eIF2-P to manifest (124, 125).

ISRIB is a potent small molecule that can significantly reduce ISR activity. It has been found to improve cognitive deficits in mice with traumatic brain injury, Down syndrome, normal aging, and other brain disorders without any harmful effects (120, 126-128). ISRIB targets eIF2B, binding to a central groove that bridges the symmetry interface between eIF2B $\beta,\gamma,\delta,\epsilon$ tetramers. This binding promotes the assembly of two eIF2B $\beta,\gamma,\delta,\epsilon$ tetramers into eIF2B($\beta,\gamma,\delta,\epsilon$)₂ octamer as an active enzyme, acting as a 'molecular staple'(122, 125).

The eIF2B is a heterodecamer that comprises two copies each of alpha, beta, gamma, delta, and epsilon subunits, which assemble into a two-fold symmetric structure (124, 129) (Figure 1.6). The eIF2B-epsilon subunit contains the enzyme's catalytic center and is closely associated with eIF2Bgamma. Two copies of the eIF2B-beta and delta subunits form the complex's core, bridged by two eIF2B-alpha subunits across the symmetry interface (124, 130, 131). Structural studies of eIF2B-eIF2 complexes using cryo-electron microscopy (cryo-EM) have shown that eIF2 snaked across the surface of eIF2B in an elongated conformation. It contacts eIF2B at four interfaces, referred to as IF1-IF4 (124, 130). Upon S51 phosphorylation, eIF2alpha adopts a new conformation that renders it incompatible with IF3-IF4 binding. Instead, phosphorylation leads to a new binding mode on the opposite side of eIF2B, where eIF2alpha-P binds to a site between eIF2B1 and eIF2B4. This new binding mode can sterically block eIF2gamma of a simultaneously bound unphosphorylated eIF2 substrate from productive engaging with eIF2B5's active site (132, 133) (Figure 1.7).

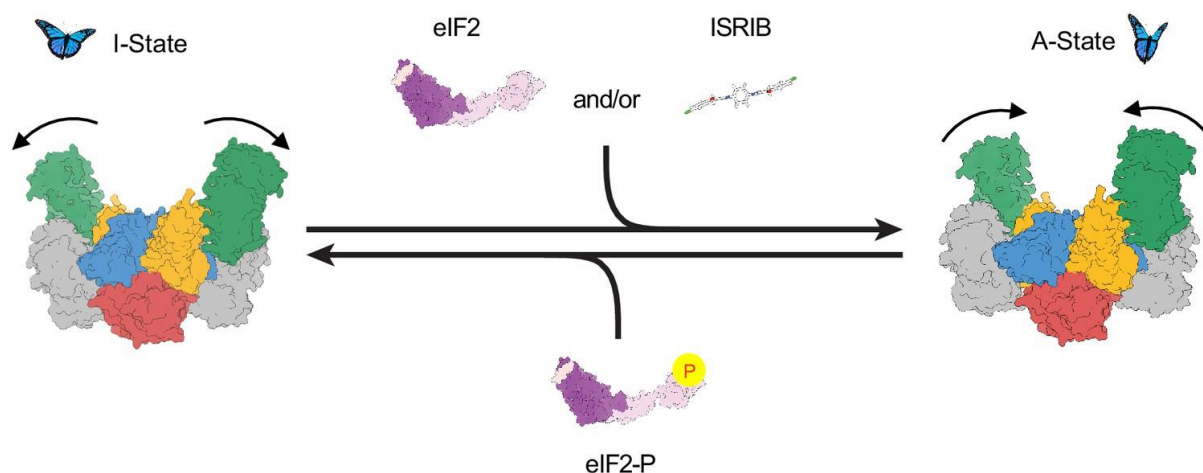


Figure 1.7 Modulation illustration of eIF2B activity. The active conformation (A-state) of eIF2B is stabilized by ISRIB and eIF2 binding, while the inactive conformation (I-state) is stabilized by eIF2-P. The equilibrium between the two conformations is likely biased towards the active state, which is further stabilized by substrate eIF2 and ISRIB binding. The two states are mutually exclusive and define an on-off switch of eIF2B's GEF activity. The transition from the active to the inactive state is the central mechanism underlying ISR activation. Adapted from (130).

Genetic and biochemical studies have identified residues responsible for eIF2B's catalytic activity and suggested how eIF2 binding to eIF2B may differ following eIF2- α -S51 phosphorylation (124, 134, 135). ISRIB is a drug-like inhibitor of the integrated stress response that alleviates the effects of eIF2 α phosphorylation by activating eIF2B. Upon adding ISRIB, cells undergoing the ISR resume translation (136-138). ISRIB bridges the symmetric interface of two eIF2B subcomplexes to enhance the formation of the decameric eIF2B holoenzyme (122, 139), enhancing available GEF activity by promoting higher-order assembly of the eIF2B decamer. However, the question of why decameric eIF2B would be more active than its unassembled subcomplexes remains enigmatic (Figure 1.7).

1.5 eIF2B dysregulation in human cancer

eIF2B, a GEF for eIF2, is considered to be the master regulator of translation initiation and composed of five subunits (α , β , γ , δ and ϵ) which are encoded by genes *eIF2B1*, *eIF2B2*, *eIF2B3*, *eIF2B4* and *eIF2B5*, respectively (140). The mutations in the *eIF2B2* and *eIF2B5* genes have been reported to be the cause of an inherited disease called vanishing white matter

(VWM) (141). ISRIB has been employed as a singular agent in targeting lung adenocarcinoma and aggressive prostate cancer, with no toxic side effects observed in mice and prolonged survival observed in both models (142, 143). In combination therapies, ISRIB has been shown to sensitize pancreatic cancer cells to Gemcitabine treatment and breast cancer cells to bortezomib (106, 118).

As the largest subunit, eIF2B ϵ contains the catalytic domain and promotes GDP/GTP exchange on eIF2. Additionally, eIF2B ϵ is found to be upregulated in live cancer and its expression is related to histologic grade, clinical stage and vital status. Furthermore, high eIF2B ϵ expression correlates with poor prognosis and an independent risk factor for liver cancer, while the downregulation of eIF2B ϵ expression leads to reduction in GEF activity and global protein synthesis, as well as significant reduction in cell growth rate, colony formation and tumor progression in nude mice (144)

1.5.1 Unleashing the Potential of PROTACs to Target eIF2B for Novel Therapeutic Strategies

PROTAC (Proteolysis-Targeting Chimera) is an innovative approach to drug discovery. It involves selectively using small molecules called PROTACs to degrade disease-causing proteins within cells (145). PROTACs consist of two molecules bound together by the linker to form a two-headed molecule. One end of the molecule binds to an E3 ubiquitin ligase, while the other binds to the target protein for destruction, such as eIF2B. Unlike conventional protein inhibitors that require a perfect degree of target engagement over a long period to be pharmacologically effective, PROTACs engage in a strategy to be optimized for fast degradation rates in relatively short exposure to therapeutic doses, resulting in the complete elimination of the target protein (146, 147) (Figure 1. 8).

The most popular ligands in PROTACs are those that bind to von Hippel-Lindau (VHL) or Cereblon (CRBN) E3 ligase (148).

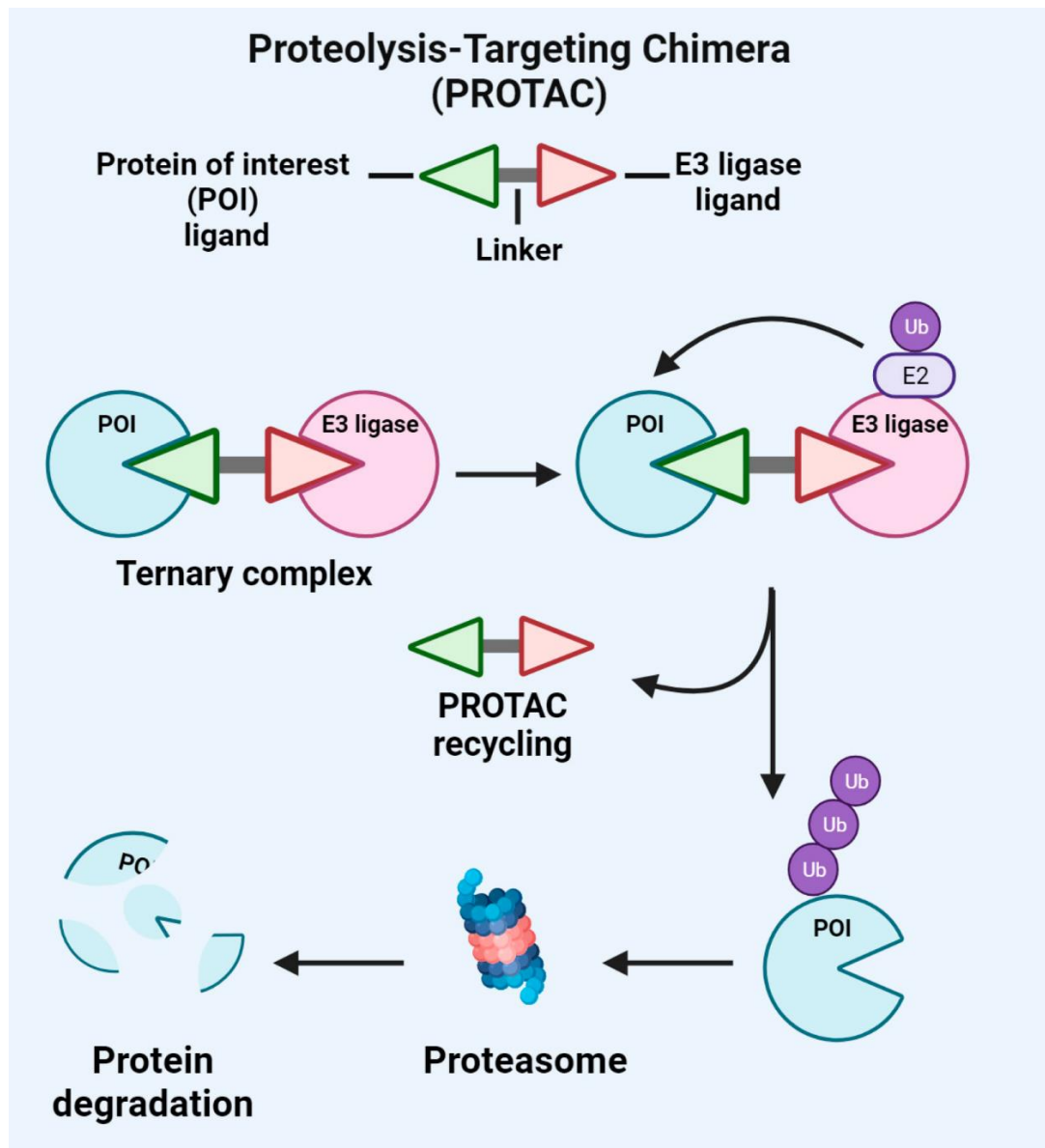


Figure 1.8 Schematic illustration of PROTAC mechanisms of action. General mechanism of PROTAC-mediated ubiquitination and proteasomal degradation of target protein. The heterobifunctional PROTAC comprises a ligand that binds to the target protein and a ligand that attaches to the E3 ubiquitin ligase by a linker. Adapted from (149).

As illustrated in Figure 1.8, when both parts bind, they bring the target protein and the E3 ligase together, leading to the proteasome's transfer of ubiquitin and subsequent degradation

of the target protein. This targeted protein degradation approach offers advantages over traditional methods, as it can target previously "undruggable" proteins and restore normal cellular function. PROTACs have the potential to be used in various diseases, and research in this field is ongoing to optimize designs and expand the range of targets (150).

One ligand binds to a protein of interest (POI). In contrast, the other binds an E3 ubiquitin ligase to create a ternary complex (TC) from which the POI is ubiquitinated and targeted for degradation by the cell's ubiquitin-proteasome system. PROTACs have garnered significant interest in the past two decades, with several candidates progressing to clinical trials for treating cancers (151, 152).

1.6 Rational, study design and hypothesis

1.6.1 Rational

Herein, we investigate the mechanisms and biological effects of functional interaction between eIF2B and mKRAS in tumorigenesis and its implications in treatments targeting mKRAS cancers.

In recent years, there has been significant progress in the cancer field by the generation of drugs targeting mKRAS. In contrast, the initial success of drugs in the clinics that lock mKRAS in an inactive conformation (2) is hindered by the development of resistance (3, 4). Based on recent studies (153) (154) and Dr. Koromilas' lab data (142, 155) show that eIF2B promotes the maintenance of mKRAS in an active state, leading to stimulation of proliferation and tumor growth and development of resistance to mKRAS inhibition. Hence, understanding the biology of mKRAS proteins that reveal a new mode of regulation of mKRAS function by the translation initiation factor eIF2B is necessary to design treatments with long-term anti-tumor effects. To date, the function of eIF2B has been linked to the synthesis of proteins with roles in the survival and adaptation of cells to stress (5).

The interaction between eIF2B subunits and mutant forms of KRAS 4B findings demonstrate a contributory role of eIF2B in the stimulation of MAPK signaling downstream of mutant KRAS (142, 156). The data further suggest that eIF2B is a guanine exchange factor (GEF) for mutant

KRAS. With the cell-free system experiment, the active form of the KRAS increased when treated with ISRIB.

Interestingly, Dr. Koromilas' lab data showed that the interaction between KRAS and eIF2B with SOS1 also increased simultaneously. That displays that eIF2B can act as GEF for mutant KRAS. EIF2B, KRAS, and SOS1 make a huge cluster complex and then interact with the RAF binding domain by GST-RAF1-Binding domain pull-down kit. These results show that eIF2B can act as GEF for mutant KRAS. EIF2B, KRAS, and SOS1 make huge complex clusters and interact with the RAF binding domain. So, utilizing computational structural analysis could assist in elucidating the interacting domains and residues involved in these protein interactions between eIF2B and mutant KRAS with SOS1.

1.6.2 Hypothesis

We hypothesize that eIF2B is a valid target to impair mutant KRAS function in tumours. Considering that mutant KRAS inactivation by a new generation of drugs leads to the development of resistance, understanding eIF2B function may help to design new approaches to:

- 1) Combat mutant KRAS function in cancers**
- 2) Defecting adaptation processes depending on the translational effects of eIF2B**

1.6.3 Specific aims

Aim 1: Understand the structural characteristics of the eIF2B/KRAS/SOS complex by computational analysis of existing structures of KRAS/SOS and eIF2B and assessing Clinical relation of mutant KRAS in patients Lung tumors with eIF2B subunits' mutations

Aim 2: Identify signalling pathways orchestrated by eIF2B specifically in mutant KRAS tumour cells by RNA-seq analysis of tumours with intact or impaired eIF2B

Aim 3: Develop strategies to impair eIF2B for the treatment of mutant KRAS cancers by Development of ISRIB PROTACS and its function on KRAS downstream

1.6.4 Study design

In 2020, KRAS-PROTACs developed as a druglike compound to targeting KRAS protein as a new therapeutic approach and affected KRAS to inhibit its downstream signaling pathways, so we decided to develop the PROTACs targeting eIF2B as it has potential interaction with mutant KRAS to inhibit downstream of KRAS and translational pathways simultaneously. Also, the ISRIB-modified compound based on the published paper in 2018 mentions when they modified the ISRIB and added a linker, which is also attached to fluorescein called FAM tagged ISRIB, treat cells with it, which is functional. We wondered whether the eIF2B as a potential target for modified ISRIB could be used with KRAS inhibitors in combination therapies.

Hence, innovative therapeutic approaches using ISR inhibitors like ISRIB may be valuable for treating one of the deadliest forms of mutant KRAS-driven cancer. ISRIB functions as a molecular glue by binding to the eIF2B protein in a deep binding pocket between beta and delta subunits that bridges the eIF2B tetramer-tetramer interface. The binding of ISRIB antagonizes the inhibition of eIF2B by phosphorylated Serine 51 eIF2 α in the eIF2B/p-eIF2 α complexes, as it facilitates the assembly of new eIF2B complexes in a conformation that is resistant to inhibition by p-eIF2 α (139).

Our research aims to develop strategies to impair eIF2B in wild-type and mutant KRAS cells to block its translation and regulation signaling by leveraging the proteolysis-targeting chimeras (PROTACs) technology. This study intends to investigate the mechanisms underlying eIF2B's cytoprotective function in tumor cells under stress. Additionally, we explored whether converting ISRIB from an inducer to an eIF2B complex destructor using the proteolysis-targeting chimeras (PROTACs) technology is a viable approach to impair mKRAS tumorigenesis. Therefore, utilizing modified ISRIB as ISRIB-PROTACs can suppress eIF2B by targeting it, suggesting anti-tumor effects in human LUAD cells as well.

Bond *et al.* investigated the targeting of mKRAS by developing LC-2 compound as the first PROTAC capable of degrading endogenous KRASG12C. The LC-2 compound includes a MRTX849 warhead (as POI ligand) covalently binds with KRASG12C as its target and recruits the E3 ligase VHL (E3 ligase ligand). This lead to rapid and sustained KRASG12C degradation, diminishing oncogenic KRAS levels and downstream signaling in cancer cells. The study

demonstrates the potential viability of PROTAC-mediated degradation in achieving this objective. The degradation of endogenous KRASG12C modulates ERK signaling in homozygous or heterozygous KRASG12C cell lines, and the attenuation of p-ERK occurs dose-dependently (150).

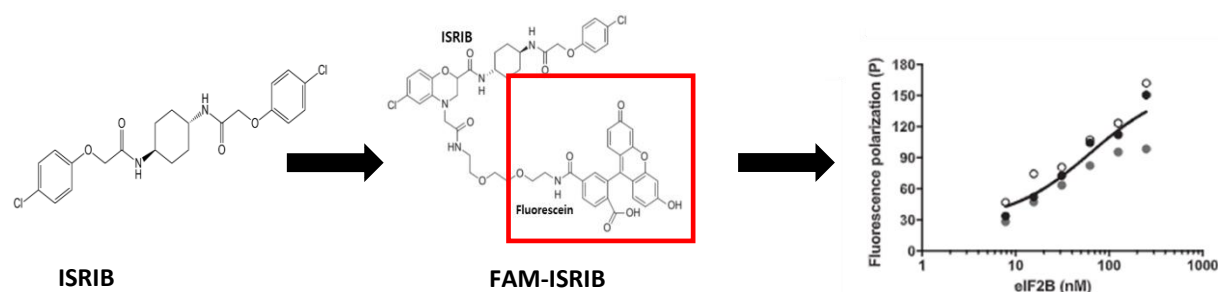


Figure 1.9 Plot of relative FP signal from samples of fluorescein-ISRIB interacted with purified hamster eIF2B. It shows that the FP signal from fluorescein-ISRIB is still functional even with some modification to its structure. Adapted from (139)

In-vitro experiments measuring the binding of the fluorescent derivative of ISRIB (FAM-labeled ISRIB) to eIF2B illustrate the binding of the small FAM-ISRIB has a similar marked increase in the fluorescence polarization signal. However, the challenge of the eIF2B-FAM-ISRIB complex with the p-eIF2 α displayed a concentration-dependent decrease in the fluorescence polarization signal at a steady state (Figure 1.9). These results revealed portions of ISRIB that can be chemically modified to create a FAM-ISRIB derivative that retains low nanomolar affinity for the eIF2B binding pocket and cooperative process consistent with an enhanced displacement of FAM-ISRIB when eIF2B is bound by two molecules of the p-eIF2 α and ISRIB, interaction on eIF2B did not change (139, 157).

To demonstrate the potential of a modified ISRIB-derivative to bind eIF2B complex while it is reported KRAS4b interacts with eIF2B δ through its C-terminal Hypervariable Region (HVR) with KRAS proteins. It suggests that KRas4b isoform may regulate protein translation initiation by interacting with eIF2B (146), can interact with KRAS4B isoform showed that a bifunctional derivative of ISRIB could be synthesized to bind eIF2B in complex with mKRAS to be utilized in treatment approaches.

Chapter 2

Material and Methods

All experimental protocols and procedures were performed in accordance with McGill University Regulations.

2.1 Computational Structural Biology analysis

2.1.1 Blind Protein-Protein Docking of existing structures of KRAS/SOS1 and eIF2B

To investigate the interactions between eIF2B and mutant KRAS in lung cancer, a computational structural modelling approach was employed, which can help to understand the associated biological processes, structure and function and reduce the number of further experiments. First, the available crystalized structures through the PDB database (<https://www.rcsb.org>) has been checked. The experimental data such as X-ray crystallography with higher resolution and lowest missing residues and atoms, including eIF2B Homo sapiens apo form (PDB ID:7L70)(130) and SOS1 in complex with KRAS (G12C)(PDB ID: 6EPL)(158) has been chosen. Even these experimental structures are not perfect and often contain errors, including issues like incorrectly fitted sidechains, flipped amides and imidazoles, incorrect sugar conformations, misoriented ligands, misidentified water molecules, and local errors in chain tracing.

The protein preparation by MolProbity (159) has been done to get structures with favorable thermodynamic parameters close to the biological situation. Structure optimization started by adding hydrogens that can improve the analysis's reliability. Most homology modeling programs do not include hydrogens because hydrogens are not observed (mostly) in X-ray crystallography experiments. Then, it flips hydrogen bonding to optimize them and make Electron clouds appropriate for the structure.

Then, the ClusPro (160) web tool used for the rigid-body blind docking method between these two structures was done, and 1000 low-energy results were output. So far, the most stable docked and top-ranked structures with the lowest energy scores predict the interaction between eIF2B-SOS1 and KRAS, which were more stable thermodynamically, were filtered. As a brief explanation, the way ClusPro works is to rotate the ligand (6EPL structure) with 70,000 rotations and 1000 rotation/translation combinations with the lowest score choice with a 9- angstrom C-alpha RMSD (Root Mean Square Deviation) radius. This means we find

the ligand (SOS1 bounded KRAS) position with the most "neighbors" in 9 angstroms of complex, and it becomes a cluster center, and its neighbors are the cluster members. Then, these are removed from the set, and a second cluster center is assessed.

Molecular graphics and analyses were performed with the Pymol software (161), which was developed by the Resource for Biocomputing, Visualization, and Informatics.

2.1.2 Assessing Clinical relation of mutant KRAS in patients Lung tumors with eIF2B subunits' mutations

To detect mutations within tumor samples, whole exome sequencing (WES) has traditionally been the preferred method for identifying somatic mutations.(162, 163)

The Genomic Data Commons (GDC) portal (<https://portal.gdc.cancer.gov>) offers access to the processed WES data typically utilized for gene expression measurement and the identification of transcript and splicing isoforms for the Cancer Genome Atlas Lung Adenocarcinoma (TCGA-LUAD) dataset. Nonetheless, it is possible to identify genomic variants from RNA-seq data (164), allowing for somatic mutation detection, with a particular focus on the mutational changes observed in RNA-seq.

This approach has gained prominence, especially in the context of emerging targeted therapies, primarily those targeting KRAS-related pathways. However, these therapies often encounter issues related to drug resistance (165), underscoring the importance of discovering new target genes.

Analyzing the complete set of TCGA database somatic mutation files comprising 567 patients of LUAD data has been done. In our investigation, we placed emphasis on the utilization of MuTect2 tool from GATK v4 (166), a sensitive and rapid tool widely employed for local assembly and realignment, particularly for the detection of single nucleotide variations (SNVs) and insert or deletion (indels).

Briefly, the utilized pipeline includes sample preprocessing, alignment to the human reference genome and somatic variant calling with variant annotation and aggregation. Variants recovered in Variant Call Format (VCF) files were used to annotate variants relative to RefSeq annotations. Finally, somatic mutations were utilized to compare the effects of

different mutations in the patient's tumor genome considering KRAS and eIF2B structure modifications for further analysis.

This approach emerging new targeted therapies (mostly targeting KRAS-related pathways) while unfortunately encountering problems of drug resistance, discovering new potential target genes of foremost importance.

2.2 Cell culture and impairing eIF2B

2.2.1 Cell culture

The NSCLC cell line, H358 with heterozygous missense KRAS mutation at codon 12 (G12C or Gly to Cys) were cultured in Roswell Park Memorial Institute (RPMI) 1640 Medium (Wisent) and human colon cancer cell line HCT-116 containing a mutated KRAS at codon 13 (G13D or Gly to Asp) and its KRAS-disrupted subclones, HK2-8 (isogenic of HCT116 cell line), with wildtype KRAS were maintained in Dulbecco's Modified Eagle Medium (DMEM) (Wisent). Both mediums were supplemented with 10% fetal bovine serum (FBS, Wisent) and 1% antibiotics (penicillin/streptomycin, 100 units/mL; Life Technologies). All cell lines were cultured at 37 °C with 5% CO₂.

2.2.2 Knocking down eIF2B5 by shRNA

H358 cells were engineered to down regulated eIF2B5 (epsilon) by Human eIF2B5 shRNAs (listed in Table 2.1) by infection with pLKO.1 lentiviruses and selection at 2.5 µg/mL puromycin. The functionality efficiency of eIF2B5 cDNAs was determined by western blot for three biological replicates.

2.2.3 Knocking down eIF2B5 by si-RNA

Downregulation of Human eIF2B5 (epsilon subunit) was performed by treatments with a mix of 4 siRNAs (Dharmacon) as Human siGeNOME SMARTpool containing the sequences listed in Table 1 in H358, HCT116 and HK2-8 cell lines.

6*10⁵ cells were seeded in 60mm plate. Next day, lipid-based transfection was performed on cells using Lipofectamine™ RNAiMAX Transfection Reagent (Catalog number: 13778075). 24 hours after transfection, targeted cells were seeded for either protein or RNA extraction. The extraction has been done in four biological replicates.

Table 2.1. Sequences of shRNA and siRNA of the corresponding target genes

Application	Target Gene	Sequence	ID
shRNA	Empty vector	-	pLKO_TRC001
	eIF2B5	5'-CCGG-CCAAAGAGATACAACTGACAA-CTCGAG-TTGTCAGTTGTATCTCTTTGG-TTTTGG-3'	shRNA TRCN0000083989
siRNA	eIF2B5	5'-GCAUGAAGCUCUUGGUAAUU-3'	siGENOME Human EIF2B5 siRNA-SMARTpool (D-012625-01)
		5'-GCACGUAACAGCUAAGGAA-3'	siGENOME Human EIF2B5 siRNA-SMARTpool (D-012625-03)
		5'-UCUCAAUGUGGUUCGAAUA-3'	siGENOME Human EIF2B5 siRNA-SMARTpool (D-012625-17)
		5'-CGACCAUUUGGAAGCGUUA-3'	siGENOME Human EIF2B5 siRNA-SMARTpool (D-012625-18)
	Control	5'-UAGCGACUAAACACAUCAA-3'	siGENOME non-targeting siRNA Pool (D-001206-13-20)
		5'-UAAGGCUAUGAAGAGAUAC-3'	
		5'-AUGUAUUGGCCUGUAUUAG-3'	
		5'-AUGAACGUGAAUUGCUCAA-3'	

2.3 RNA-seq data analysis

Total RNA of eIF2B5 sh-RNA and si-RNA in H358, HCT116 and HK2-8 with control (empty PLKO.1 vector and non-targeting siRNA, respectively) (all replicates) was isolated with Qiazol buffer and then RNA was extracted by miRNeasy Micro Kit (Qiagen, 217004) based on the manufacturer protocol. The quality and integrity of RNA assessed by Bioanalyzer 2100 (Agilent). RNA-seq libraries was prepared by Genome Québec (Montreal, Canada) using polyA-enriched RNA (Illumina mRNA TruSeq) protocols. The sequencing of samples was prepared at a depth of >25 million using paired-end mode (PE100) reads on an Illumina Novaseq 6000 instrument. Before analysis, the raw paired reads with FASTQ format were used for quality control by MultiQC and Trimmomatic tool to cut Adaptor and low-Quality bases.

Adapter sequences include 5'-TCGTCGGCAGCGTCAGATGTGTATAAGAGACAG-3' for read 1 and 5'-GTCTCGTGGGCTCGGAGATGTGTATAAGAGACAG-3' for read 2.

HISAT2 (167)(a fast and sensitive spliced alignment program) utilized to align RNA-Seq data mapped to Human (homo sapiens-hg19) as the reference genome

We used FeatureCounts (168), to extract the quantification of transcript level expression and store sequencing data as BAM file for further analysis.

An expression matrix was generated after normalization, and statistical methods were used to identify differentially expressed genes (DEGs) by DESeq2 (169) and edgeR packages (170) in R to perform this task. All condition types were compared in a pairwise manner with all other conditions to test for any genes that were differentially expressed.

Differentially expressed genes (DEGs) calculated and visualized as PCA and heatmap by the ggplot2 package (171).

The DEGs data for each cell line with FDR less than 0.05 and $|\log FC| > 0.58$ shows that overexpressed genes and downregulated genes.

For further functional analysis, clusterProfiler (172) and Genekitr (173) packages in R software were utilized to conduct KEGG and GO enrichment analysis. For pathway analysis, p-

value<0.05 considered for the significant gene functionals, and the results were visualized using the “ggplot2” and “GOplot” packages in R, as well.

For survival plots, Gepia2 (174) and kmplotter (www.kmplot.com) web-based tools used for Overall Survival estimation by utilizing median to define the border of High and Low groups. 95% confidence interval was set for analysis.

2.3.1 Data analysis for common genes in mKRAS cell lines

The significant DEGs in Knocked-down eIF2B5 cells were screened by the Venn diagram (175) for shared genes between different cell lines (H358, HCT116 and HK2-8). Dysregulated genes based on the given criteria ($|\log_2FC| \geq 0.58$ and adjusted p-value <0.05) illustrated the overlapped up and down-regulated genes by eIF2B in KRAS mutant cells, respectively.

2.4 Develop strategies to impair eIF2B for the treatment of mutant KRAS cancers

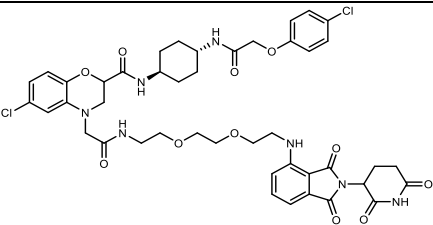
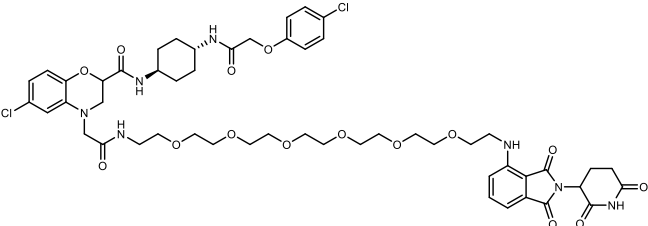
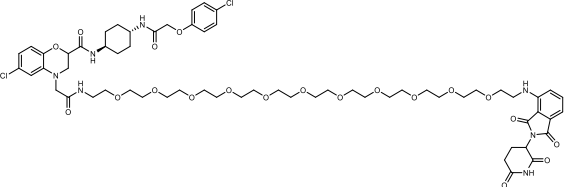
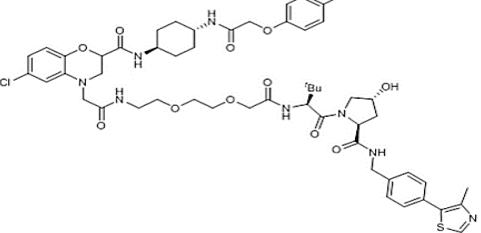
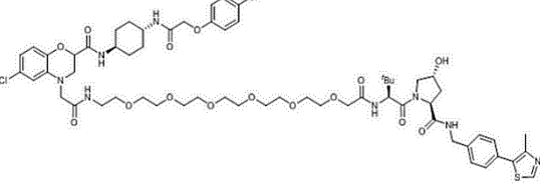
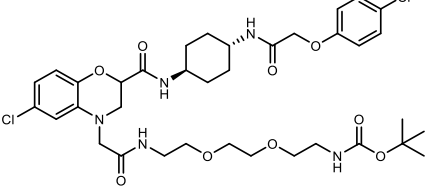
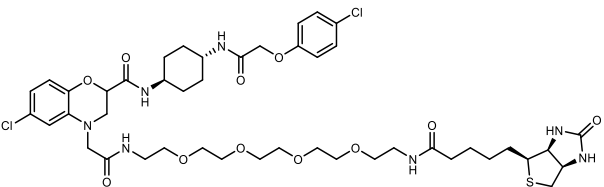
To target eIF2B, we decided to use ISRIB, which can interact with eIF2B and is the activator of it. So, Girardini and Zyryanova *et al.* published papers that mention when they modified the ISRIB and added a linker attached to fluorescein (called FAM tagged ISRIB) and treated cells with it. The compound can interact with eIF2B and increase fluorescence. (139, 176)

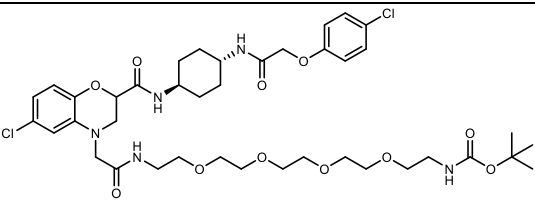
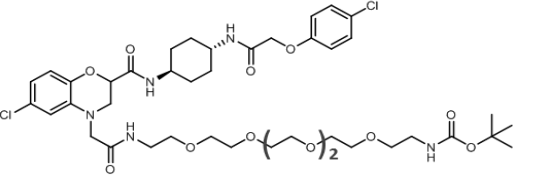
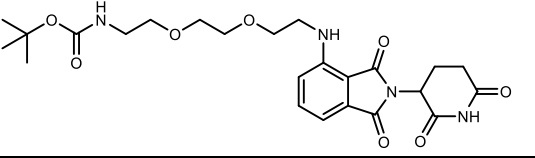
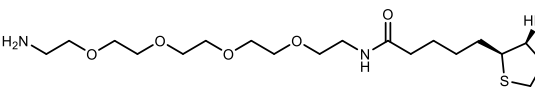
Our collaborator, Dr. Jean-Philip Lumb at the Chemistry Department at McGill University, synthesized ISRIB-PROTACs, which include ISRIB attached to an E3 ligase ligand with variable length linker that includes Cereblon and VHL. They can act as E3 ligands and interact with E3 ligase and E2 ligase to Eubiquitinate the eIF2B and be degraded by proteasome specifically.

2.4.1 Developing ISRIB-PROTACs Structures

The synthesized compounds of ISRIB-PROTACs are illustrated in Table 2.2. We used Synthesized ISRIB-PROTAC with different PEG (polyethylene glycol) units and E3 ligase ligands, including CRBN and VHL. These PROTAC molecules include different lengths (carbon chains or polyethylene glycol (PEG) chains) to give derivatives for linkers in ISRIB-PROTACs structure to evaluate sufficient length to escape the immediate steric interaction of eIF2B complex and cell permeability.

Table 2.2. Summary of the chemical structures and properties of ISRIB-PROTACs.

ID	Structure	E3 ligase ligand	Linker length (# PEG unit)	Type of compound	Chemical Formula and Molecular weight
ISRIB-CRBN-PEG2		CRBN	2	ISRIB-PROTAC	C44H49Cl2N7O11 (922.81 gr/mol)
ISRIB-CRBN-PEG6		CRBN	6	ISRIB-PROTAC	C52H65Cl2N7O15 (1099.03 gr/mol)
ISRIB-CRBN-PEG11		CRBN	11	ISRIB-PROTAC	C62H85Cl2N7O20 (1319.29 gr/mol)
ISRIB-VHL-PEG2		VHL	2	ISRIB-PROTAC	C53H66Cl2N8O11S (1094.12 gr/mol)
ISRIB-VHL-PEG6		VHL	6	ISRIB-PROTAC	C61H82Cl2N8O15S (1270.33 gr/mol)
ISRIB-PEG2		-	2	Control	C36H49Cl2N5O9 (766.71 gr/mol)
ISRIB-PEG4-Biotin		-	4	Pull-Down	C45H63Cl2N7O11S (981 gr/mol)

ISRIB-PEG4		-	4	Control	C40H57Cl2N5O11 (854.82 gr/mol)
ISRIB-PEG6		-	6	Control	C44H65Cl2N5O13 (942.93 gr/mol)
CRBN-PEG2		CRBN	2	Control	C24H32N4O8 (504.54 gr/mol)
Biotin-PEG4		-	4	Pull-Down Control	C20H38N4O6S (462.61 gr/mol)

Furthermore, the control compounds, including ISRIB bonded to the linker and CRBN bonded to linker, were utilized to check the efficiency of PROTAC compounds.

To evaluate other interacted proteins with eIF2B, we also developed a PROTAC molecule with a similar linker length (PEG4) incorporated with Biotin. Through Pull Down Assay with streptavidin beads, we can capture biotinylated eIF2B and co-associated proteins.

The experiment was done with control compounds in vitro by utilizing KRAS wildtype and mutant cell lines.

2.4.2 Evaluation of ISRIB-PROTACs function in cell culture

To detect degradation targets and evaluate the efficiency of the mentioned compounds' function, Human embryonic kidney 293T (HEK293T) and H358 cells were plated at a density of 6×10^5 per 60mm plate. Cells were treated with different concentrations of ISRIB-PROTAC compounds mentioned in Table 2.2, covering ISRIB-CRBN and ISRIB-VHL with different linker lengths (from 2 to 11 PEGs) with controls including DMSO, ISRIB-linker, CRBN-linker, Thapsigargin (Sigma- Aldrich, cat number T9033), and ISRIB (Selleck Chemical, cat number S0706) in cell culture and incubated for different time points with fixed concentration as well.

It should be noted that based on The Human Protein Atlas database (<https://www.proteinatlas.org/>), H358 cells have unusually low ATF4 and CRBN protein, 10% and 80% less than HEK293T cell lines with wildtype KRAS, respectively, so we used HEK293T cells for ISRIB-CRBN-PEG2 as 1st generation compound, and it helps us to detect the lowest activity of ISRIB-PROTACs via impairing eIF2B and triggering ISR through up-regulation of ATF4 and eIF2B subunits in protein level compared to H358 cell lines.

A density of 6×10^5 cells were seeded in 60mm plates, incubated for 24 h to reach the desired confluency (70-80%), and then treated with DMSO (as control) or the specified concentration of a test compound.

2.5 Immunoblotting (western blot)

The cells were subjected to an ice-cold phosphate-buffered saline (PBS) wash followed by direct lysis in ice-cold 1X modified Radioimmunoprecipitation Assay (RIPA) lysis buffer containing phosphatase inhibitors. The lysis buffer comprised of 10 mM Tris-HCl (pH 7.5), 50 mM KCl, 2 mM MgCl₂, 1% Triton X-100, 3 µg/ml aprotinin, 1 µg/ml pepstatin, 1 µg/ml leupeptin, 1 mM dithiothreitol (DTT), 0.2 mM Sodium Vanadate (Na₃VO₄), 0.01 µM Okadaic acid, 10 mM Sodium Fluoride (NaF), 2mM Tetra Sodium pyrophosphate, 2mM beta-glycerophosphate, and 1 mM phenylmethylsulfonyl fluoride. The lysate was scraped and transferred to a 1.5 ml microtube using a cell scraper or silicone spatula, followed by incubation on ice for 15 minutes. The lysate was then centrifuged at $16,000 \times g$ for 15 min (4 °C), and supernatants were stored at -80 °C. Protein quantification was performed using the Bradford assay (Bio-Rad protein assay dye reagent, cat number 5000006). The expression of various proteins was analyzed by loading 30 µg of protein extracts from the same set of samples in 1X SDS sample buffer, boiling for 5 min, and running in parallel on two identical 12% sodium dodecyl sulfate (SDS)-polyacrylamide gels. The proteins were then transferred to a polyvinylidene fluoride membrane (Millipore, Ireland), blocked with 5% skim milk for two hours and washed with TBST three times (each for 10 minutes). The two identical blots were cut into smaller pieces based on the size of proteins to be incubated with primary antibodies overnight at 4 °C. After washing with TBST and incubating with the secondary antibodies for 1 h at room temperature, the bands were visualized using enhanced chemiluminescence (ECL)

as per the manufacturer's specification (Thermo Fisher Scientific, cat number 1859701). One piece of the blot was probed for proteins of interest, while the other identical piece was used for the corresponding total and reference protein as an internal control. The antibodies used for immunoblotting are listed in Table 2.3. Band quantification within the linear exposure range was performed using the ImageJ 1.51e software (NIH, Maryland, USA).

Table 2.3 List of antibodies used in the study.

Antibody	Species	Company	Cat number	Dilution Ratio in WB
eIF2B1 (alpha)	Rabbit	Proteintech	18010-1-AP	1:1000
eIF2B2 (beta)	Rabbit	Proteintech	11034-1-AP	1:1000
eIF2B3 (gamma)	Mouse	Santa Cruz Biotechnology	Sc-9980	1:1000
eIF2B4 (delta)	Rabbit	Proteintech	11332-1-AP	1:1000
eIF2B5 (epsilon)	Rabbit	Cell Signaling	3595S	1:1000
SOS1	Rabbit	Cell Signaling	12409S	1:1000
SOS2	Rabbit	abcam	ab154999	1:1000
Tubulin	Mouse	Cell Signaling	3873S	1:1000
ERK1/2-P	Rabbit	Cell Signaling	4370S	1:1000
ERK1/2-total	Rabbit	Cell Signaling	9102S	1:1000
MEK1/2-P	Rabbit	Cell Signaling	9154S	1:1000
MEK1/2-total	Rabbit	Cell Signaling	8727S	1:1000
ATF4	Rabbit	Cell Signaling	11815S	1:1000
KRAS	Mouse	Abnova	H00003845-M01	1:1000
Mouse IgG-horserdish peroxidase-conjugated	Goat	KPL	474-1806	1:2000
Rabbit IgG-horserdish peroxidase-conjugated	Goat	Jackson immunoResearch	111-035-144	1:1000

2.6 Statistical analysis of patient data

For patient data, statistical analysis was performed using Rstudio in Ubuntu (v22.04).

Patient survival was visualized by Kaplan-Meier plots and significance assessed by a log-rank test and Cox Proportional regression for univariate survival models. The associations between patient survival and eIF2B subunits were examined using overall, cancer-specific, and recurrence-free survival endpoints. All experimental data were expressed as means \pm S.D. To establish significance, data were subjected to unpaired student's t-tests or one-way ANOVA followed by the Tukey's multiple comparison test using the GraphPad Prism software

statistical package 7 (GraphPad Software version 7.03). The criterion for significance was set at $p < 0.05$.

Chapter 3

Results

3.1 KRAS(G12C) bonded SOS1-eIF2B Protein Interaction evaluation via Blind docking

Docking methods are used in several stages during the design of protein-protein interaction inhibitors. Even before docking methods are applied to find the interface residues, the first question is how and through which domains the two proteins of interest interact with one another. To assess proteins to interact with each other, their respective binding sites must be in direct physical contact, either in a stable or transient mode. These binding sites with three-dimensional structures formed by sets of amino acid residues directly responsible for the recognition of binding partners. Deleterious or beneficial mutations occur, especially on interfaces, affecting binding affinity due to impairment or improvement of protein electrostatic and structural properties (177).

Most proteins are composed of multiple domains that have specific biological functions. Protein-Protein Interactions can be better understood when they are seen from the level of Domains interactions (178, 179).

Conversely, proteins with multiple interfaces tend to establish simultaneous interactions with multiple domains. Such proteins are likely to arrange themselves via stable Domain's interactions (180).

Figure 3.1 presents the top three models using the ClusPro balanced coefficient set score. Based on these scores the lowest energy structures illustrated the stability of structures' interaction displayed in table 3.1. For each cluster, the table shows the member (i.e., the number of docked residues in structures), the energy of the cluster center (i.e., the system that has the highest number of neighbor structures in the cluster), and the energy of the structure in the cluster with the lowest energy.

The atomic models of interacted subunits of two docked structures were visualized (Figure 3.1) and model 0 (the most stable model) shows the interaction between SOS1 and eIF2B gamma and epsilon subunits (Fig 3.1-A). Model 1 (the next stable model) illustrates the interaction between alpha and beta subunits of eIF2B with SOS1 (Fig 3.1 –B). Model 7 (last top stable model) includes interaction between SOS1 and KRAS interaction simultaneously with alpha, gamma, and delta subunits (Fig 3.1 C). These predicted models would help us

determine which domains and residues are most critical for the interaction between these structures, impairing them in IP experiments and enhancing the inhibitors effect to target these structures specifically and overcome drug resistance in lung cancer.

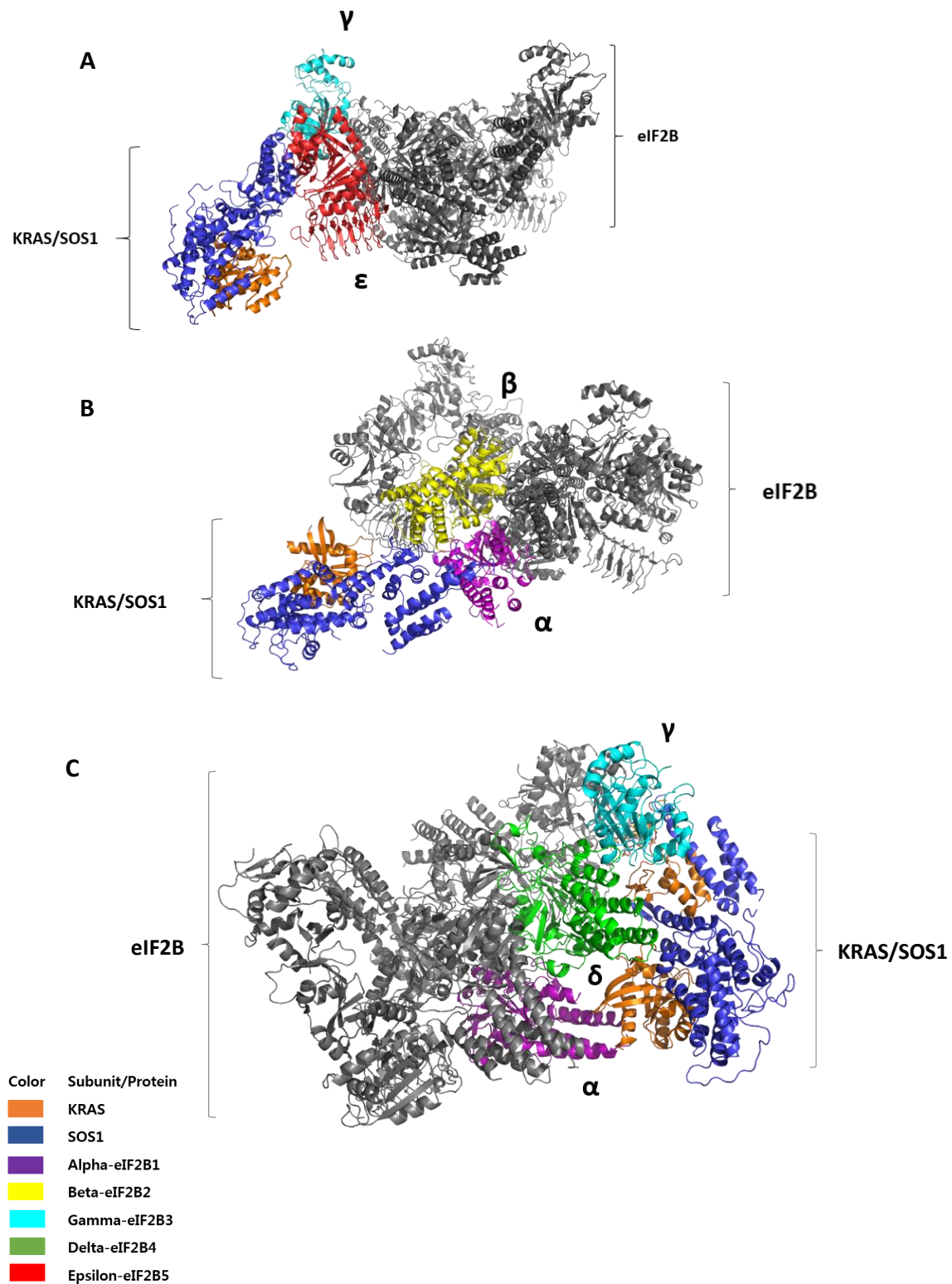


Figure 3.1. 3D ribbons representation for the crystal structure of protein complexes 7L70 and 6EPL, along with the predicted domain interactions. Three top structures predicted by ClusPro of eIF2B is in gray and predicted interacted domains and subunits are colorful based on legend. All 3D crystal structures of top models follow the same color illustration.(A) model 0, (B) model 1 and (C) model 7.

Table 3.1. Model scores for the balanced coefficient set when docking the eIF2B to SOS1 interacted with KRAS G12C.

Model ID	Member	Balanced		Electrostatic Favored		Hydrophobic favored		VdW/Electrostatic	
		Center	Lowest Energy	Center	Lowest Energy	Center	Lowest Energy	Center	Lowest Energy
0	316	-936.7	-1001.1	-1308.8	-1419.7	-936.7	-1001.1	-427.6	-482.7
1	236	-931.1	-986.6	-1285.9	-1374.3	-931.1	-936.6	-449.3	-481.6
7	14	-943	-943	-	-	-943	-943	-	-

Due to the mode of interaction and number of interface residues, changes in the residues are likely to impair some interactions with specific partners. Interestingly, most proteins interfering with cell signaling and regulatory pathways perform dynamic interactions with the proteins, leading to severe changes in cellular metabolism. Compared to stable (domain–domain) interactions, dynamic interactions are under-represented in Protein-Protein Interaction databases due to limitations in utilized methods to obtain protein–protein interaction data; so, assessing any changes in interface residues and their impact on these interactions is an asset.

3.2 eIF2B somatic mutations in LUAD patients

Our data analysis result among 567 TCGA lung adenocarcinoma patients' tumor samples illustrated that 151 samples carry KRAS mutation (~26.5%). Also, eighteen samples bear mutations in eIF2B subunits.

Out of all the samples with KRAS mutant, 6 samples carry at least one mutation in eIF2B subunits with amino acid change and missense variants (~4 %).

Interestingly, all the eIF2B mutations correlate with KRAS G12 missense variants (G12C, G12D and G12V) when KRAS G12 missense variants include 111 samples out of 151 samples of

mutant KRAS. The frequency of eIF2B mutations in G12 variants is 6.3% in TCGA Lung Adenocarcinoma (LUAD) patients which include eIF2B α (K35N), eIF2B γ (A413S) or eIF2B δ (S139L, R306L) (Table 3.2).

Table 3.2. Somatic mutation in eIF2B subunits in mutant KRAS LUAD patients in TCGA.

Sample_ID	Gene	Ref allele	Alt allele	Amino_Acid Change	Effect	Gene	Ref allele	Alt allele	Amino_Acid Change	Effect
TCGA-44-7671-01A	EIF2B3	C	A	p.A413S	missense_variant	KRAS	C	A	p.G12C	missense_variant
TCGA-69-7978-01A	EIF2B2	C	T	-	5_prime_UTR_variant	KRAS	C	A	p.G12C	missense_variant
TCGA-05-4249-01A	EIF2B4	C	A	p.R306L	missense_variant	KRAS	C	A	p.G12C	missense_variant
TCGA-55-8097-01A	EIF2B4	T	G	-	intron_variant	KRAS	C	A	p.G12C	missense_variant
TCGA-44-A47A-01A	EIF2B1	C	G	p.K35N	missense_variant	KRAS	C	T	p.G12D	missense_variant
TCGA-17-2022-01A	EIF2B3	A	G	-	3_prime_UTR_variant	KRAS	C	A	p.G12C	missense_variant
	EIF2B4	G	A	p.S139L	missense_variant; splice_region_variant					

These somatic mutations in Lung tumors with KRAS G12 mutation are synchronized with the interacted subunits of eIF2B protein in Model 7 docking structures with KRAS and SOS1 structures (Figure 3.2). These results confirm the possibility of balanced and stable interaction of these structures in KRAS G12 mutant tumors at the clinical level.

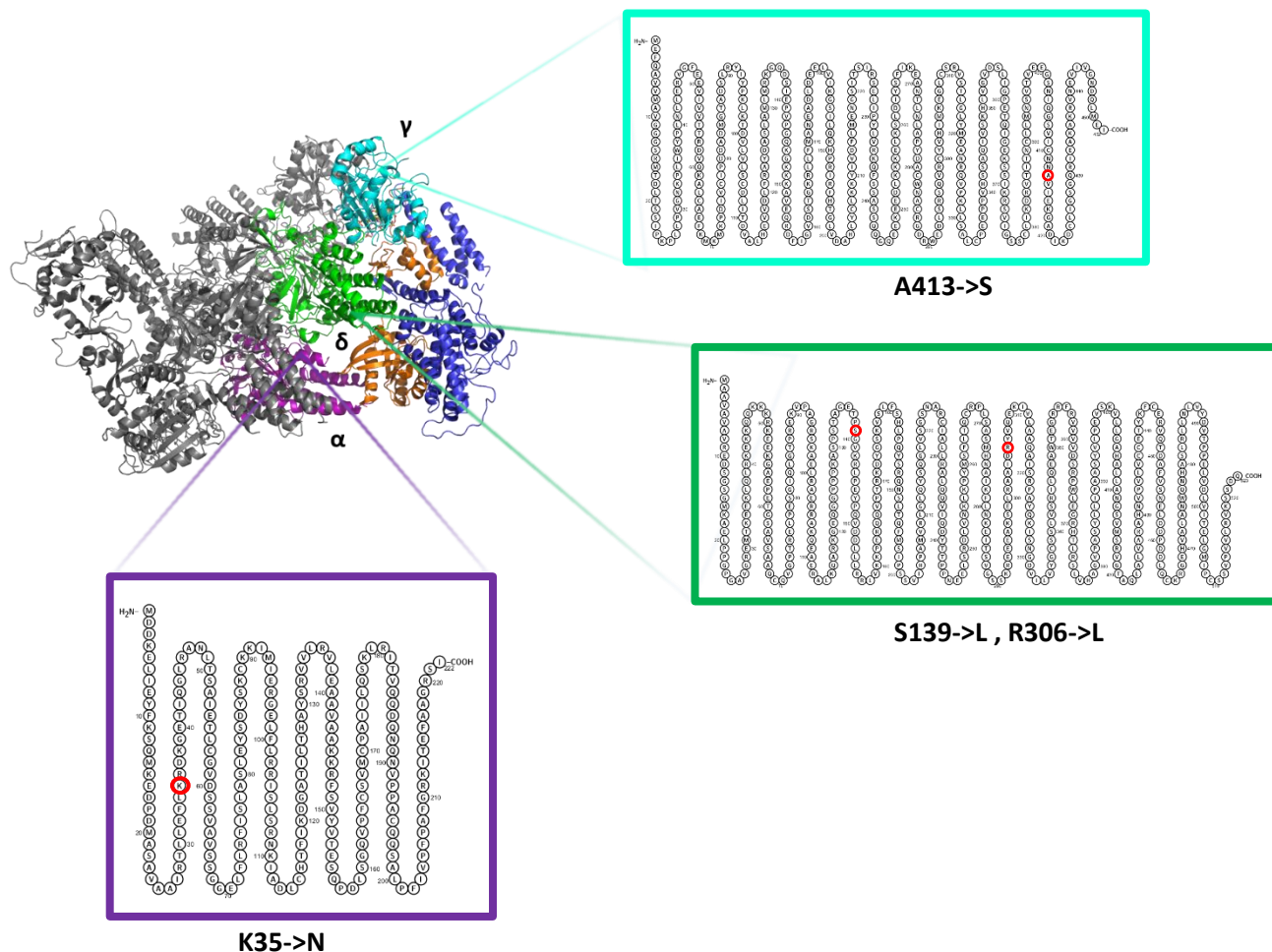


Figure 3.2. Ribbons representation of the eIF2B (PDB ID: 7L70) interacted with SOS1-KRAS G12C (PDB ID: 6EPL) complex based on model 7 in docking analysis highlighting interacted-subunits. The eIF2B α , eIF2B γ and eIF2B δ subunits are colored purple, turquoise and green, respectively. The amino acid sequences for each subunit are represented in boxes. The missense mutations for each subunit existing in KRAS G12 mutant lung tumors are shown in red circles.

3.3 Identify signaling pathways orchestrated by eIF2B specifically in mutant KRAS tumor cells

Our research focused on investigating the impact of eIF2B5 knockdown on cellular signaling pathways. We were able to validate successful knockdown in colon and lung tumor cell lines and noted substantial changes in the downstream protein expression through western blotting. These changes were consistently observed in mentioned cell lines, suggesting a uniform involvement of eIF2B5 in the regulation of cellular signaling pathways .

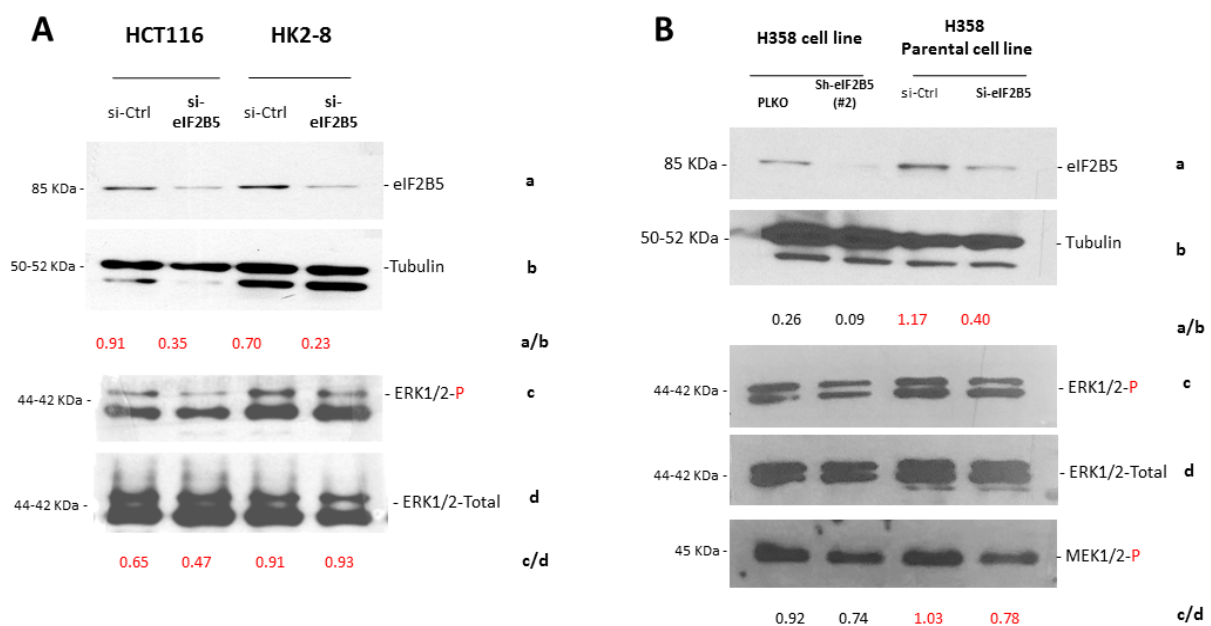


Figure 3.3 Estimation of eIF2B5 knockdown efficiency and MAPK pathway regulation in protein level. The knockdown of eIF2B5 has been verified by western blotting in colon (A) and lung (B) tumor cell lines and samples' RNA have been extracted and sent out for bulk RNA sequencing. The mutant KRAS cells HCT116 with G13D and H358 with G12C mutations in KRAS displayed the role of eIF2B in phosphorylation of ERK and MEK regulation in MAPK pathway.

Further, the previous experiments in our lab showed that genetic inactivation (knocking down) of eIF2B epsilon subunit by siRNA in lung adenocarcinoma cell line with G12C KRAS mutation (H358 parental cell line) and the knock-down of eIF2Bε in H358 led to lower expression of p-ERK in western blot (WB), and also provide solid evidence that eIF2B

stimulates the KRAS signaling in KRAS mutant cells when compare colorectal adenocarcinoma cell line with G13D KRAS mutation (HCT116) to its isogenic cells with wild type KRAS (HK2-8 cell line) (Figure 3.3). Also, eIF2B5 shRNA H358 cell lines (Knock-down), strongly decreased phosphorylation and activation of KRAS downstream signaling compared to H358 cells were infected with lentivirus expressing Scrambled (PLKO).

To uncover the role of eIF2B in mutant KRAS tumors, we compared the p-ERK expression between isogenic mutant and wild-type KRAS human colorectal cell lines (Figure 3.3-A) and p-MEK in lung cancer cells via immunoblotting (Figure 3.3-B). Indeed, p-ERK was downregulated in cells having mutant KRAS G12C after knocking down eIF2B5 (HCT116 and H358) compared to a colon cancer cell line with wild-type KRAS (HK2-8) (Figure 3.3).

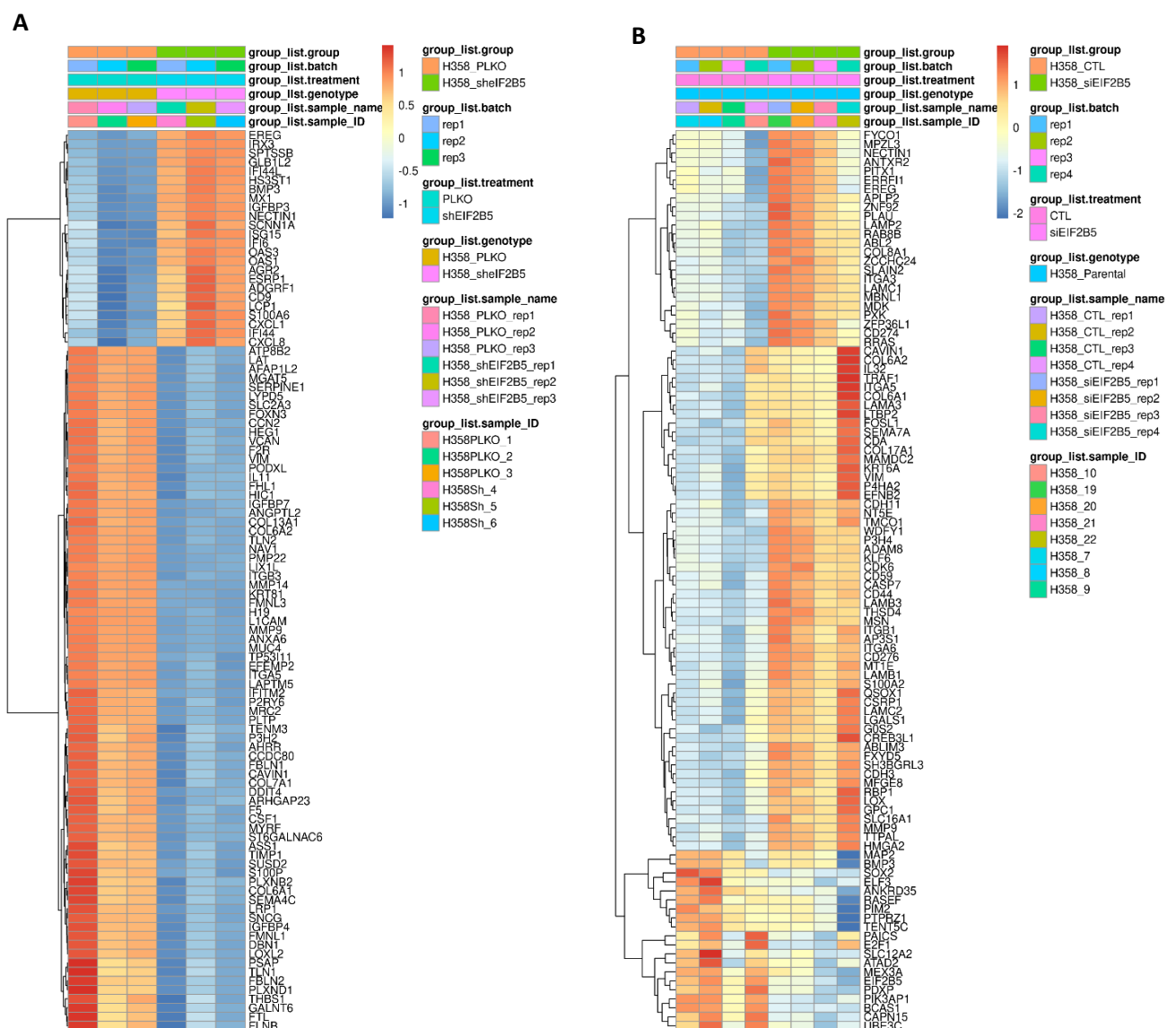
Together, these results suggest that eIF2B has a role in MAPK signaling pathway regulation in tumor cells in terms of effect on tumor progression and proliferation in mutant KRAS cells compared with wild-type KRAS cells (Figure 3.3). This is the case with cells that express mutant KRAS G13D compared to their isogenic wild-type KRAS counterparts.

To examine the effects of knocking down of eIF2B on transcriptional changes in 4 model cells, we selected eIF2B5 knocking down cells with 60% efficiency that was associated with minimal effects on cell death and physiology by western blot, and the cells were subjected to RNA-seq analysis. Knocking down eIF2B5 impairs the GEF activity of eIF2B complex that is required for TC to start translational initiation, as a result of defecting this GEF activity, ISR triggered in the cell. For this purpose, total RNA was extracted, and libraries for mRNA-sequencing were constructed from two independent intact and impaired eIF2B5 groups.

3.3.1 Analysis of gene expression as a result of eIF2B function in mutant KRAS cells

A study conducted in 2018 by Vihervaara and colleagues highlighted that the Integrated Stress Response (ISR) triggers rapid and comprehensive reprogramming of transcription at both genes and enhancer regions. Comprehensive genome-wide assessments, which monitor RNA polymerase II (Pol II) engaged in transcription at the nucleotide level, have provided valuable insights into the underlying molecular mechanisms governing transcriptional responses to stress. While eIF2B primarily operates at the translational level, it is important to note that

mRNA translation is often closely linked to transcriptional reprogramming due to the regulated synthesis of transcription factors (181). Therefore, we hypothesized that analyzing changes in gene expression through RNA-seq could serve as an appropriate initial approach to elucidate the observable phenotypic characteristics in cells affected by eIF2B impairment. To further expand the scope of our investigation, we performed whole transcriptome analysis [Bulk RNA sequencing (RNA-seq)] on four different cell line models mentioned in material and methods section 2.1 in all biological replicates. Results validated the transcriptional induction of impairing eIF2B dysregulates several genes.



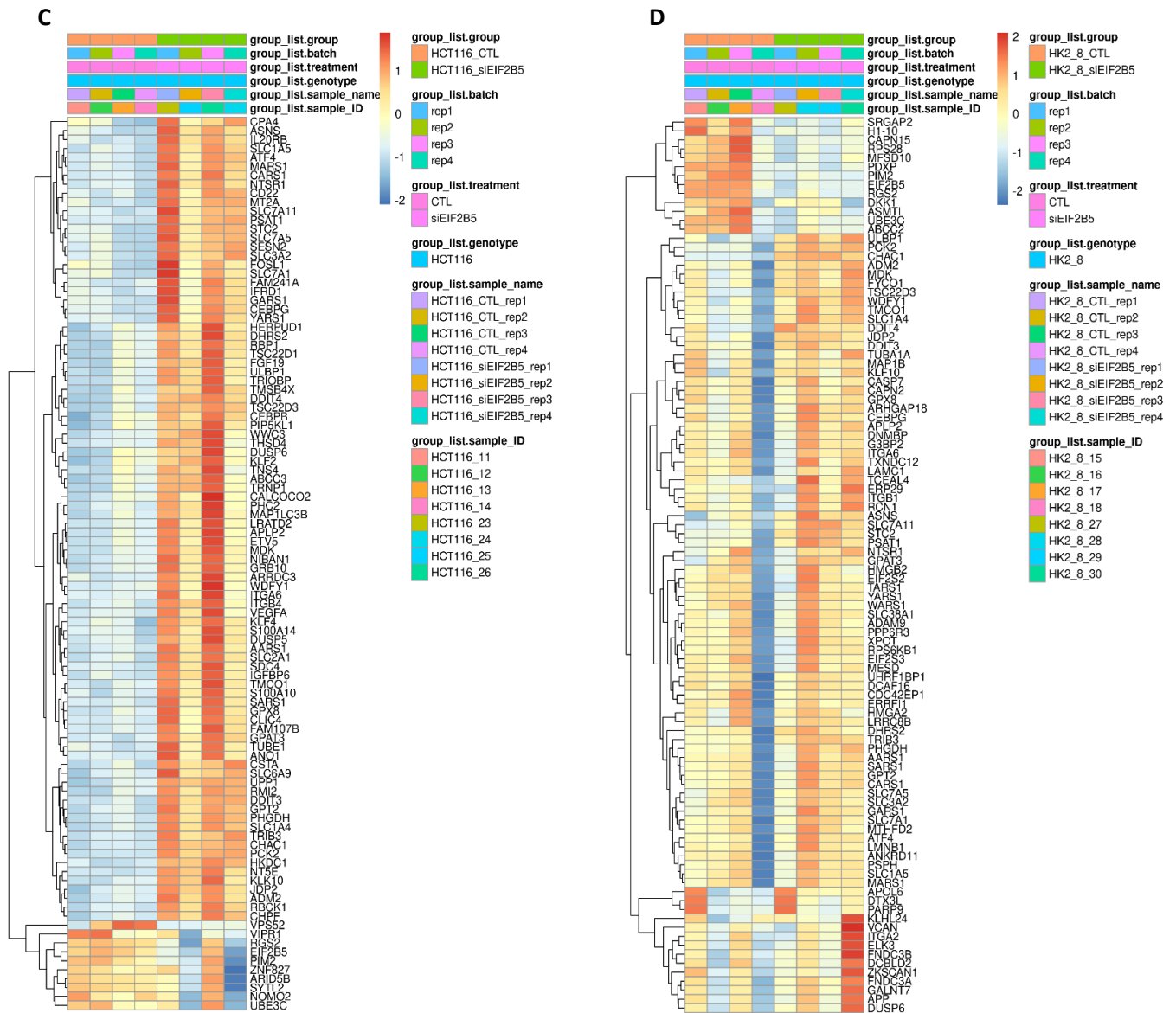


Figure 3.4 eIF2B regulates important genes involved in tumorigenesis in mutant and wildtype KRAS lung and colorectal tumors as revealed by RNA-seq analysis of knocked-down eIF2B genes. Heatmap plots showing the top 50 dysregulated genes in mRNA expression between intact and impaired eIF2B groups in H358 cell line treated with shRNA-eIF2B5 (A), H358 cells treated with siRNA-eIF2B5 (B), HCT116 (C) and HK2-8 (D) cells treated with siRNA-eIF2B5, respectively. (The given criteria are $|\log_2FC| \geq 0.58$ and adjusted p-value < 0.05)

After filtering and analyzing the RNA-seq data, a differentially expressed genes (DEGs) list of transcripts for each cell group was obtained. To test congruency among biological replicates,

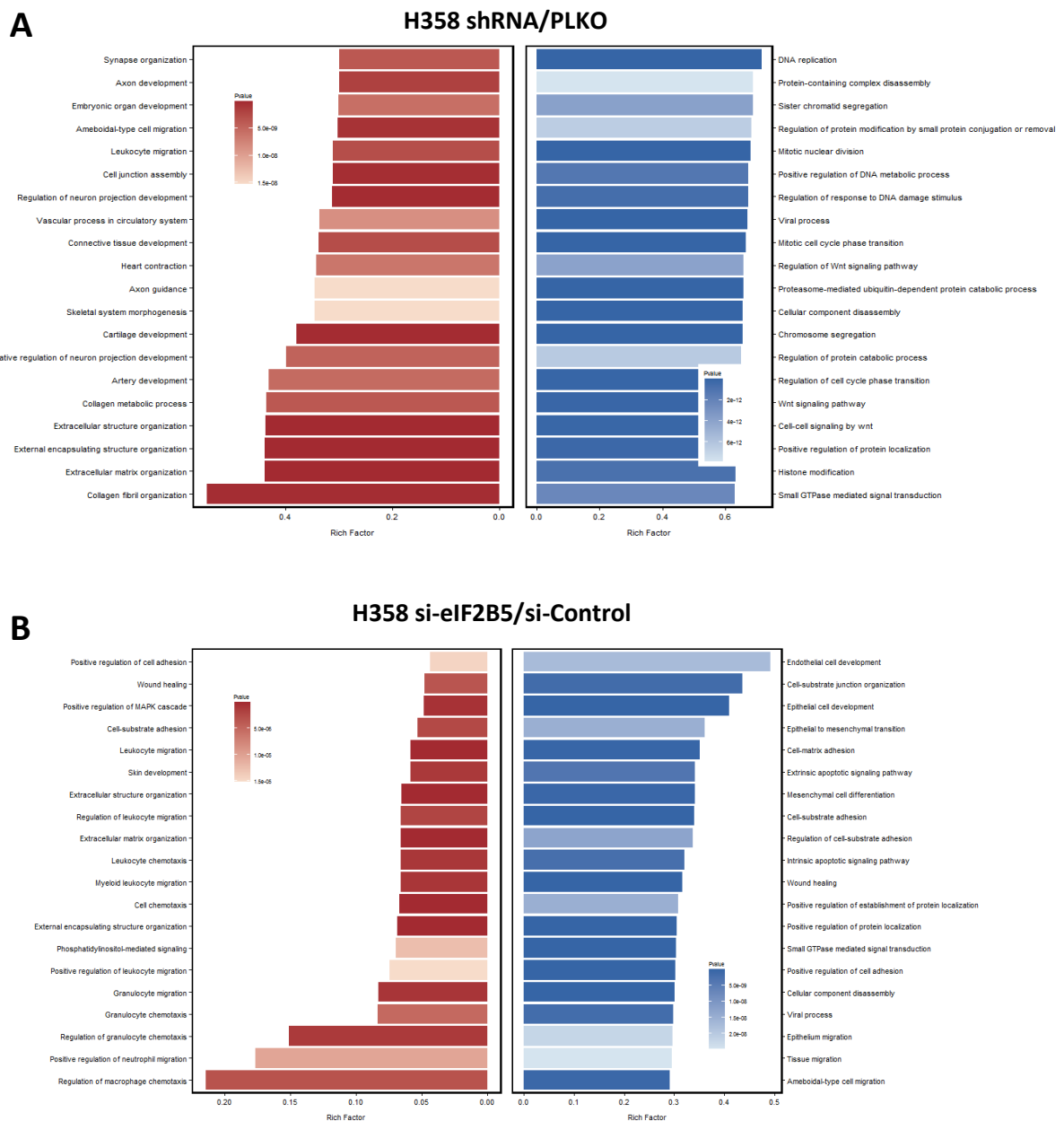
the principal component analysis (PCA) using DESeq revealed that impaired eIF2B accounted for the largest variance among test and control groups in each model generated using the RNA-seq platform. The cluster between the biological replicates of each experimental group was shown together, confirming high reproducibility between each replicate (Figure supplementary S1). Application of DESeq with a conservative approach to the RNA-seq data obtained from the impaired eIF2B versus control cells identified 4991, 392, 85, and 23 differentially expressed genes (DEGs) for H358 shRNA treated, H358 siRNA treated, HCT116 siRNA treated, and HK2-8 siRNA treated to knock down eIF2B5, respectively. (utilized criteria is $|\log_2FC| > 0.58$, $p\text{-value} \leq 0.05$).

Downregulated genes for H358 shRNA treated, H358 siRNA treated, HCT116 siRNA treated, and HK2-8 siRNA treated to knock down eIF2B5, were 3167, 182, 27 and 6 respectively, when upregulated genes for H358 shRNA treated, H358 siRNA treated, HCT116 siRNA treated, and HK2-8 siRNA treated to knock down eIF2B5, were 1824, 210, 58 and 17 in order (utilized criteria is $|\log_2FC| > 0.58$, $p\text{-value} \leq 0.05$).

To identify the expression pattern of mRNAs during eIF2B knock-down in each cell group, heat maps were constructed to profile the top 50 transcriptome differences. The heat maps for KRAS mutant cell lines showed a decisive shift in the knocked-down eIF2B with control transcriptome in the form of upregulated and downregulated transcripts in comparison with wild-type KRAS cell line (HK2-8) with a small shift of dysregulation (Figure 3.4)

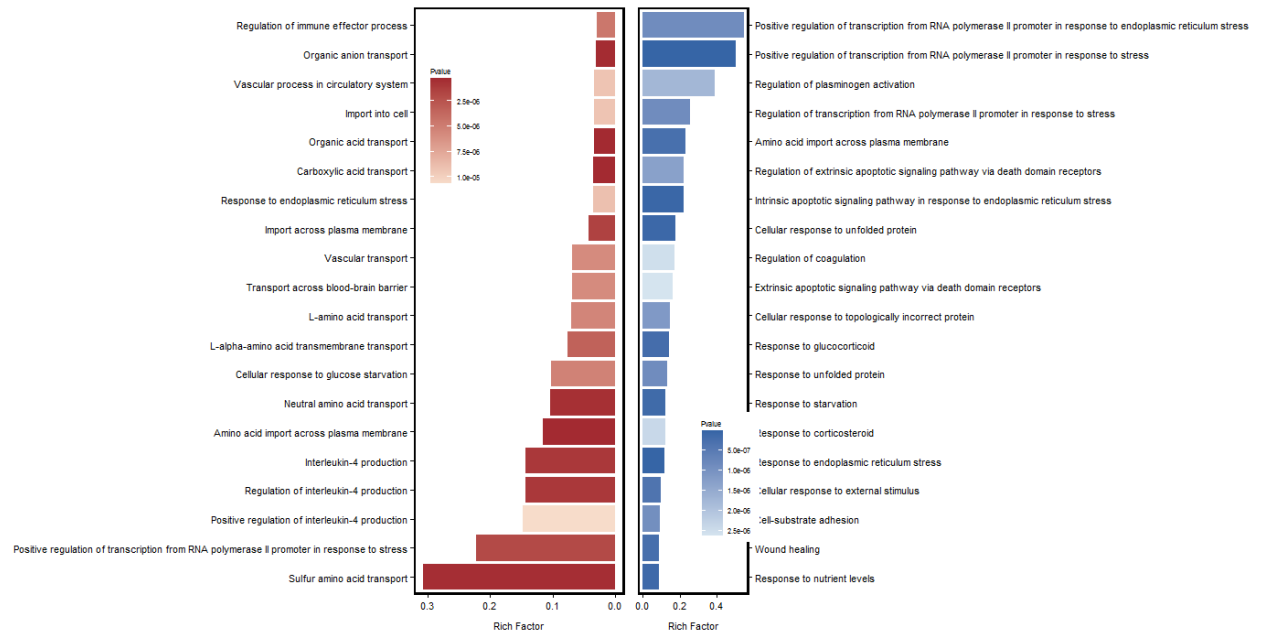
Furthermore, a significant increase in the number of dysregulated genes has been observed in sh-eIF2B5 H358 cells compared to si-eIF2B5 H358 cells. This is attributed to the longer-term or stable expression of shRNA, which can be integrated into plasmid vectors and result in a prolonged knockdown of the target mRNA through antibiotic selection. On the other hand, siRNA exhibits low stability and poor pharmacokinetic behavior for target gene knockdown, with detectable effects as early as four hours and lasting up to around 5 days. The ideal time period for assessing gene knockdown by siRNA and investigating functional effects in cell culture is between 24 and 96 hours (182).

Figure 3.5 Top Gene Ontology enrichment pathways in biological processes to illustrate up (Red) and down (Blue) regulated pathways for impaired and intact eIF2B groups in H358 cell line treated with shRNA-eIF2B5 (A), H358 cells treated with siRNA-eIF2B5 (B), HCT116 (C) and HK2-8 (D) cells treated with siRNA-eIF2B5, respectively.(The criteria for enrichment analysis is $p\text{value} < 0.05$). X-axis: Rich Factor (ratio of DEGs annotated in a pathway to all genes annotated in this pathway), Y-axis: pathways annotations.



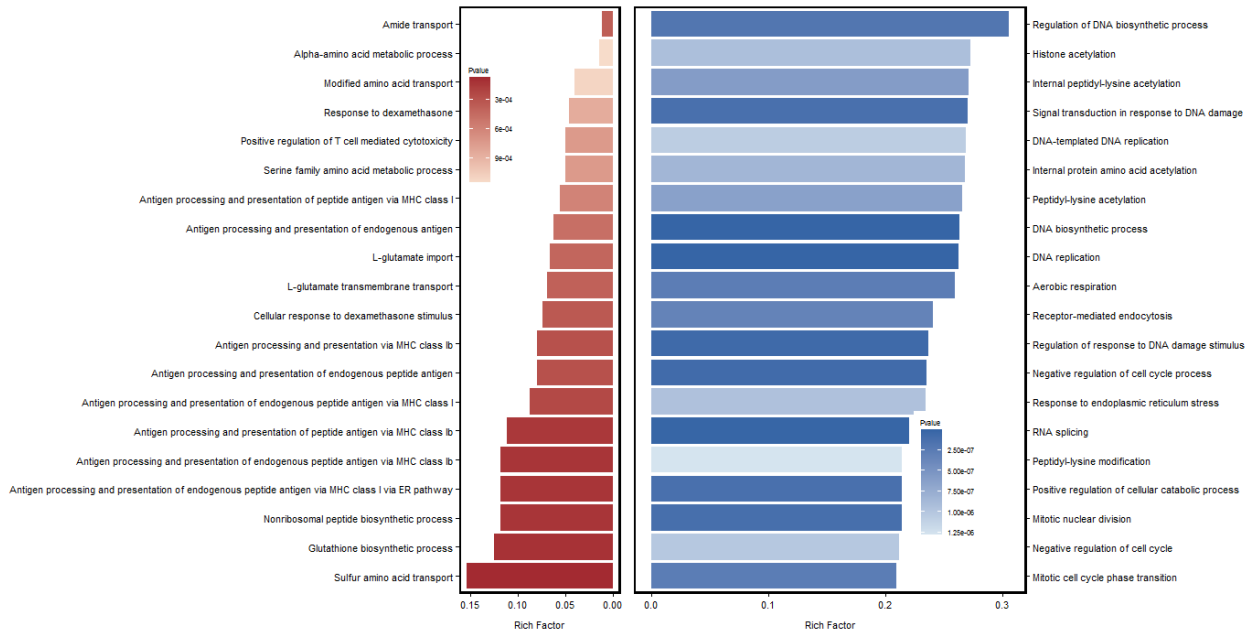
C

HCT116 si-eIF2B5/si-Control



D

HK2-8 si-eIF2B5/si-Control



3.3.2. Gene Ontology (GO) and KEGG pathway enrichment analysis

To identify the transcriptomic pathways regulated by eIF2B, the subset of DEGs that were significantly affected by knocking-down eIF2B5 were subjected to GO annotation using Gene Ontology Consortium (<http://geneontology.org/>) bioinformatics resource. For each category, these results were defined to be statistically significant at $p < 0.05$. The analysis was performed to identify GO pathways in the biological processes category (Figure 3.5). The upregulated and downregulated genes were independently subjected to GO analysis to distinguish them according to their functional roles in red and blue color (based on their expression patterns) and not merely according to their gene names.

The biological processes, which were significantly enriched, were mainly involved in the negative regulation of Wnt signaling and cell-cell signaling by Wnt and proteins localization regulation when upregulated pathways, including leukocyte migration, cell junction assembly, skeletal system morphogenesis and extracellular matrix organization for H358 cells impaired eIF2B5 by shRNA (Figure 3.5-A). Other top pathways include MAPK signaling pathways, cell adhesion, artery development, which are important pro-tumorigenic pathways upregulated by eIF2B while Endothelial cell development, EMT transition and apoptotic signaling pathway downregulated in biological processes for H358 cells impaired eIF2B5 by siRNA (Figure 3.5-B). Furthermore, response to ER stress, importing across plasma membrane and IL-4 production and regulation to be positively regulated and Regulation of transcription by RNA pol II to stress, apoptotic signaling pathways and amino acids import via plasma membrane in HCT116 of cell regulated negatively (Fig 3.5-C). The validation datasets consisted of Schmitt *et al.*'s research about the depletion of eIF2B5 and enhances the translation of MYC through an internal ribosomal entry site (183). Another research data of Cai *et al.* has been used as it focuses on identifying eIF2B5 as a central co-regulator of HRAS proliferation and cell fate choice and provide direct evidence that oncogene-induced loss of progenitor self-renewal is driven by eIF2B5-mediated translation of ubiquitination genes (184, 185). These datasets were used to validated by the DEGs and enriched pathways gained in our data analysis and were common between our results and their reported significant results to illustrate reproducibility (Figure 3.5-C & D, Supplementary tables 1-3).

For HK2-8 cell lines, the biological processes significantly enriched were involved in the negative regulation of DNA replication and cell cycle, DNA biosynthesis process, and response to the ER and DNA damage stress. Nevertheless, upregulated pathways applied to amino acids metabolism, including alpha-amino acids and serin family amino acids, the metabolic process of Glutathione biosynthesis process, L-Glutamate importing and transporting and Antigen processing and presentation via MHC class I and Ib for HK2-8 cell lines with impaired eIF2B by siRNA. All calculated parameters in enrichment analysis pathways are reported in supplementary tables 1 & 2.

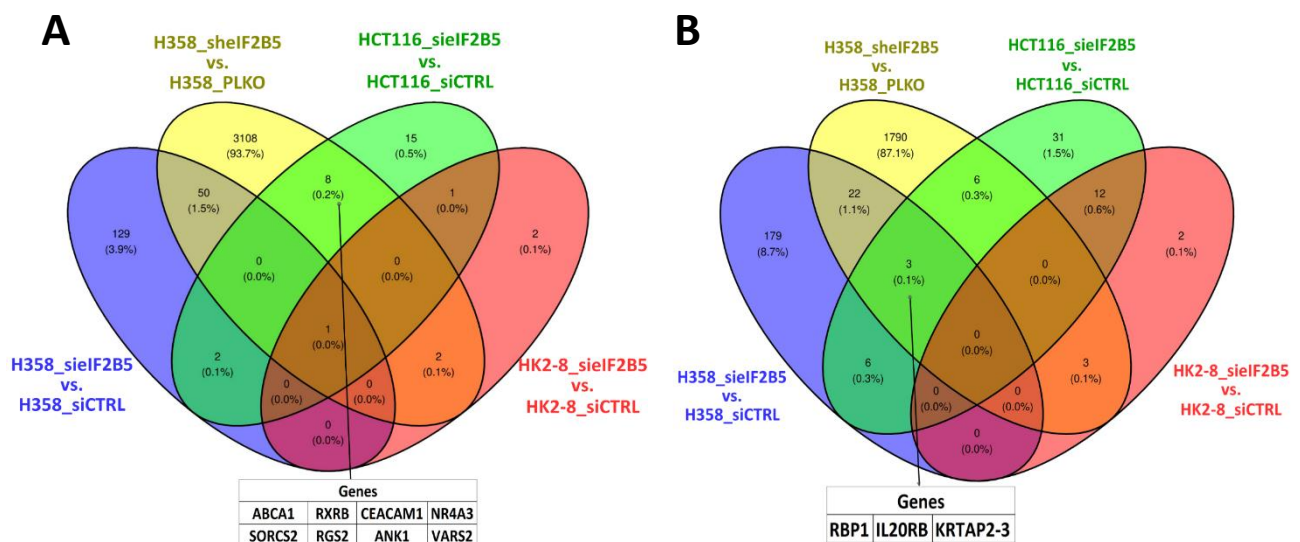


Figure 3.6. Shared genes regulated by eIF2B in mutant KRAS cells. The significant differentially expressed genes (DEGs) in knocked-down eIF2B5 cells were screened by Venn diagram for shared genes between different cell lines (H358, HCT116 and HK2-8).

Dysregulated genes based on the given criteria ($|\log_2FC| \geq 0.58$ and $p\text{-value} < 0.05$) illustrate overlap up (A) and down-regulated (B) genes by eIF2B5 in KRAS mutant cells which are shown in the table, respectively.

3.3.3 Analysis of eIF2B-dependent genes in mutant KRAS cells

To disclose the eIF2B regulated genes exclusively in mutant KRAS tumors, the significant differentially expressed genes (DEGs) in Knocked-down eIF2B5 cells were screened by the Venn diagram for shared genes between different cell lines (H358, HCT116 and HK2-8).

Dysregulated genes based on the given criteria ($|\log_2FC| \geq 0.58$ and $p\text{-value} < 0.05$) illustrate overlap up and down-regulated genes by eIF2B5 in KRAS mutant cells which are shown in the table of each Venn diagram (Figure 3.6).

The common genes between each group are also reported in Supplementary table 3.

Function of common dysregulated genes by eIF2B5 in KRAS mutant cells has been indicated diverse functions and activities in cancer and cellular pathways. A comprehensive compilation of these genes, along with their corresponding full names and functional annotations, is presented in Table 3.3 which assist our understanding of the intricate interplay between these genes in colon and lung cancer progression to make it a proceed to valuable reference for further investigation.

Table 3.3 Annotated function of common down-regulated and up-regulated genes by eIF2B in mutant KRAS cell lines.

Status	Gene Symbole	Gene name	Gene Function	Citation
Down regulated by eIF2B	RBP1	Retinol-binding protein type 1	<ul style="list-style-type: none"> Transporting retinol and plays a crucial role in retinoic acid metabolism Upregulated expression is correlated with lung adenocarcinoma and laryngeal cancer In lung adenocarcinoma, correlates with increased tumor grade and reduced OS 	[197-202][205-206]
	IL20RB	IL receptor 20 subunit β	<ul style="list-style-type: none"> Tumoral response to osteoclasts, and bone metastasis in lung cancer. Promoted metastatic growth of lung cancer cells in bone. Tumor cells induced osteoclasts to activate downstream JAK1/STAT3 signaling. 	[207]
	KRTAP2-3	Keratin-associated protein 2-3	<ul style="list-style-type: none"> Regulator of dual effects of TGF-β Correlated with tumor progression in head and neck cancer patients, migratory and metastatic potentials of oral cancer cells mediating EMT pathways to generates two populations of mesenchymal cancer cells with differential cell-cycle status by TGF-β 	[208]

			<ul style="list-style-type: none"> • inducing EMT for cancer cell proliferation and migration by and mediating TGF-β 	
Up regulated by eIF2B	ABCA1	ATP-binding cassette transporter (member 1 of the human transporter sub-family ABCA)	<ul style="list-style-type: none"> • maintain metabolism of intracellular cholesterol by mediation of transmembrane transport of free intracellular cholesterol and phospholipids to apo A-I • Enhance drug resistance by its upregulation in non-small cell lung carcinoma cells • Associated with a poor prognosis by down regulated status in breast cancer • Poorer overall and relapse-free survival in patients with CEACAM1-positive tumors 	[209-213]
	SORCS2	Sortilin-related VPS10 domain-containing receptor 2	<ul style="list-style-type: none"> • Intracellular trafficking and lysosomal processing • Prognostic marker for poor outcomes in patients with lung adenocarcinomas • <i>in-vitro</i> sensitivity to chemotherapeutics in human gastric cancer cell lines 	[215]
	RXRB	Retinoid X receptor beta	<ul style="list-style-type: none"> • Cancer development and stemness 	[216]
	RGS2	Regulator of G-protein signaling 2	<ul style="list-style-type: none"> • Reduced overall and disease-free survival rates in patients with lung adenocarcinoma • Associated with increased invasion and metastasis of human non-small cell lung cancer cells • Mediation the translational effects of eIF2B in stressed cells • Regulator of dormancy and tumor relapse in lung adenocarcinomas • The inhibitory effect of RGS2 on mRNA translation is mediated by a specific region within the RGS2 protein 	[227-231]
	CEACAM1	Carcinoembryonic antigen-related cell adhesion molecule 1	<ul style="list-style-type: none"> • Drug resistance with cytoprotective effects of eIF2B against mKRAS drug inhibitors. • Tumoral and immune-mediated effects in mKRAS cancers • Initiates signaling by its phosphorylated form to activates RAS-MAPK and PI3K-AKT pathways 	[233-236]

			<ul style="list-style-type: none"> • induces the survival/proliferation of mKRAS cells to increase their susceptibility to mKRAS inhibitors 	
	ANK1	Ankyrin-1	<ul style="list-style-type: none"> • Prognostic marker/therapeutic target in colorectal cancer (CRC) and lung cancer • ANK1 mutations predict poor prognosis in CRC independently • ANK1 knockdown affects the expression of genes and molecular pathways in lung cancer development and progression • Expression regulator of miR-486-5p, contributing to smoking-induced lung adenocarcinoma • Correlation of ANK1 mutation with immune cell infiltration for CRC 	[217-219]
	NR4A3	Nuclear receptor 4A3	<ul style="list-style-type: none"> • Transcriptional activator for steroid-thyroid hormone-retinoid receptor superfamily • With fusion mutations in various cancers including lung adenocarcinoma • Breast cancer cells anti-proliferative effects by collaborating with p53 • Correlation with the survival rates of patients with breast and lung cancer 	[220-223]
	VAR2	Valyl-tRNA synthetase 2	<ul style="list-style-type: none"> • Role in respiratory chain protein synthesis • Prognostic biomarker of the early stages of colon and breast cancers • Provide a new link between mKRAS and mitochondrial metabolism in tumor cells 	[232]

Assessing the survival rate of LUAD patients by a Web-Based Survival Analysis Tool (kmplot.com) showed the shared genes regulated by eIF2B have a significant effect on LUAD patients' survival rates; although, it needs to be considered that the survival rate report included wildtype and mutant KRAS together (Figure 3.7).

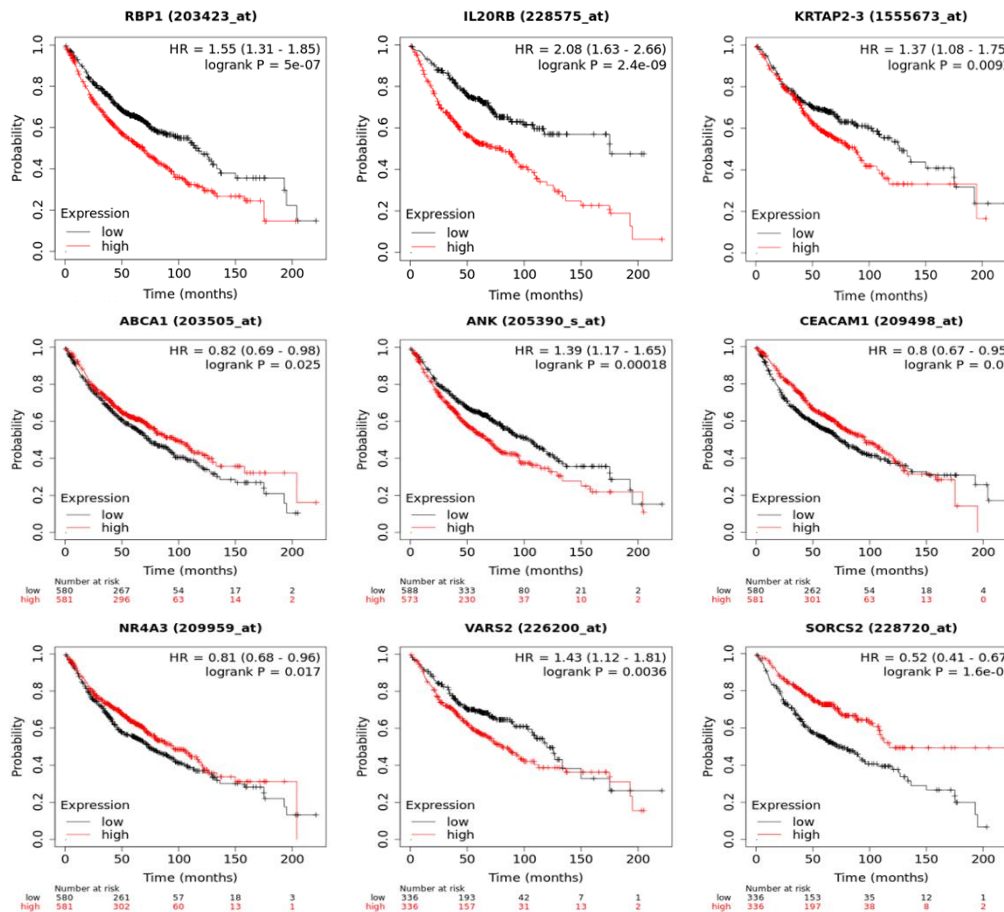


Figure 3.7 Kaplan–Meier survival analysis of lung cancer patients of TCGA database for common genes regulated by eIF2B. Comparison of Overall Survival were used to estimate the significant effects on survival rate in LUAD patients (p -Value < 0.05). Kaplan-Meier curves for the common genes with high and low levels illustrate their critical roles as tumor suppressors or oncogenes for lung cancer progression. Significantly dysregulated genes illustrated in patients' tumor somatic mutations are a combination of wildtype and mutant KRAS genotypes. Black and red curves are for low-risk and high-risk groups, respectively. HR: hazard ratio

To analyze the expression signature for commonly dysregulated genes by eIF2B, in mutant KRAS cell lines as prognostic biomarkers, publicly available data and tools from TCGA databases were utilized. As shown in Figure 3.7, the Kaplan–Meier survival analysis results show the high expression levels of RBP1, IL20RB, KRTAP2, ABCA1, ANK1, and VARS2 are the

risk factors affecting the prognosis of LUAD patients ($p < 0.05$). However, the patients with lower SORCS2 ABCA1, CEACAM1, NR4A3, and SORCS2 gene expression levels showed lower overall survival rates. In contrast, the expression of the RXRB and RGS2 genes did not significantly affect the patient's prognosis ($p > 0.05$)(Data has not been shown).

Therefore, the increase in survival is most probably attributed to the decrease in aggressiveness of tumors and tumor proliferation with less eIF2B, which validates the assumption that eIF2B can indeed act as a potential target in LUAD patients.

The clinically striking role of eIF2B in LUAD patient survival and tumor progression prompted the investigation of the possible biological and mechanistic effects of this factor in LUAD progression and development.

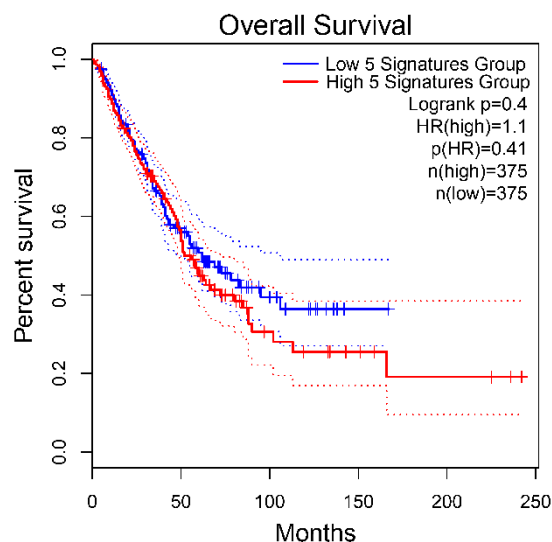


Figure 3.8 Survival Rate analysis of all eIF2B subunits expression in Lung and colon adenocarcinoma. The Kaplan –Meier plot illustrated the high expression of eIF2B protein complex has negative correlation with adenocarcinoma lung and colon patients' survival rate of TCGA database. Patients' tumor somatic mutations combine wildtype and mutant KRAS genotypes.

Also, the high expression of eIF2B in lung and colon adenocarcinoma patients is correlated with a low survival rate based on the TCGA database (Figure 3.8). Even though the KRAS

inhibitors promoted death in lung cancer mutant KRAS tumors, drug resistance to treatment is still critical for patients' survival and tumor recurrent which could be affected by eIF2B, which can reduce the effect of drug treatment stress in the cell with KRAS interaction and aid cells abscond of this stress. Therefore, mutant KRAS Lung and colon adenocarcinoma rely on eIF2B for proliferation and survival.

3.4 Probing PROTAC Efficacy: Characterizing its Function in Targeting eIF2B

Under normal conditions, ISRIB restores cellular GEF activity by replenishing the supply of uninhibited eIF2B decamers from a limiting pool of building blocks. Under stress, high levels of eIF2 phosphorylation would sequester all decameric eIF2B complexes in an inactive state and eliminate ISRIB's effect. ISRIB interacts with the eIF2B internal pocket through beta and delta subunits to stabilize the complex (132). So, utilizing modified ISRIB (ISRIB-PROTAC) as an inhibitor of the eIF2B complex would be a good approach to targeting this protein specifically. ISRIB-PROTAC compounds were conducted to determine: (1) The viability of these compounds binding to Eukaryotic Initiation Factor 2 beta (eIF2B); (2) Impact of linker chain length on the compound's ability to recruit von Hippel-Lindau disease tumor suppressor (VHL) or cereblon (CRBN).

We have investigated the effects of the integrated stress response inhibitor (ISRIB), which antagonizes the translational effects of p-eIF2 α by deactivating eIF2B, on KRAS G12C LUAD progression. Firstly, we tested the implications of ISRIB on the MAPK pathway in H358 cells. ISRIB treatment with high to low concentration (20uM to 250nM) before and during ISR, enhanced with thapsigargin (TG) treatment, in H358 cells were shown in Figure 3.9.

ATF4 displayed a decreasing synchronization with a lower concentration of ISRIB and high efficiency at 10uM concentration of ISRIB. Interestingly, SOS1 and p-ERK displayed upregulation with no stress and downregulation during stress by decreasing ISRIB concentration. This suggests a positive correlation between SOS1 and p-ERK and decreasing ISRIB during stress regulation, which indicates a decrease during ISR status.

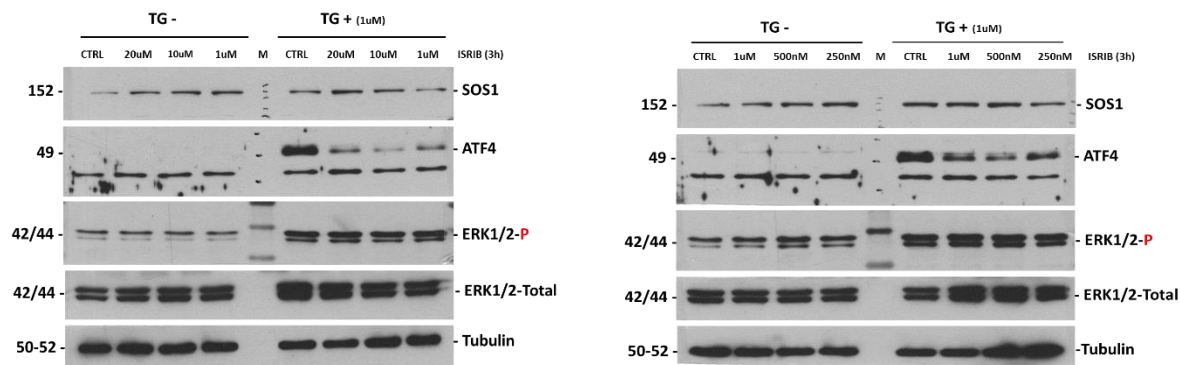


Figure 3.9 ISR inhibition by ISRIB antagonizes eIF2B function in mutant KRAS lung tumor cells. The ISR increases ATF4 and stimulates p-ERK in human LUAD cells under stress. Human LUAD cells with KRAS G12C (H358) were treated with 1 μ M thapsigargin (TG) for 30 min followed by treatments with increasing concentration of ISRIB for 3h at the indicated different concentrations (250nM to 20uM). Protein extracts (30 μ g) were immunoblotted for the indicated proteins. p-ERK was normalized to total ERK-total whereas ATF4 and SOS1 expression to Tubulin.

Human lung cell lines with mKRAS G12C (H358) were treated with fixed concentration (20uM) of ISRIB, ISRIB-biotin, and ISRIB-PEG4 (as ISRIB-Biotin control) in two different time-point (1 and 3 hours) illustrated that ISRIB has a more significant effect on ATF4 to inhibit it during stress induced by thapsigargin; ISRIB-Biotin has an upregulation effect on phosphorylated ERK in comparison to other compounds and less ability to overcome ATF4 expression during stress (Figure 3.10 A, B). ISRIB-linker (PEG4) has more ability to increase phosphorylated ERK pre- and post-stress in comparison with control and ISRIB; however, it has less effect for overcoming ATF4 expression compared with ISRIB but less effect versus ISRIB-Biotin during stress (Figure 3.10 C, D). Further, in the context of treatment with the ISRIB-linker (PEG6), both pre- and post-stress results indicate that the linker PEG6 does not impair the ability of ISRIB to interact with eIF2B and dysregulate ATF4 to overcome ISR. However, the polarity of the linker reduces the solubility of ISRIB and enables lower concentrations of ISRIB-linker (PEG6) to overcome ISR effectively (Figure 3.10 E, F).

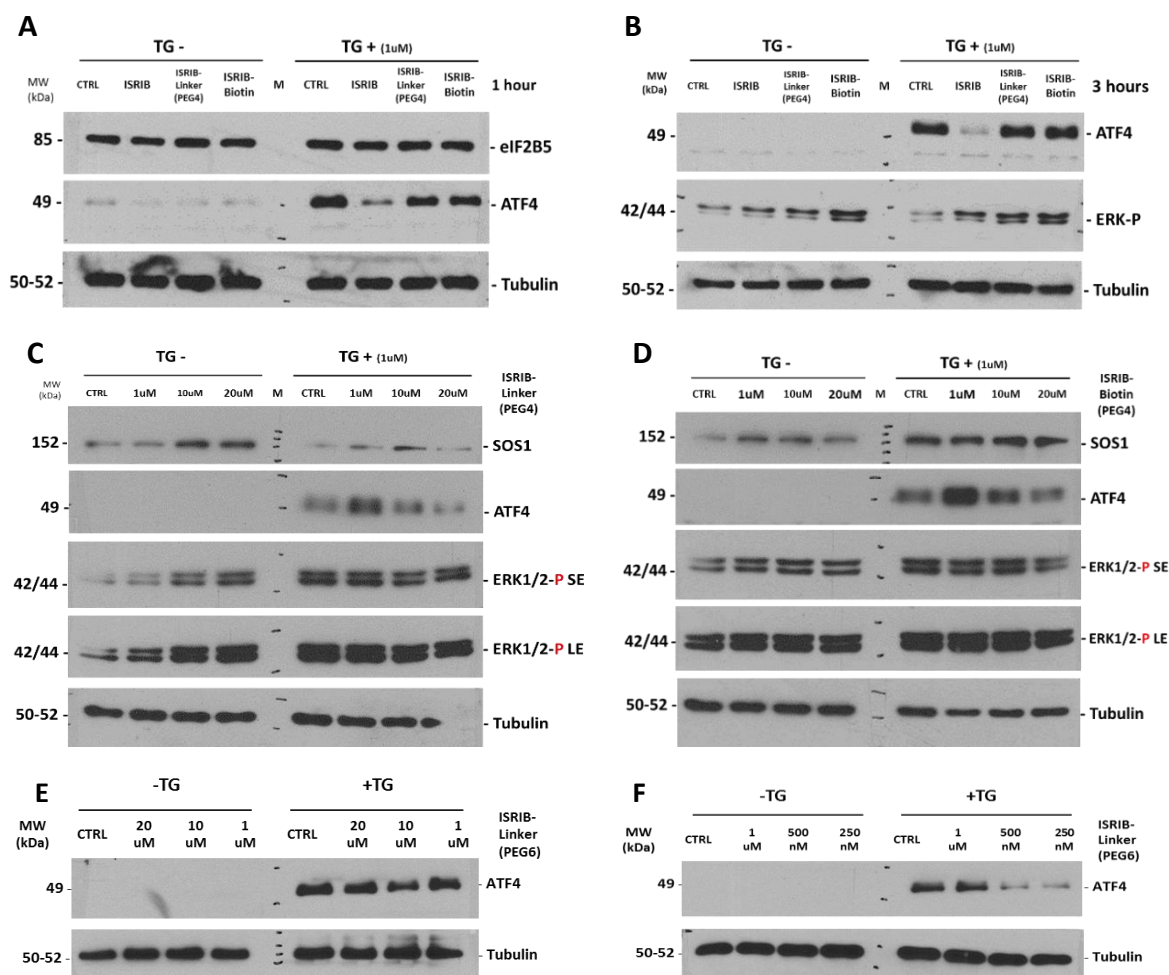


Figure 3.10 Immunoblotting of H358 cells treated with biotinylated ISRIB and ISRIB-linkers (PEG 4-6) to dysregulate ATF4 in mutant KRAS lung tumor cells. Treatment of Human LUAD cells with KRAS G12C (H358) with Biotin-ISRIB, ISRIB-linker(4-6PEG) and ISRIB in 20uM concentration for 1 hour (A) and 3 hours (B). ISRIB-Biotin (C) and ISRIB-linker (PEG4) (D) cell treatment in different concentrations (250nM to 20uM) with fixed time points (3h) was evaluated pre and post-stress induced by treated with 1μM thapsigargin (TG) for 30 min, followed by treatments. ISRIB bounded to the PEG6 linker with increasing concentrations of ISRIB-linker(PEG6) (E, F) for 3h, still acts as ISRIB in low concentrations, at the indicated different concentrations (250nM to 20uM). Protein extracts (30 μg) were immunoblotted for the indicated proteins. All compound structures are available in Table 2.2.

To scrutinize the functional effect of ISRIB-Biotin and ISRIB-linker (PEG4) in cell treatment, protein dysregulation with different concentrations (1, 10 and 20uM) of compounds pre- and

post-ISR by thapsigargin treatment has been evaluated. The revealed blots for SOS1 decreased by increasing the concentration of ISRIB-linker (PEG4) in the absence of stress but showed an increase with decreasing both compounds' concentrations during ISR. ATF4 expression increased with decreasing concentration in both treatments, showing a negative correlation. Even more, phosphorylated ERK (p-ERK) decreased with decreasing the concentration of ISRIB-linker (PEG4) without stress and vice versa, increasing during stress, while ISRIB-biotin showed the same pattern with SOS1 without stress and the same pattern with ATF4 in ISR for both compounds (Figure 3.10 C,D).

Downstream of eIF2B inhibition, ATF4 is activated to regulate genes that can overcome a stressed microenvironment. Therefore, we speculated that ATF4 downregulation after ISRIB-PROTACs with linker PEG6 in ISR status might be arising from the ISRIB-PROTAC effect on eIF2B-eIF2 interaction to overcome the ISR effect in the cell, which suggests that these compounds were able to interact with eIF2B and other interacted proteins in stress condition. However, inhibiting eIF2B using different ISRIB-PROTACs did not affect ATF4 and eIF2B subunits' levels out of stress condition. In addition, immunoblotting of ISRIB, ISRIB-linker (PEG4 and 6) and ISRIB-biotin revealed that p-ERK level is much higher in the presence of ISRIB-Biotin as it has less effect on ATF4 in comparison with ISRIB as it was significantly downregulated in the H358 cells to eliminate the ISR (Figure 3.10 E,F).

HEK293T cell lines were treated with the first generation of ISRIB-PROTAC, including PEG2 as a linker and CRBN as E3 ligase ligand, with multiple time points (6 to 24 hours) and fixed concentrations (20uM). Protein extracts (30 µg) were subjected to immunoblotting for the indicated proteins (Figure 3.11). This experiment normalized the time-response curves for different eIF2B, ATF4 and SOS1 protein expression subunits to GAPDH, which did not reach significant changes. (Figure 3.11-C,E). ATF4 was used as a marker of the antagonistic effects of ISRIB on mRNA translation in the tumor cells (142).

EIF2B subunits did not decrease as we expected for the ISRIB-PROTACs effect to facilitate the degradation of this complex by the proteasome after ubiquitination. Also, ATF4 expression did not increase due to ISR triggering by the ISRIB-PROTACs effect (Figures 3.11 & 3.12).

In addition, the experiments for assessing the second generation of PROTAC compounds have been done, which included different lengths of polyethylene glycol (PEG) linker (from 2 to 11 units) and other E3 ligase ligands, including CRBN and VHL in H358 cells, with different concentrations (0.5 μ M to 20 μ M) at a fixed time point for 4 hours (Figure 3.12).

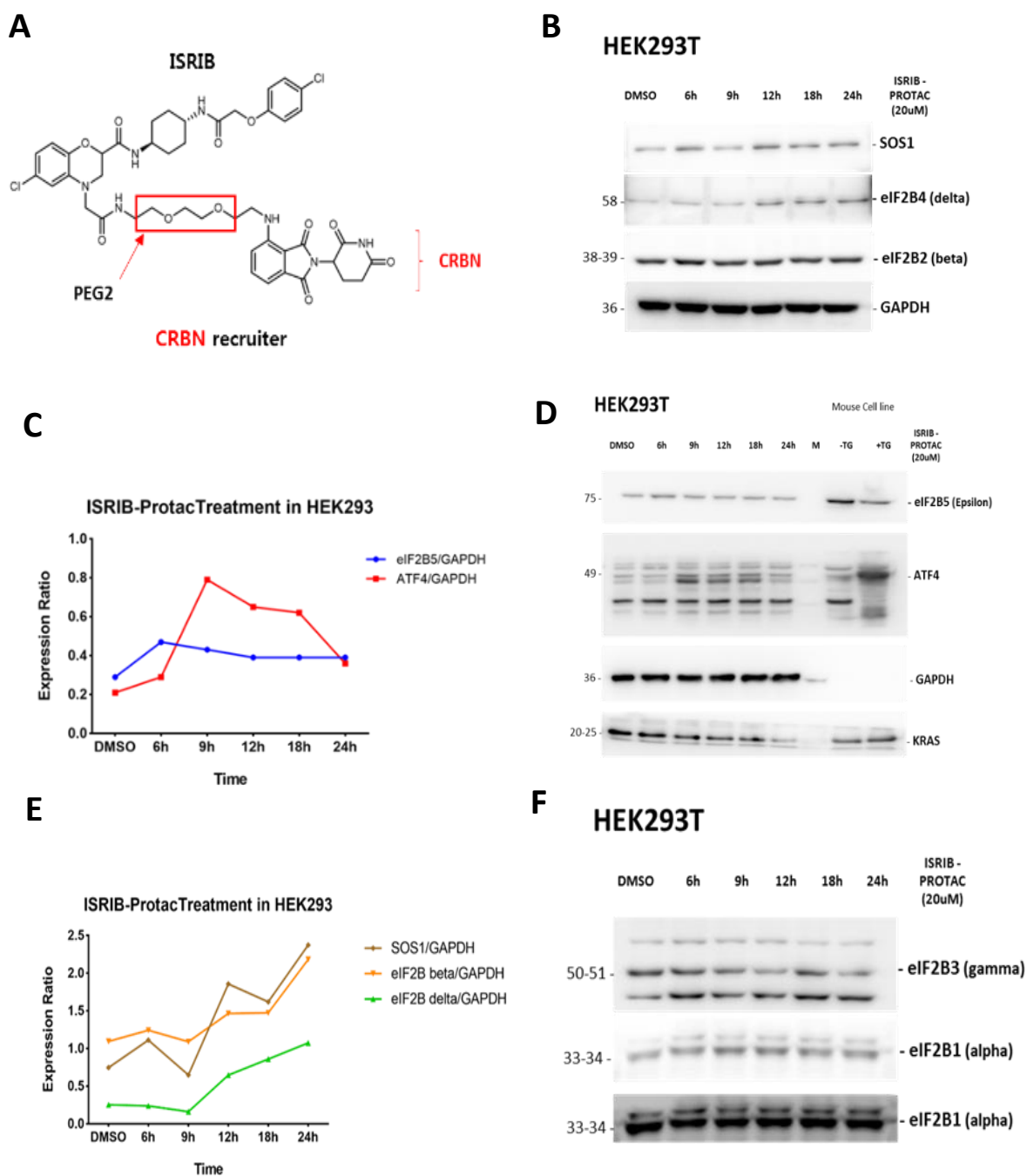


Figure 3.11 Immunoblotting of HEK293T cells treated with the first generation of ISRIB-PROTAC (ISRIB-CRBN-PEG2) with fixed concentration (20uM) and different time points. The

chemical structure of first-generation ISRIB-CRBN-PEG2 (A) is illustrated. The mouse lung tumor cell lines treated with DMSO and Thapsigargin were utilized as control for ATF4 expression level. eIF2B subunits and ATF4 protein levels were not affected by ISRIB-CRBN-PEG2 compound (C,D). Data in each plot represents the normalized expression of each protein, illustrating that ISRIB-CRBN-PEG2 was not functional to degraded eIF2B subunits in the mentioned circumstances (B, F).

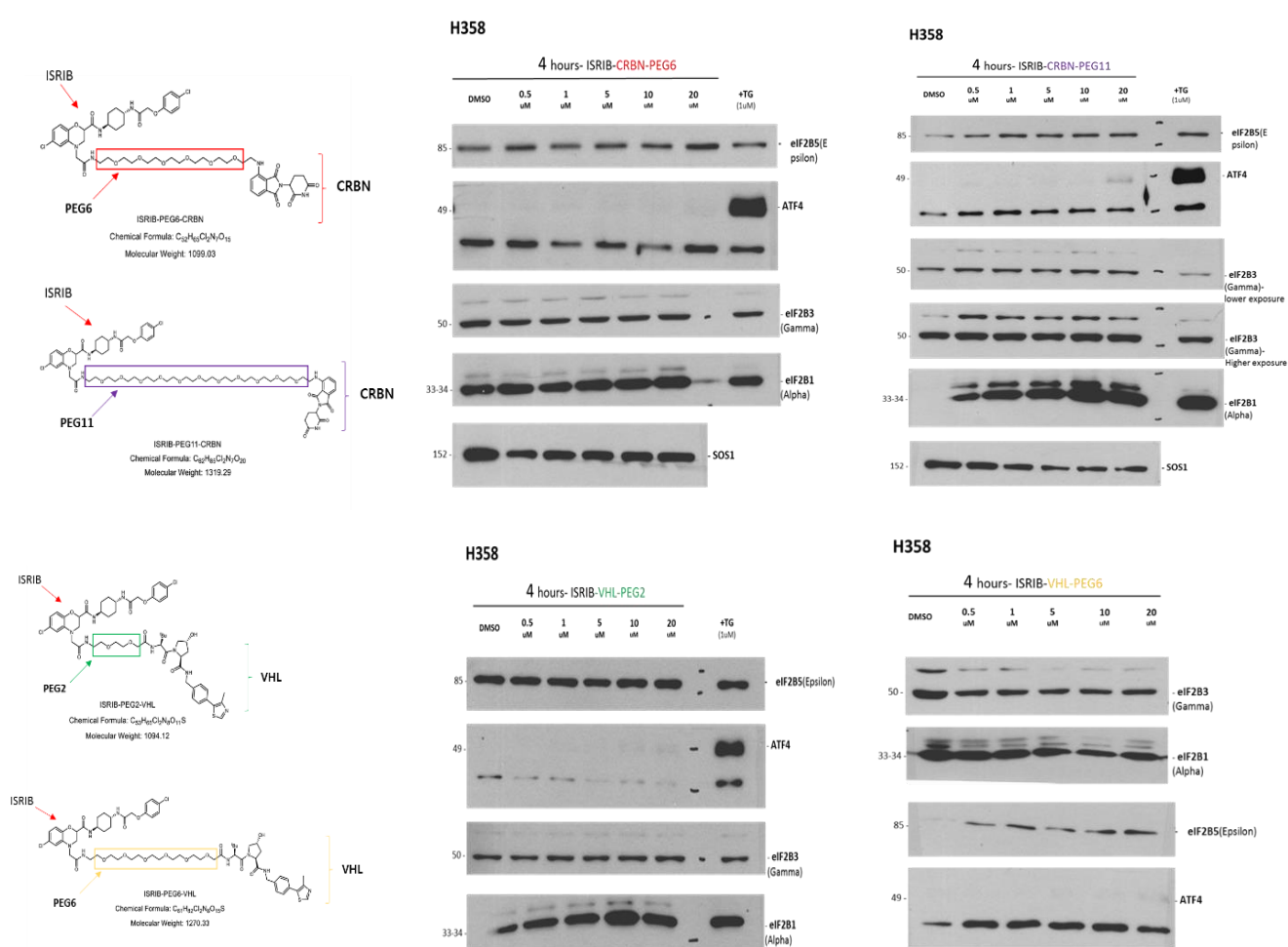


Figure 3.12 Immunoblotting of H358 cells treated with second generation of ISRIB-PROTAC. The chemical structure of each compound is illustrated. The experiment was done with different E3 ligase ligands (CRBN or VHL) and linkers length (PEG2-11) in different concentrations with fixed time point (4h). eIF2B subunits and ATF4 protein expression were not affected by the second generation of ISRIB-PROTAC compounds.

Although we expected the degradation of eIF2B by ISRIB-PROTAC treatment, ISR has been triggered, which eventuated in ATF4 expression; both generations of ISRIB-PROTAC compounds were ineffective. It resulted in evaluating ATF4 protein and eIF2B subunit degradation through immunoblotting and did not show any dysregulation via these compound treatments in different concentrations for a fixed time (4 hours) (Figures 3.11 & 3.12).

Such observations contribute to our understanding of the complex mechanisms underlying ISRIB-mediated stress response and could have implications for developing novel therapeutic strategies. As with the effects of ISRIB-PROTACs, after induction of the UPR with TG, ISRIB downregulated SOS1 and p-ERK, followed by upregulation with no stress. However, it had decreasing effects on the MAPK pathway in H358 cells (Figure 3.10). These findings suggest that ISRIB-PROTACs are capable of cellular diffusion and target engagement but do not degrade eIF2B or other interacting proteins.

We also sought to explore possible therapeutic compounds in targeting eIF2B in KRAS mutant lung cell lines, H358, by ISRIB-PROTACs.

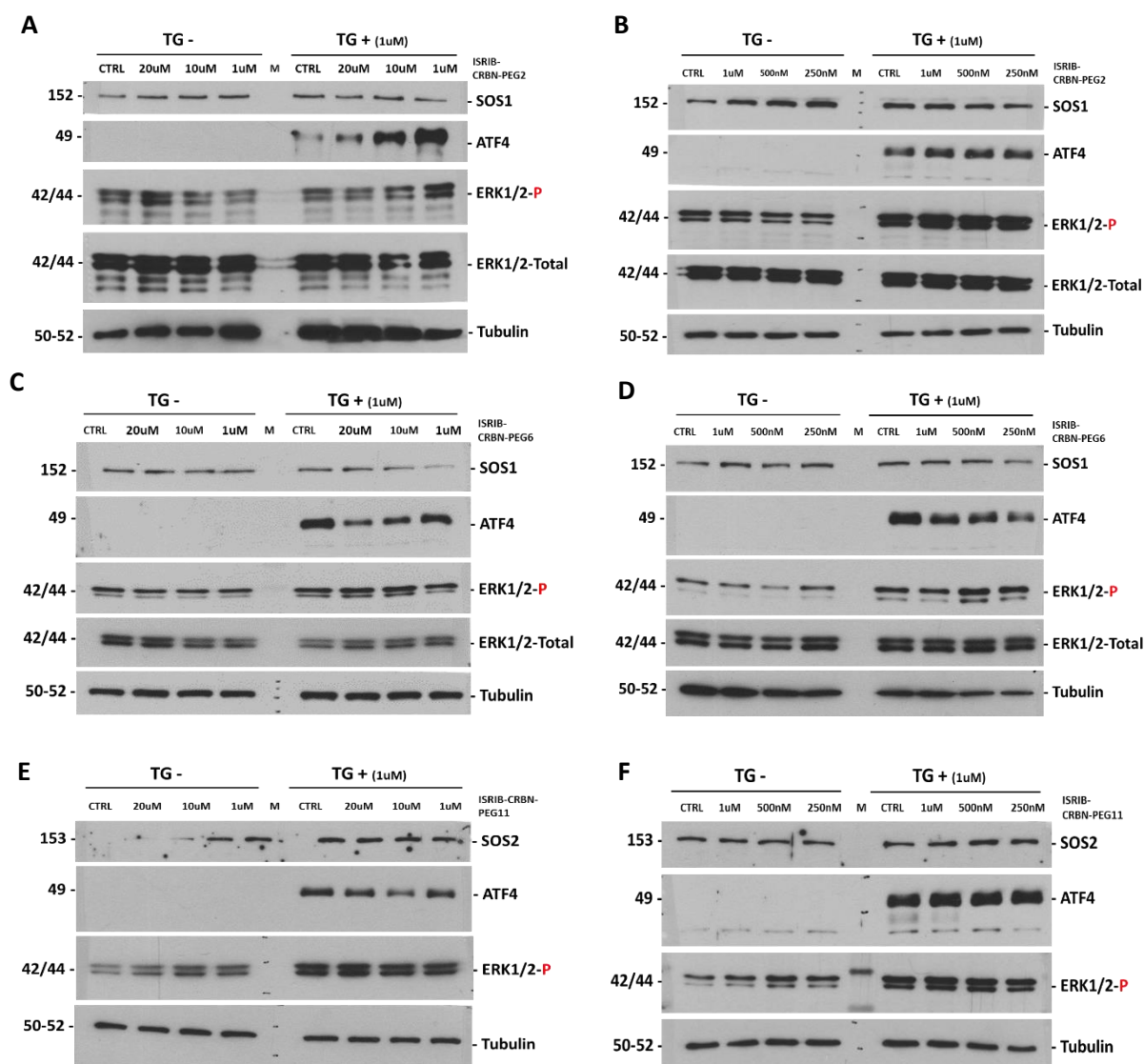


Figure 3.13 ISIRI-PROTACs with CRBN ligand and different linker lengths affect ISR in the presence of thapsigargin via ATF4 expression. Treatment of ISIRI-PROTACs with CRBN ligand, and different linker lengths (4-11PEGs) cell treatment in different concentrations with fixed time points (3h) was evaluated pre- and post-stress induced by thapsigargin. ATF4, SOS1 and p-ERK protein expression were used to evaluate the effects of ISIRI-PROTACs via translational and KRAS signaling pathways. Human LUAD cells with KRAS G12C (H358) were treated with 1μM thapsigargin (TG) for 30 min, followed by treatments with increasing concentrations of ISIRI-CRBN (PEG2) (A, B), ISIRI-CRBN (PEG4) (C, D), and ISIRI-CRBN (PEG11) (E, F) for 3h at the indicated different concentrations (250nM to 20uM). Protein extracts (30 μg) were immunoblotted for the indicated proteins.

While ISRIB-CRBN-PEG2 increases the ATF4 and p-ERK during stress along with increasing its concentration simultaneously (Figure 3.13 A, B), ISRIB-CRBN-PEG6 upregulates the p-ERK and SOS1 in H358 with no stress and then decreased with decreasing concentration to 1uM and then started to increase in lower concentrations (500 and 250 nM) during stress, while ATF4 increased but less than control (thapsigargin) (Figure 3.13 C, D). Immunoblot analysis of ISRIB-CRBN-PEG11 in H358 cells prior and after treatment with 1μM thapsigargin (TG) for 3 hours also displayed an increase of SOS1 and p-ERK level, which indicated a negative correlation with this compound concentration treatment. ATF4 level during stress status decreased until 10uM and then increased along with decreasing compound concentration (Figure 3.13 E, F).

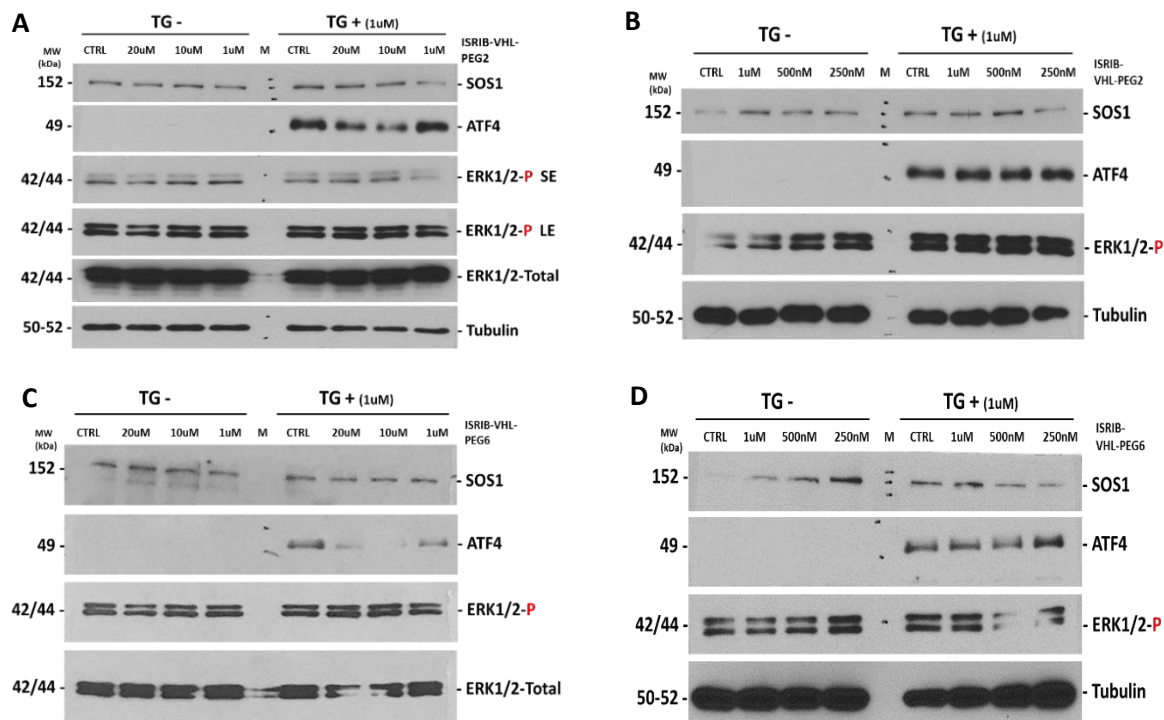


Figure 3.14 The PROTAC-PEG6 dysregulates ATF4 levels in H358 cells with mKRAS G12C.

Immunoblotting of H358 cells treating with ISRIB-PROTAC-VHL-PEG2 (A,B) and -PEG6 (C,D) with KRAS G12C. p-ERK, ATF4 and eIF2B were normalized to corresponding total proteins, including total ERK and tubulin. SE: Short Exposure. LE: Long Exposure.

Immunoblotting of ATF4, ERK phosphorylation and SOS1 in lung tumor cells pre and post-treatment with ISRIB-PROTACs combination with Thapsigargin indicated different

concentrations of ISRIB-VHL-PEG2 for 3h had an effect of reducing ATF4 during stress in high concentration (Figure 3.14 A, B).

Treating H358 cell line with ISRIB-VHL-PEG2 did not change the SOS1 level prior to stress but increased it until 1uM and then showed the same level in lower concentration during stress, as the ATF4 level also synchronized with SOS1. Level of p-ERK increased and negatively correlated with compound concentration pre- and post-stress (Figure 3.14 A, B).

Evaluation of protein levels by western blots after treating with ISRIB-VHL-PEG6 were performed for SOS1, phosphorylated ERK (p-ERK), and ATF4 were normalized to corresponding total protein whereas H358 cell were under stress response with thapsigargin treated and without stress. With no stress, the SOS1 increased with decreasing level of the compound, but p-ERK did not change; whereas, during stress, SOS1, p-ERK and ATF4 displayed a positive correlation with decreasing compound concentration as they also were decreasing (Figure 3.14 C, D).

ISRIB-PROTACs could not initiate degradation of eIF2B; however, whether these PROTACs will elicit degradation by recruiting the associated ligase is unclear. Similar challenges are often encountered in PROTAC campaigns and are best addressed by changing the linker domain's length, rigidity, and polarity. Depending upon preliminary results, the Lumb group will synthesize a series of additional linkers, including those possessing alkyne subunits to increase rigidity and piperidine subunits to increase polarity, flanked by PEG-units of varying length to extend the ligase further into a solvent-accessible region. We will also assess the effects of ISRIB-PROTACs on degrading eIF2B-interacting proteins (e.g., mKRAS or SOS) and may prevent the E3 ligase of PROTACs from accessing eIF2B (POI- Target). Moreover, we will use our ISRIB-biotin analogs with the highest affinity to eIF2B to identify interacting proteins by Mass spectrometry for lysate of IP for eIF2B that could provide additional targets for an ISRIB-PROTAC.

Chapter 4

Discussion and Conclusion

4.1 Discussion and Contribution to original knowledge

In 2018, Zhang *et al.* reported KRAS4b interacts with eIF2B δ through its C-terminal HVR in HEK293T Cells by SILAC and AP-MS based interactome studies and using immunoprecipitation of FLAG-tagged KRAS proteins. They confirmed biochemically that eIF2B δ only interacted with KRAS4b but not KRAS4a in a nucleotide-independent and the C-terminal HVR-dependent manner, which suggests that KRas4b isoform may regulate protein translation initiation by interacting with eIF2B(153).

Additionally, Dr. Koromilas' labs data in collaboration with Dr. Atsuo Sasaki's lab (University of Cincinnati) who also performed mass spectrometry (MS) analysis of immunoprecipitated (IPed) FLAG-tagged KRAS proteins transiently expressed in HEK293 cells to identify interacting partners (155). The results illustrate that all five eIF2B subunits were bound to mutant G12V but not wild-type (WT) KRAS. While all eIF2B subunits interacted with 4B as the major KRAS isoform (154), 4A isoform of KRAS G12V does not interact with eIF2B. Mutations in the carboxyl-terminal hypervariable region of KRAS, which abolish the binding of KRAS to the plasma membrane (PM), also impaired the interaction of KRAS G12V with eIF2B (155).

It should be considered SOS1/2 are the *bone fide* GEF of RAS proteins (186). While, other GEFs, such as eIF2B, generally dissociate from their substrates after GDP-GTP exchange, SOS proteins remain bound to RAS-GTP, leading to an allosteric stimulation of their GEF activity that further increases the rates of GDP release from RAS (187).

In order to decipher the potential domains involved in eIF2B-mutant KRAS interaction, blind docking for these proteins, utilizing available crystallography structures, has been done for KRAS carrying G12C mutation to interact with SOS1 with the apo form of eIF2B. These crystal structure analyses predicted valuable insights into the molecular mechanisms underlying eIF2B-mutKRAS interaction with each other. The significance of our findings in a clinical context is reinforced by the analysis of the collection of 567 cohort human LUADs, which revealed that eIF2B carries somatic missense mutations in alpha, gamma, and delta subunits that interact with KRAS G12C and SOS1 structures through rigid protein-protein docking, elevated in a way that these subunits have a critical role for this interaction between these proteins structures (Fig 3.2).

One of the biggest challenges in this analysis is access to the complete structure of desired proteins in high resolution and quality for further analysis as a positive and negative control for this process. Accurate computational approaches are required to address this limitation and enable us to access large-scale three-dimensional structures that a protein will adopt based solely on its amino acid sequence or the structure prediction component of available homologous structures. The *in-silico* modeling approach incorporates physical and biological knowledge about protein structure, leveraging multi-sequence alignments to design more accurate structures close to biological form. So, utilizing a prediction model for unavailable or missed parts of the proteins seems inevitable. One of the tools that can be used for homology modeling and superimposing is to evaluate structural properties based on the homologous sequence of proteins for these structures by modeling and computational tools, including modeller, Swiss model, and alpha fold (188-190).

To figure out the involved precise residues in the interacted proteins, it is also necessary to compare the biological control complexes through structural analysis, including eIF2-eIF2B and KRAS-SOS1/2 associated with individual structures in each analysis like KRAS (WT and mutant), SOS1/2, and eIF2B (active and inactive apo form) as well.

Also, the molecular dynamic simulation to decipher dynamic interaction domains in protein structures and the stability of the interaction close to biological systems is another complementary approach to illustrate the interaction mechanism between residues in these complexes.

These results suggested that mKRAS may be subjected to a similar "allosteric" regulation by eIF2B. It is also possible that eIF2B acts with another GEF, like SOS, to stimulate the GTP-bound state of mutant but not WT KRAS. Experimental procedures such as co-immunoprecipitation, pull-down assay, and protein chip- or mass spectrometry-based assays can be used to identify these protein partner interactions.

In order to validate these results and evaluate mutations that affect eIF2B complex formation and stimulation of GTP-bound mKRAS, detection of the stoichiometric formation of eIF2B complex in glutathione-sepharose pull-down assays with ectopic tagged eIF2B (i.e., α , γ , δ , ϵ subunits) and tagged forms of either WT or eIF2B mutant in protein extracts of transfected cells can be done (125). This approach not only assesses the role of the mutations

in the stabilization of the eIF2B complex in the absence or presence of ISRIB, a small compound that acts as a molecular glue to stabilize eIF2B decamers and stimulate GEF activity for eIF2-GDP in cells (65), can be determined, but also the effects of the mutations on the interaction of eIF2B with either WT or mKRAS (e.g. G12V, G12C, G12D, etc.) in co-IP assays of MYC-eIF2Bs and FLAG-KRASs in cells can be evaluated.

Previous genetic studies reveal that eIF2B is crucial for the survival and proliferation of tumor cells with KRAS mutations, providing a link between mutant KRAS and mRNA translation. Translational inhibition of eIF2B using siRNAs in KRAS-mutant cells demonstrates stimulation of p-ERK and p-MEK. Researchers also suggest that increased expression of eIF2B5 is associated with transformation and tumorigenesis, with knockdown experiments showing reduced cell growth, proliferation, and tumor formation(144, 191).

Although eIF2B predominantly functions at the translational level, mRNA translation is usually coupled with transcriptional reprogramming due to controlled transcription factor production, revealing impaired eIF2B changed gene expression sets related to RNA processing and regulation (181). Also, as we considered the eIF2B as a potential targeted therapy in mKRAS tumors, it is conducive to assessing the defecting eIF2B's impact on cell biology and the regulation of genes.

Using genetic approaches, we decipher tumor cells with KRAS mutations that need eIF2B for survival and proliferation via the stimulation of MAPK signaling. Dr. Koromilas's lab data also show that eIF2B increases the tumor cells' resistance to pharmacological inhibition of mutant KRAS forms. We illustrate the translational inhibition of eIF2B accounts for the stimulation of p-ERK and p-MEK in mutant KRAS cells, so it is characterized by inhibiting GEF activity of eIF2B through downregulating epsilon subunit with siRNAs in KRAS G12C lung cancer cells (H358) and KRAS G13D HCT116 with its isogeneic cells with wild-type KRAS in HK2-8 cells. In contrast, its high expression in lung and colon adenocarcinoma patients decreases the survival rate. Our findings reveal a stimulatory role of eIF2B in mutant KRAS signaling and provide a remarkable link between mutant KRAS and mRNA translation with an affect on the growth and treatment of cancers with KRAS mutations (156).

Using external datasets, we also validate a transcriptomic gene signature in an independent cohort for colon cancer cells with mutant KRAS. GO and pathway enrichment analysis was

performed and correlated with signature gene expression in our data. Differentially expressed genes validated biomarkers for mutant KRAS tumors as well. The validation datasets consisted of Schmitt *et al.*'s research about the depletion of eIF2B5, which induces an integrated stress response and enhances the translation of MYC through an internal ribosomal entry site. This status disrupts the balance of cellular amino acids and nucleotides, depletes energy resources and induces apoptosis dependent on the MYC gene. eIF2B5 serves to restrict MYC expression and prevent apoptosis in APC-deficient murine and patient-derived organoids, as well as in APC-deficient murine intestinal epithelia in vivo (183) and research data of Cai *et al.* who focus on identifying eIF2B5 as a central co-regulator of HRAS proliferation and cell fate choice and provide direct evidence that oncogene-induced loss of progenitor self-renewal is driven by eIF2B5-mediated translation of ubiquitination genes (185).

Our validated diagnostic gene signature with KRAS mutation analysis significantly improves the diagnostic accuracy of current standard procedures. It could feasibly be implemented into clinical practice to reduce the need for repeat procedures. Consistent with the RNA-seq data, top GO and KEGG pathway enrichment analysis has been assessed and confirmed (Figure 3.5).

Similarly, the most common dysregulated mRNAs were significantly increased and decreased in HCT116 cells with external datasets (Fig.3.4).

A recent study showed that stimulation of p-ERK by the translational suppression of ISR is lower than the threshold required to induce anti-proliferative effects in the mutant KRAS G12D lung tumors. In addition to p-ERK stimulation, the roles of adaptive ISR in driving secondary changes in the transcriptome outcome have been pinpointed in additional changes to metabolic and signaling pathways with established roles in cancer (142). Specifically, common dysregulated genes enrichment analysis of our RNA-seq data indicated a role of eIF2B in the activation of pro-tumorigenic and invasion pathways under the control of RBP1, IL20RB, KRTAP2-3, ABCA1, RXRB, CEACAM1, NR4A3, SORCS2, RGS2, ANK1, VARS2, and NF-kB pathway involved in upregulation of Twist-1-mediated epithelial-mesenchymal transition (EMT) that is critical for cancer cell invasion and metastas (132, 192).

Retinol-binding protein type 1 (RBP1) is a protein that transports retinol and plays a crucial role in retinoic acid metabolism (193), which has significant implications for the proliferation and differentiation of epithelial cells (194). Studies have shown that RBP1 expression is correlated with various cancers, with downregulated expression associated with prostate cancer, endometrial cancer, and ovarian cancer. In contrast, upregulated expression is correlated with lung adenocarcinoma and laryngeal cancer (195-198). RBP1 is hypermethylated in Coronary Artery Disease and multiple cancers, and its expression levels in different cancers have been associated with poor prognosis (197, 199-201). RBP1 has also been correlated with tumor mutation burden (TMB), Microsatellite Instability (MSI), Mismatch Repair (MMR), cancer-associated functional status, and immune checkpoints in various cancers, and its expression has been related to the sensitivity of six anti-cancer drugs (202).

Additionally, RBP1 is associated with immune cell activation, immune response, and cancer development. The distribution of RBP1 expression is markedly different among different types of cancers, suggesting that it could be a candidate molecular marker for predicting patient outcomes (183, 203-205). The high expression of RBP1 in lung adenocarcinoma correlates with increased tumor grade and reduced OS, probably increasing Akt/Erk/EGFR-mediated cell proliferation and differentiation. Studies have also shown that restored RBP1 expression in NSCLC cells reduced proliferation and viability, down-regulating AKT-related gene levels. These findings suggest that RBP1 could be a potential markers for assessing prognosis and improving the efficacy of retinoid anti-cancer adjuvant therapy (206).

A recent study found that IL receptor 20 subunit β (IL-20RB) played a crucial role in the tumoral response to osteoclasts, leading to bone metastasis in lung cancer. The study also revealed that IL-20RB promoted metastatic growth of lung cancer cells in bone. The mechanism behind this was that tumor cells induced osteoclasts to secrete the IL-20RB ligand IL-19, which then stimulated IL-20RB-expressing tumor cells to activate downstream JAK1/STAT3 signaling. This resulted in the enhanced proliferation of tumor cells in bone. The study further showed that blocking IL-20RB with a neutralizing antibody significantly suppressed bone metastasis of lung cancer. These findings suggest that IL-20RB-targeting approaches could potentially treat metastasis (207).

A recent research paper reveals that the keratin-associated protein 2-3 (KRTAP2-3) plays a vital role in regulating the dual effects of TGF- β . The study found that the expression of KRTAP2-3 has a correlation with tumor progression in head and neck cancer patients and the migratory and metastatic potentials of oral cancer cells. Furthermore, the study showed that TGF- β generates two populations of mesenchymal cancer cells with differential cell-cycle status through two distinctive EMT pathways mediated by Slug/HMGA2 and KRTAP2-3. The KRTAP2-3-induced expression of ZBED2/ENC1 regulates cell motility and proliferation, suggesting motile cancer cells arrested in the G1 phase as a target to suppress metastasis. Overall, the study highlights the significant role of KRTAP2-3 in orchestrating cancer cell proliferation and migration by inducing EMT and mediating both tumor-suppressive and tumor-promoting effects of TGF- β (208).

Another research paper highlights the role of intracellular cholesterol and the ATP-binding cassette transporter (ABCA1) protein, member 1 of the human transporter sub-family ABCA, in regulating cancer cell proliferation, metastasis, and invasion. The report suggests that ABCA1 mediates the transmembrane transport of free intracellular cholesterol and phospholipids to apo A-I, which maintains the normal metabolism of intracellular cholesterol (209). Overexpression of ABCA1 has been found to enhance drug resistance in non-small cell lung carcinoma cells. The down regulation of ABCA1 in breast cancer has also been associated with a poor prognosis (209, 210). The paper further suggests that targeting ABCA1 could potentially treat lung cancer, with microRNA-200b-3p acting as an oncogene in lung adenocarcinoma cells by targeting ABCA1. Further, another article focuses on Carcinoembryonic antigen-related cell adhesion molecule 1 (CEACAM1) as a therapeutic target in lung diseases. The paper discusses the structure, sub-types, and biological function of CEACAM1 and its potential role in lung diseases. Alterations in CEACAM1 expression and CEACAM1-S/CEACAM1-L ratio have been found to promote the growth and metastasis of non-small cell lung carcinoma (211). CEACAM1 also mediates bacterial adherence and transcellular transcytosis, suppressing immune cell activities and inflammatory responses, which may trigger acute exacerbation of chronic obstructive pulmonary disease. The research work concludes that CEACAM1 can serve as a diagnostic biomarker and therapeutic target in lung diseases, playing a critical role in their development (212).

According to another study, tumors were classified as CEACAM1-positive, and the rest of them were classified as CEACAM1-negative. Patients with CEACAM1-positive tumors had significantly poorer overall and relapse-free survival than those with CEACAM1-negative tumors. These observations seem to contrast with the report of Laack *et al.*, who identified CEACAM1 expression as a prognostic marker for poor outcomes in patients with adenocarcinomas of the lung (213). However, Sienel *et al.* suggested that the unfavorable prognostic influence of CEACAM1 might be derived from its angiogenic impact, leading to an increased angiogenic activity and microvessel density (MVD) in non-small-cell lung cancer. It is also possible that the expression of other CEACAMs in NSCLC cells could overcome the CEACAM1-mediated contact inhibition in these cells (214).

On the other hand, sortilin-related VPS10 domain-containing receptor 2 (SORCS2) contains a VPS10 domain that plays a role in intracellular trafficking and lysosomal processing. Although it differs from other members of the gene family, SORCS2 is mainly located on the cell surface and has been found to be highly expressed in the brain and central nervous system and the developing and adult lungs. Studies hypothesized a role for SORCS2 in clinical outcomes in breast cancer and lymphatic metastasis after treatment for oral carcinoma.

Moreover, SORCS2 gene expression has been strongly related to sensitivity to chemotherapeutics in human gastric cancer cell lines *in-vitro*. The data indicate that rs10937823 mutation in SORCS2 may be associated with overall survival in NSCLC patients. However, additional studies are necessary to determine the function of SORCS2 in NSCLC and establish rs10937823 as a candidate SNP for poor overall survival outcomes in this patient population (215).

Retinoid X receptor beta (RXR-beta) with RAB39A in an axis plays an eminent role in cancer development and stemness, and targeting RAB39A causes inhibiting its downstream molecular effector RXRB strongly impairs tumorigenesis and cancer stemness. Overall, the study highlights the significance of these genes in cancer biology and proposes their potential as prognostic markers or therapeutic targets (216).

The ANK1 (ankyrin-1) is a potential prognostic marker and therapeutic target in both colorectal cancer (CRC) and lung cancer. In CRC, subclonal ANK1 mutations predict poor prognosis independently (217, 218).

In lung cancer, ANK1 knockdown affects the expression of genes and molecular pathways implicated in cancer development and progression. ANK1 also regulates the expression of miR-486-5p, contributing to smoking-induced lung adenocarcinoma (217). The significant correlation between subclonal ANK1 mutation, ANK1-driven genes, and immune cell infiltration suggests its role in guiding immunotherapy strategies for CRC (219).

The nuclear receptor 4A3 (NR4A3), also known as NOR1 or neuron-derived orphan receptor 1, encodes a protein that functions as a transcriptional activator and is part of the Nur77 steroid-thyroid hormone-retinoid receptor superfamily. Fusion mutations in NR4A3 are observed in various cancers, including extraskeletal myxoid chondrosarcoma, lung adenocarcinoma, myxoid chondrosarcoma, astrocytoma, and breast invasive ductal carcinoma, showing the highest prevalence (220-223).

NR4A3 inhibits the proliferation of p53-positive MCF7 breast cancer cells and collaborates with p53 to induce the expression of pro-apoptotic genes. NR4A3 expression correlates with the survival rates of patients with breast and lung cancer, and is altered in 0.05% of all cancers (224, 225). Overall, NR4A3 is a promising target in cancer therapy, with its regulation by p53, anti-proliferative effects, and clinical correlations highlighting its potential significance in cancer treatment (226).

Recently, the impact of RGS2 (Regulator of G-protein signaling 2) expression on clinical outcomes of patients with NSCLC has been determined. Although no significant correlation was found between RGS2 mRNA expression and NSCLC histological subtype, patients with lung adenocarcinoma and elevated RGS2 mRNA expression exhibited significantly reduced overall and disease-free survival rates (227). In contrast, upregulation of RGS2 is related to poor survival in lung adenocarcinoma patients. At the same time, downregulation of RGS2 is associated with increased invasion and metastasis of human non-small cell lung cancer cells. Additionally, the downregulation of RGS2 illustrates a possible tumor suppressor role, but this may not hold for all cancer types. For instance, upregulation of RGS2 is related to poor survival in lung adenocarcinoma patients by losing Med1/TRAP220 (228, 229).

Future studies will investigate the function of other eIF2B-dependent genes, such as RGS2 and VARS2. RGS2 mediates the translational effects of eIF2B in stressed cells and is a regulator of dormancy and tumor relapse in lung adenocarcinomas (230).

RGS2 has emerged as a crucial protein that inhibits the activation of G protein-coupled receptors and eIF2B activity.

Several forms of stress upregulate RGS2 and inhibit protein synthesis, an established response to stress typically achieved via the phosphorylation of the initiation factor, eIF2, to conserve energy and resources. The study uncovers a novel function of RGS2 in the control of protein synthesis, which is unique to RGS2 and not a general characteristic of all RGS proteins. The inhibitory effect of RGS2 on mRNA translation is mediated by a specific region within the RGS2 protein. These novel findings highlight the potential therapeutic value of targeting eIF2B in mutant KRAS lung cancer by investigating its role in translational control, interaction with mutant KRAS, and involvement in MAPK signaling. These exciting discoveries open up a new avenue for research in the field of lung cancer treatment and offer hope to patients suffering from this deadly disease (231).

Meanwhile, Valyl-tRNA synthetase 2 (VARS2) plays a key role in respiratory chain protein synthesis and is a prognostic biomarker of the early stages of colon and breast cancers. VARS2 upregulation by eIF2B may provide a new link between mKRAS and mitochondrial metabolism in tumor cells (232).

Focusing on ABCA1 and CEACAM1 are particularly interesting due to their established roles in cancer among the genes upregulated by eIF2B in mKRAS cells. ABCA1 is known to play a role in drug resistance (233), which may explain the cytoprotective effects of eIF2B against mKRAS drug inhibitors. On the other hand, eIF2B upregulation of CEACAM1 may exert tumoral and immune-mediated effects in mKRAS cancers. Phosphorylation of CEACAM1 by RTKs initiates signaling that activates RAS-MAPK and PI3K-AKT pathways (234).

ABCA1 is also implicated in membrane phosphatidylserine turnover (235), which may partially explain the stimulation of mKRAS binding to the plasma membrane (PM) by eIF2B.

Further, cell imaging experiments provide evidence for the implication of eIF2B associated with mutant KRAS with the plasma membrane of tumor cells (156).

For future studies, we suggest that further experiments will assess whether impairing ABCA1 induces the survival/proliferation of mKRAS cells to increase their susceptibility to mKRAS inhibitors. Additionally, the study will examine whether knocking down ABCA1 decreases phosphatidylserine in PM and impairs mKRAS PM localization.

The study also can examine whether knocking down CEACAM1 impairs the survival and proliferation of mKRAS cells in culture and whether these effects are more robust in tumor cells that are replete rather than depleted of eIF2B. CEACAM1 also functions as an immune checkpoint inhibitor (236).

As such, its upregulation could account for the more substantial tumorigenic effects of eIF2B in mKRAS cells grown in immune-competent than immune-deficient mice. In future experiments, an assessment of whether knocking down CEACAM1 decreases the growth of mouse KRAS G12D lung tumors in immune-competent B6 mice and whether such an effect is more robust in replete rather than eIF2B-deplete tumors can be done.

Correspondingly, KRas4b has more lysosome localization than KRas4a, suggesting that KRas4a and -4b have different intracellular localizations, which may contribute to KRas4a and -4b signaling functions. Although KRas4b is reported to mainly localize on the plasma membrane, Zhang *et al.*'s study illustrated that KRas4b can localize on the lysosome via its interaction with v-ATPase. Another KRas4b interacting protein, eIF2B, is the GEF of eIF2 α , which plays a pivotal role in canonical translation initiation. They suggested that KRas4b, by interacting with eIF2B, may regulate protein translation initiation. These previously unknown interacting proteins and our data show isoform specificity may uncover therapeutic functions or new regulatory mechanisms of KRas4b to overcome drug resistance challenges in cancer (153, 156).

Using crystallography structures of KRAS G12C interacted with SOS1 and eIF2B structures, we demonstrate that the predicted interactions with eIF2B is an important mechanism of mutant KRAS tumorigenesis, which can be reinforced by the somatic mutations in LUAD patients with KRAS G12 mutations. At the same time, its increased expression is linked to poor prognosis and decreased survival rate in LUADs and COADs patients.

Furthermore, our investigation portrayed the effects of inhibiting the translational function of eIF2B on mutant KRAS lung cancer using RNA-seq analysis and immunoblotting. These results showed that downregulating eIF2B by genetic or pharmacological means impaired p-

ERK in human mutant KRAS LUADs, suggesting that knocking down eIF2B translational repression is responsible for downregulating the MAPK pathway. The results also highlighted the importance of eIF2B-dependent genes in tumorigenic pathways in mutant KRAS tumor cells and identified common dysregulated genes in eIF2B and mutant KRAS-mediated signatures.

Hence, innovative therapeutic approaches using ISR inhibitors like ISRIB may be valuable for treating one of the deadliest forms of mutant KRAS-driven cancer. ISRIB functions as a molecular glue by binding to the eIF2B protein in a deep binding pocket between beta and delta subunits that bridges the eIF2B tetramer-tetramer interface. The binding of ISRIB antagonizes the inhibition of eIF2B by phosphorylated Serine 51 eIF2 α in the eIF2B/p-eIF2 α complexes, as it facilitates the assembly of new eIF2B complexes in a conformation that is resistant to inhibition by p-eIF2 α (139).

Our research aims to develop strategies to impair eIF2B in wild-type and mutant KRAS cells to block its translation and regulation signaling by leveraging the proteolysis-targeting chimeras (PROTACs) technology. This study aims to investigate the mechanisms underlying eIF2B's cytoprotective function in tumor cells treated with mKRAS drug inhibitors. Additionally, we explored whether converting ISRIB from an inducer to a destructor of the eIF2B complex using the proteolysis-targeting chimeras (PROTACs) technology is a viable approach to impair mKRAS tumorigenesis. Therefore, utilizing modified ISRIB as ISRIB-PROTACs can suppress eIF2B by targeting it, suggesting anti-tumor effects in human LUAD cells as well.

Two studies have shown promising results in cancer research. Bond *et al.*'s study developed LC-2 as the first PROTAC capable of degrading endogenous KRASG12C, demonstrating the potential of PROTAC-mediated degradation in attenuating KRAS levels and downstream signaling of this oncogene in cancer cells. Zyryanova *et al.*'s research suggests that the phosphorylated alpha subunit of eIF2 and ISRIB bind to eIF2B in a mutually antagonistic manner (150, 176).

While many PROTACs portrayed substantial degradation efficiencies, in parallel, they have weak binders of the POI; such potencies are adequate to elicit a pharmacological response if retained in the final construct.

To demonstrate the potential of a modified ISRIB-derivative to bind eIF2B complex while also being accessible to streptavidin with the IP method, Dr. Jean-Philip Lumb's group in the Department of Chemistry at McGill, synthesized a Biotin derivative compound of ISRIB. Koromilas' lab data successfully showed that a bifunctional derivative of ISRIB could be synthesized to bind eIF2B in complex with mKRAS using a streptavidin-agarose pull-down assay in the cell-free system. A library of ISRIB-PROTACs that links core structure to either CRBN or VHL recruiters has been synthesized through PEG linkers with different lengths. Screening the preliminary library of PROTACs in tumor cells and selecting a single stereoisomer champion for further optimization based on its ability to degrade eIF2B and inactivate mKRAS has been done. The lead compounds tested for their effects on eIF2B subunit degradation, ISR triggering by ATF4 expression and MAPK signaling alteration through p-ERK dysregulation to estimate their effect on cell survival and proliferation, and for future studies, their anti-tumor impacts will be evaluated in xenograft tumor assays in mice.

In preliminary results of unpublished data from Koromilas' lab, a streptavidin-agarose pull-down assay for the eIF2B complex, which was stabilized by the co-expression of KRAS G12V, demonstrated that a bifunctional derivative of ISRIB could be synthesized to bind eIF2B in complex with mKRAS, and that the chosen vector for chemical modification was appropriate for the continued development of a PROTAC.

Several successful PROTAC campaigns have highlighted the importance of linker length, rigidity, and polarity on activity (152, 237). The source for many of these effects remains poorly understood, and there is consensus that a small library of PROTACs should be evaluated in the initial stages of development. Therefore, Lumb's group has created a small library of ISRIB-PROTACs that links the core structure of ISRIB to either CRBN or VHL recruiters through linkers with different lengths of 2, 6, and 11 PEG units. The aim of the study was to assess the adequacy of linker length for binding to eIF2B and recruiting CRBN or VHL to activate the PROTAC degradation pathway; so, the longer linkers probably are capable of positioning the CRBN or VHL domains beyond the eIF2B γ -subunit to escape the immediate steric bulk forcefield of eIF2B complex and recruiting the associated ligase.

The findings indicate that the shortest PEG linker (n=2) is not sufficiently long to recruit CRBN or VHL. In contrast, PROTACs 6 and 11, with significantly longer PEG linker chains, may recruit E3 ligase ligands on these planes, which suggests that PEG6 and PEG11-linker PROTACs may be long enough to escape the steric bulk of eIF2B and recruit CRBN or VHL.

Experimental screening of these LEADs library data presented a low ability to degrade endogenous eIF2B subunits and trigger ISR by ATF4 upregulation, ISRIB PROTACs examined in human HEK293T cells in different concentrations and time points.

As these LEAD compounds of PROTAC generated from ISRIB were ineffective, some possibilities and reasons for these results can be illustrated, including that the permeability of ISRIB to the cell is low and it can not reach functional concentration or effect. Probably, compounds can not diffuse across the lipid bilayer or other parts of the cell membrane, so testing the ISRIB-PROTACs in protein extract of the cell (cell-free system approach) has been done in Koromilas' lab and the result shows the compound is effective. The biotinylated forms of the ISRIB-PROTACs, with streptavidin beads in IP experiments, used with overexpression of wild-type and mutant KRAS and MYC-eIF2B5 and flag-KRAS in HEK293T cells protein extract (cell-free system), displayed interaction between mutant KRAS (4B-G12V) with eIF2B in this system and the ISRIB-biotinylated is functional as ISRIB-PROTACs are.

Further experiments have been done in H358 cells with mKRAS, pre- and post-stress by thapsigargin, which activates the UPR, to simulate tumor stress under different conditions, such as treatment in cells with PROTAC controls, ISRIB, and LEAD treatment impacts.

ISRIB-Biotin acts as a weaker inducer for eIF2B (based on ATF4 expression) and has a higher impact on KRAS downstream activity by increasing p-ERK in comparison with ISRIB and ISRIB-linker (PEG4).

Although the pattern of knockdown of eIF2B5 with ISRIB-PROTAC treatment was not as efficient as impairing it with si/sh-RNA, on downstream pathways. LUAD has relatively low expression of p-ERK and ATF4 in CRBN or VHL with linker with 6 PEGs during stress status, suggesting that these compounds may have reduced eIF2B or KRAS signaling activity,

mirroring the potential function of these compounds for combination therapy with other drug treatment.

Among all compounds, it seems that the ISRIB-PROTACs effect is concentration dependent, as observed in altering ATF4 with PEG6 linker (CRBN or VHL) illustrated a similar impact on ATF4 during stress with ISRIB. However, p-ERK regulations, considering MAPK signaling, are dose-dependent for ISRIB-PROTACs in pre-stress conditions, as no significant alterations were observed during stress.

The data show that the ISRIB-PROTACs act as weak inducers like ISRIB for eIF2B based on ATF4 in stress status during cell culture treatment, and these LEAD compounds are effective *in-vitro*.

The data also suggest the stabilization of the KRAS-eIF2B-SOS1, which affected downstream pathways, including MAPK, by changing p-ERK.

Another limitation of these compounds' function is that eIF2B interacting proteins may prevent the E3 ligase of PROTACs from accessing eIF2B as the target. Furthermore, the study revealed that the PEG6-linker PROTAC can form the ternary complex with VHL, to interact with E3 ligase. Notably, VHL is significantly smaller than CRBN, implying that less steric penalty is expected when forming the ternary complex of the PROTAC system.

Mass spectrometry for lysate of IP for eIF2B will illustrate auxiliary proteins that interact with eIF2B. Also, trying different PEG lengths to change the compound's permeability is another solution for these mentioned challenges. The team will choose the two most effective ISRIB PROTACs and further optimize them as required. The work serves as a proof-of-principle approach for the design of new strategies to target protein synthesis machinery in cells and may have significant implications for developing effective therapies for viral infections.

In the future, the lead compounds will be further tested for their effects on mKRAS cell survival and proliferation (IC50 assays, colony formation assays). Its ability to target mRNA translation will be assessed in polysome profile assays by examining the translatability of eIF2B-dependent mRNAs with roles in the mKRAS cell proliferation and/or resistance to

mKRAS inhibition. The lead compound will eventually be tested for its anti-tumor effects in xenograft tumor assays in mice compared with the ISRIB compound (142).

The study proposes the use of a cutting-edge technology called proteolysis-targeting chimeras (PROTACS) to develop effective strategies that can impair eIF2B in infected cells and block viral gene translation. The researchers aim to create an ISRIB PROTAC by chemically linking an E3 recruiting ligand to ISRIB, which can convert it from an activator to a degrader of eIF2B. To achieve this, the Lumb Group will make a chemical modification to ISRIB that links an E3 recruiting ligand without disrupting its affinity for eIF2B.

Nanomolar affinity for the eIF2B binding pocket. The Lumb group will create a small library of ISRIBPROTACs by replacing the carboxyfluorescein dye with a suitable E3 recruiter. After screening the compounds in human HEK293T cells, the team will select two lead ISRIBPROTACs. The Koromilas lab will then perform a screening of the ISRIB-PROTACs libraries synthesized by the Lumb lab to identify hit ISRIB-PROTACs with the highest ability to degrade endogenous eIF2B and stimulate the synthesis of ATF4 in HEK293 cells. Finally, the two most effective ISRIB-PROTACs will be further optimized as required. This work serves as a proof-of-principle approach for designing new methods to target protein synthesis machinery in cells and may have significant implications for developing effective therapies for viral infections.

These data support the notion that inhibiting the translational function of eIF2B can efficiently impair p-ERK in human mutant KRAS LUADs. So, expect to reproduce these dysregulations through ISRIB-PROTACs treatment in cancer cells.

Consistent with the eIF2B-dependent regulation of MAPK responses observed in our RNA-seq analysis with immunoblotting results, we assumed ISRIB-PROTACs treatment was likewise able to diffuse into cell and interact with eIF2B complex, while not able to degrade it to trigger ISR by inducing ATF4 expression, so the evaluation of ATF4 and p-ERK proteins were done in H358 cells pre and pro stress by thapsigargin treatment and ISRIB used as control in 1 and 3 hours with 20uM concentration (Figure 3.14 C,D and 3.14 C, D) .

Eukaryotic initiation factor 2B (eIF2B), a five subunit guanine nucleotide exchange factor (GEF), plays a key role in regulating mRNA translation. Expression of its epsilon-subunit is specifically upregulated in certain conditions associated with increased cell growth.

Therefore, the present study aimed to examine the effect of repressing eIF2B5 expression on growth rate, protein synthesis, and other characteristics of two tumorigenic cell lines that display upregulated expression of the epsilon-subunit. Experiments were designed to compare spontaneously transformed fibroblasts (TMEF's) to TMEFs infected with a lentivirus containing a short hairpin (sh)RNA directed against eIF2B5. Cells expressing the shRNA displayed a reduction in eIF2B5 abundance to 30% of the value observed in uninfected TMEF's with no change in the expression of any of the other four subunits. Reductions in GEF activity and global rates of protein synthesis accompanied the repression of eIF2B5 expression. Moreover, repressed eIF2B5 expression led to marked reductions in cell growth rate in culture, colony formation in soft agar, and tumor progression in nude mice. Similar results were obtained in MCF-7 human breast cancer cells in which eIF2B5 expression was repressed through transient transfection with a siRNA directed against the epsilon-subunit. Overall, the results support a role for eIF2B5 in regulating cell growth and suggest that it might represent a therapeutic target for treating human cancer.(citation)

Our study portrays the adaptive mutant KRAS and eIF2B interaction as an essential component of tumorigenesis and a valid target of therapeutic intervention for mutant KRAS cancer treatment.

4.2 Conclusion

eIF2B enables high proliferative capacity in mKRAS lung and colon tumor cells due to the induction of the MAPK pathway. Nevertheless, RNA seq data analysis reveals the importance of other tumorigenic programs employed by eIF2B that are essential for mKRAS tumor growth, survival, and differentiation. Our findings demonstrate a new role and function of eIF2B, making it a potential therapeutic vulnerability for treating mKRAS cancers by impairing it to overcome translational and MAPK roles in drug resistance.

Furthermore, Our study aimed to impair p-ERK signaling in mutant KRAS lung adenocarcinomas using ISRIB-PROTACs treatment as a degrader of eIF2B. However, the expected impairment has not been observed as hypothesized, highlighting the complexity of cellular signaling pathways. Despite the unexpected findings, our study provides valuable insights for future therapeutic interventions in these challenging diseases.

Appendices

Figure Supplementary 1. PCA plot. These plots shown the clusters of samples based on their similarity in impaired and intact eIF2B groups in H358 cells treated with shRNA-eIF2B5 (A), H358 cells treated with siRNA-eIF2B5 (B), HCT116 (C) and HK2-8 (D) cells treated with siRNA-eIF2B5, respectively.

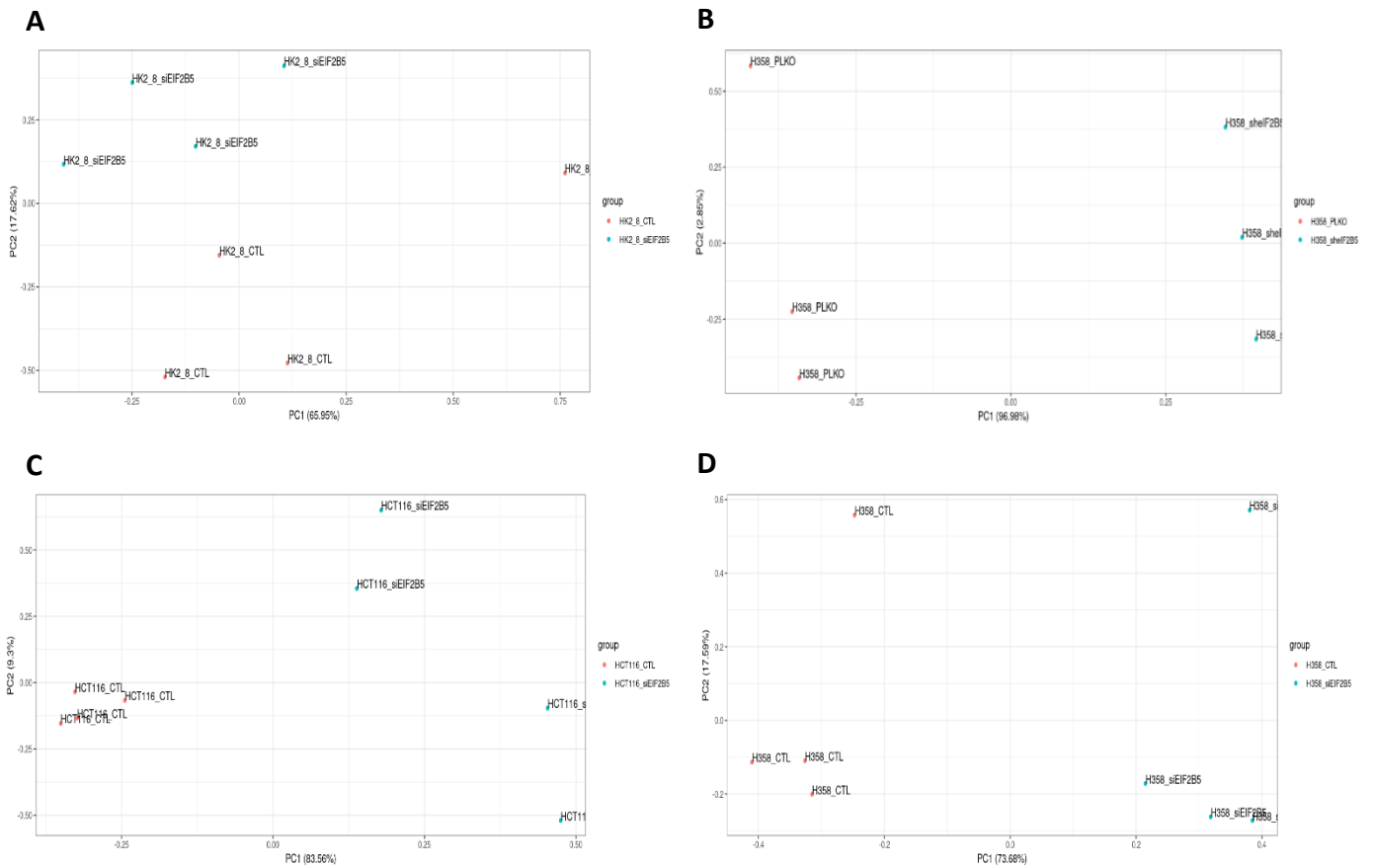


Table Supplementary 1. List of eIF2B upregulated Gene Ontology enrichment signature identified in Biological Pathway analyses. The identified pathways represent 20 top hits in four model cells

Cell line	Hs_BP_ID	Description	GeneRatio	pvalue	p.adjust	Count	FoldEnrich	RichFactor
H358-shRNA (eIF2B5)	GO:0045229	external encapsulating structure organization	0.039596	5.33E-25	1.85E-21	141	2.31413	0.437888
	GO:0030198	extracellular matrix organization	0.039315	6.02E-25	1.85E-21	140	2.319327	0.438871
	GO:0043062	extracellular structure organization	0.039315	8.74E-25	1.85E-21	140	2.312079	0.4375
	GO:0010975	regulation of neuron projection development	0.039876	1.41E-10	1.59E-07	142	1.649307	0.312088
	GO:0051216	cartilage development	0.021623	1.64E-10	1.59E-07	77	2.004561	0.37931
	GO:0030199	collagen fibril organization	0.009829	1.76E-10	1.59E-07	35	2.890098	0.546875
	GO:0034329	cell junction assembly	0.039034	2.46E-10	1.95E-07	139	1.647041	0.311659
	GO:0001667	ameboid-type cell migration	0.042123	6.18E-10	4.36E-07	150	1.594995	0.301811
	GO:0061564	axon development	0.041281	1.69E-09	1.07E-06	147	1.582196	0.299389
	GO:0061448	connective tissue development	0.026116	2.68E-09	1.48E-06	93	1.787207	0.338182
	GO:0050900	leukocyte migration	0.034541	2.80E-09	1.48E-06	123	1.645631	0.311392
	GO:0050808	synapse organization	0.039596	3.65E-09	1.65E-06	141	1.582059	0.299363
	GO:0032963	collagen metabolic process	0.013199	3.65E-09	1.65E-06	47	2.299846	0.435185
	GO:0010977	negative regulation of neuron projection development	0.016007	4.58E-09	1.94E-06	57	2.106509	0.398601
	GO:0060840	artery development	0.013199	5.25E-09	2.08E-06	47	2.278746	0.431193
	GO:0048568	embryonic organ development	0.038192	5.65E-09	2.11E-06	136	1.586592	0.300221
	GO:0060047	heart contraction	0.02387	6.25E-09	2.20E-06	85	1.811306	0.342742
	GO:0003018	vascular process in circulatory system	0.024993	8.53E-09	2.85E-06	89	1.774879	0.335849
	GO:0007411	axon guidance	0.022185	1.53E-08	4.14E-06	79	1.823124	0.344978
	GO:0048705	skeletal system morphogenesis	0.022185	1.53E-08	4.14E-06	79	1.823124	0.344978
H358-siRNA (eIF2B5)	GO:0045229	external encapsulating structure organization	0.077739	3.94E-09	1.44E-05	22	4.543358	0.068323
	GO:0060326	cell chemotaxis	0.074205	1.31E-08	1.66E-05	21	4.447334	0.066879
	GO:0030198	extracellular matrix organization	0.074205	1.72E-08	1.66E-05	21	4.377627	0.065831
	GO:0043062	extracellular structure organization	0.074205	1.82E-08	1.66E-05	21	4.363947	0.065625
	GO:0050900	leukocyte migration	0.081272	3.49E-08	2.55E-05	23	3.872049	0.058228
	GO:0043410	positive regulation of MAPK cascade	0.084806	5.77E-07	0.000352	24	3.204734	0.048193
	GO:0097530	granulocyte migration	0.045936	7.53E-07	0.000365	13	5.506223	0.082803
	GO:0097529	myeloid leukocyte migration	0.056537	8.52E-07	0.000365	16	4.396577	0.066116
	GO:0030595	leukocyte chemotaxis	0.056537	9.00E-07	0.000365	16	4.378484	0.065844
	GO:0043588	skin development	0.063604	1.06E-06	0.000388	18	3.88626	0.058442

	GO:0071622	regulation of granulocyte chemotaxis	0.028269	1.17E-06	0.000388	8	10.03747	0.150943
	GO:0002685	regulation of leukocyte migration	0.053004	2.00E-06	0.00061	15	4.374884	0.065789
	GO:0031589	cell-substrate adhesion	0.067138	2.33E-06	0.000654	19	3.519405	0.052925
	GO:0010758	regulation of macrophage chemotaxis	0.021201	3.13E-06	0.000816	6	14.24962	0.214286
	GO:0042060	wound healing	0.074205	3.37E-06	0.000821	21	3.181009	0.047836
	GO:0071621	granulocyte chemotaxis	0.038869	5.07E-06	0.001158	11	5.541519	0.083333
	GO:1902624	positive regulation of neutrophil migration	0.021201	1.04E-05	0.002225	6	11.73498	0.176471
	GO:0048015	phosphatidylinositol-mediated signaling	0.042403	1.25E-05	0.002547	12	4.612594	0.069364
	GO:0045785	positive regulation of cell adhesion	0.074205	1.45E-05	0.002683	21	2.891228	0.043478
	GO:0002687	positive regulation of leukocyte migration	0.038869	1.51E-05	0.002683	11	4.942436	0.074324
HCT116-siRNA (eIF2B5)	GO:0006520	amino acid metabolic process	0.123077	7.71E-06	0.009518	8	7.851473	0.027119
	GO:0042149	cellular response to glucose starvation	0.061538	2.44E-05	0.009518	4	23.63454	0.081633
	GO:0046942	carboxylic acid transport	0.123077	2.76E-05	0.009518	8	6.58007	0.022727
	GO:0015849	organic acid transport	0.123077	2.82E-05	0.009518	8	6.56143	0.022663
	GO:0036003	positive regulation of transcription from RNA polymerase II promoter in response to stress	0.046154	3.09E-05	0.009518	3	48.25385	0.166667
	GO:0089718	amino acid import across plasma membrane	0.061538	3.10E-05	0.009518	4	22.27101	0.076923
	GO:0034976	response to endoplasmic reticulum stress	0.107692	3.43E-05	0.009518	7	7.676748	0.026515
	GO:0015804	neutral amino acid transport	0.061538	4.78E-05	0.011591	4	19.96711	0.068966
	GO:0070059	intrinsic apoptotic signaling pathway in response to endoplasmic reticulum stress	0.061538	7.05E-05	0.014742	4	18.09519	0.0625
	GO:0042594	response to starvation	0.092308	7.93E-05	0.014742	6	8.391973	0.028986
	GO:1901605	alpha-amino acid metabolic process	0.092308	8.36E-05	0.014742	6	8.311667	0.028708
	GO:0015711	organic anion transport	0.123077	0.000118	0.019064	8	5.349156	0.018476
	GO:1902475	L-alpha-amino acid transmembrane transport	0.061538	0.00016	0.021973	4	14.6594	0.050633
	GO:0015807	L-amino acid transport	0.061538	0.000223	0.021973	4	13.46619	0.046512
	GO:0031667	response to nutrient levels	0.123077	0.000228	0.021973	8	4.855733	0.016771
	GO:1905039	carboxylic acid transmembrane transport	0.076923	0.000228	0.021973	5	9.047596	0.03125
	GO:0010232	vascular transport	0.061538	0.000233	0.021973	4	13.31141	0.045977
	GO:0150104	transport across blood-brain barrier	0.061538	0.000233	0.021973	4	13.31141	0.045977
	GO:1903825	organic acid transmembrane transport	0.076923	0.000235	0.021973	5	8.9914	0.031056

	GO:0032633	interleukin-4 production	0.046154	0.000238	0.021973	3	24.81626	0.085714
HK2-8-siRNA (eIF2B5)	GO:0000101	sulfur amino acid transport	0.105263	7.48E-05	0.012854	2	152.3806	0.153846
	GO:0006750	glutathione biosynthetic process	0.105263	0.000115	0.012854	2	123.8092	0.125
	GO:0002476	antigen processing and presentation of endogenous peptide antigen via MHC class Ib	0.105263	0.00013	0.012854	2	116.5263	0.117647
	GO:0002484	antigen processing and presentation of endogenous peptide antigen via MHC class I via ER pathway	0.105263	0.00013	0.012854	2	116.5263	0.117647
	GO:0019184	nonribosomal peptide biosynthetic process	0.105263	0.00013	0.012854	2	116.5263	0.117647
	GO:0002428	antigen processing and presentation of peptide antigen via MHC class Ib	0.105263	0.000146	0.012854	2	110.0526	0.111111
	GO:0019885	antigen processing and presentation of endogenous peptide antigen via MHC class I	0.105263	0.000241	0.016731	2	86.12815	0.086957
	GO:0002475	antigen processing and presentation via MHC class Ib	0.105263	0.000286	0.016731	2	79.23789	0.08
	GO:0002483	antigen processing and presentation of endogenous peptide antigen	0.105263	0.000286	0.016731	2	79.23789	0.08
	GO:0071549	cellular response to dexamethasone stimulus	0.105263	0.000334	0.016745	2	73.36842	0.074074
	GO:0042886	amide transport	0.210526	0.000369	0.016745	4	11.28745	0.011396
	GO:0015813	L-glutamate transmembrane transport	0.105263	0.000386	0.016745	2	68.30853	0.068966
	GO:0051938	L-glutamate import	0.105263	0.000413	0.016745	2	66.03158	0.066667
	GO:0019883	antigen processing and presentation of endogenous antigen	0.105263	0.00047	0.017708	2	61.90461	0.0625
	GO:0002474	antigen processing and presentation of peptide antigen via MHC class I	0.105263	0.000596	0.020942	2	55.02632	0.055556
	GO:0001916	positive regulation of T cell mediated cytotoxicity	0.105263	0.000736	0.022823	2	49.52368	0.05
	GO:0009069	serine family amino acid metabolic process	0.105263	0.000736	0.022823	2	49.52368	0.05
	GO:0071548	response to dexamethasone	0.105263	0.000851	0.024909	2	46.06854	0.046512
	GO:0072337	modified amino acid transport	0.105263	0.001104	0.028843	2	40.4275	0.040816
	GO:1901605	alpha-amino acid metabolic process	0.157895	0.001147	0.028843	3	14.21733	0.014354

Table supplementary 2. List of eIF2B downregulated Gene Ontology enrichment signature identified in Biological Pathway analyses. The identified pathways represent 20 top hits in four model cells

Cell line	Hs_BP_ID	Description	GeneRatio	pvalue	p.adjust	Count	FoldEnrich	RichFactor
H358-shRNA (eIF2B5)	GO:0140014	mitotic nuclear division	0.034912	1.97E-19	1.28E-15	311	1.434535	0.679039
	GO:0044772	mitotic cell cycle phase transition	0.035249	1.39E-17	4.50E-14	314	1.405413	0.665254
	GO:0022411	cellular component disassembly	0.036372	9.73E-17	1.85E-13	324	1.385589	0.65587
	GO:0006260	DNA replication	0.022339	1.32E-16	1.85E-13	199	1.512254	0.715827
	GO:0016032	viral process	0.031994	1.43E-16	1.85E-13	285	1.413356	0.669014
	GO:0043161	proteasome-mediated ubiquitin-dependent protein catabolic process	0.033004	2.34E-15	2.53E-12	294	1.386391	0.65625
	GO:0007059	chromosome segregation	0.032555	5.85E-15	5.43E-12	290	1.382963	0.654628
	GO:1901987	regulation of cell cycle phase transition	0.033229	5.38E-14	4.37E-11	296	1.362371	0.64488
	GO:0016055	Wnt signaling pathway	0.033453	9.49E-14	6.68E-11	298	1.356796	0.642241
	GO:0198738	cell-cell signaling by wnt	0.033565	1.03E-13	6.68E-11	299	1.355507	0.641631
	GO:1903829	positive regulation of protein localization	0.033565	2.26E-13	1.33E-10	299	1.349714	0.638889
	GO:2001020	regulation of response to DNA damage stimulus	0.023574	5.75E-13	3.11E-10	210	1.421939	0.673077
	GO:0016570	histone modification	0.034351	8.02E-13	4.01E-10	306	1.335649	0.632231
	GO:0051054	positive regulation of DNA metabolic process	0.022901	1.18E-12	5.47E-10	204	1.422341	0.673267
	GO:0007264	small GTPase mediated signal transduction	0.034239	2.25E-12	9.75E-10	305	1.328539	0.628866
	GO:0000819	sister chromatid segregation	0.019645	3.84E-12	1.50E-09	175	1.44982	0.686275
	GO:0030111	regulation of Wnt	0.025034	3.92E-12	1.50E-09	223	1.389701	0.657817

		signaling pathway						
	GO:0042176	regulation of protein catabolic process	0.026605	6.30E-12	2.10E-09	237	1.37174	0.649315
	GO:1903320	regulation of protein modification by small protein conjugation or removal	0.019645	6.48E-12	2.10E-09	175	1.444157	0.683594
	GO:0032984	protein-containing complex disassembly	0.018972	7.81E-12	2.42E-09	169	1.451336	0.686992
H358-siRNA (eIF2B5)	GO:0002064	epithelial cell development	0.025294	6.37E-15	4.06E-11	86	2.266714	0.409524
	GO:0031589	cell-substrate adhesion	0.035882	2.41E-13	7.69E-10	122	1.880975	0.339833
	GO:0042060	wound healing	0.040882	2.35E-12	5.00E-09	139	1.75254	0.316629
	GO:1903829	positive regulation of protein localization	0.042059	2.14E-11	2.52E-08	143	1.69125	0.305556
	GO:0007264	small GTPase mediated signal transduction	0.043235	2.18E-11	2.52E-08	147	1.677619	0.303093
	GO:0022411	cellular component disassembly	0.043824	2.37E-11	2.52E-08	149	1.669464	0.301619
	GO:0045785	positive regulation of cell adhesion	0.042941	3.17E-11	2.89E-08	146	1.673106	0.302277
	GO:0007160	cell-matrix adhesion	0.024706	1.91E-10	1.53E-07	84	1.945356	0.351464
	GO:0048762	mesenchymal cell differentiation	0.025588	5.13E-10	3.64E-07	87	1.888412	0.341176
	GO:0001667	ameboidal-type cell migration	0.042647	5.84E-10	3.73E-07	145	1.614839	0.291751
	GO:0150115	cell-substrate junction organization	0.013235	1.49E-09	8.47E-07	45	2.418204	0.436893
	GO:0016032	viral process	0.037353	1.59E-09	8.47E-07	127	1.650106	0.298122
	GO:0097193	intrinsic apoptotic signaling pathway	0.028529	2.11E-09	1.04E-06	97	1.777798	0.321192
	GO:0097191	extrinsic apoptotic signaling pathway	0.022941	3.45E-09	1.57E-06	78	1.893553	0.342105

	GO:0010810	regulation of cell-substrate adhesion	0.022059	1.27E-08	5.40E-06	75	1.869932	0.337838
	GO:0001837	epithelial to mesenchymal transition	0.018235	1.48E-08	5.56E-06	62	1.995174	0.360465
	GO:1904951	positive regulation of establishment of protein localization	0.029412	1.48E-08	5.56E-06	100	1.703077	0.307692
	GO:0001885	endothelial cell development	0.009118	1.71E-08	6.06E-06	31	2.723571	0.492063
	GO:0090132	epithelium migration	0.032647	2.20E-08	7.39E-06	111	1.642741	0.296791
	GO:0090130	tissue migration	0.032941	2.46E-08	7.83E-06	112	1.635673	0.295515
HCT116-siRNA(eIF2B5)	GO:0036003	positive regulation of transcription from RNA polymerase II promoter in response to stress	0.013255	3.57E-09	1.82E-05	9	13.85788	0.5
	GO:0034976	response to endoplasmic reticulum stress	0.045655	7.93E-09	2.02E-05	31	3.254502	0.117424
	GO:0070059	intrinsic apoptotic signaling pathway in response to endoplasmic reticulum stress	0.020619	4.99E-08	8.48E-05	14	6.062822	0.21875
	GO:0034620	cellular response to unfolded protein	0.025037	7.29E-08	9.28E-05	17	4.807836	0.173469
	GO:0031667	response to nutrient levels	0.061856	1.00E-07	0.000102	42	2.440381	0.08805
	GO:0042594	response to starvation	0.036819	1.29E-07	0.000109	25	3.347314	0.120773
	GO:0051384	response to glucocorticoid	0.029455	1.92E-07	0.000137	20	3.903628	0.140845
	GO:0042060	wound healing	0.057437	2.29E-07	0.000137	39	2.46222	0.088838
	GO:0089718	amino acid import across plasma membrane	0.017673	2.42E-07	0.000137	12	6.395944	0.230769
	GO:0071496	cellular response to external stimulus	0.047128	3.37E-07	0.000171	32	2.712245	0.097859

	GO:1990440	positive regulation of transcription from RNA polymerase II promoter in response to endoplasmic reticulum stress	0.008837	8.54E-07	0.000334	6	15.11769	0.545455
	GO:0043618	regulation of transcription from RNA polymerase II promoter in response to stress	0.014728	8.62E-07	0.000334	10	7.106605	0.25641
	GO:0006986	response to unfolded protein	0.027982	8.64E-07	0.000334	19	3.708447	0.133803
	GO:0031589	cell-substrate adhesion	0.048601	9.18E-07	0.000334	33	2.547688	0.091922
	GO:0035967	cellular response to topologically incorrect protein	0.025037	1.14E-06	0.000386	17	3.992948	0.144068
	GO:1902041	regulation of extrinsic apoptotic signaling pathway via death domain receptors	0.0162	1.29E-06	0.00041	11	6.097467	0.22
	GO:0010755	regulation of plasminogen activation	0.010309	1.74E-06	0.00052	7	10.77835	0.388889
	GO:0031960	response to corticosteroid	0.029455	2.39E-06	0.000668	20	3.339248	0.120482
	GO:0050818	regulation of coagulation	0.019146	2.52E-06	0.000668	13	4.804065	0.173333
	GO:0008625	extrinsic apoptotic signaling pathway via death domain receptors	0.020619	2.62E-06	0.000668	14	4.460007	0.16092
HK2-8-siRNA (eIF2B5)	GO:0006260	DNA replication	0.030506	6.73E-10	4.17E-06	73	2.065056	0.26259
	GO:0071897	DNA biosynthetic process	0.028416	2.17E-09	6.72E-06	68	2.072732	0.263566
	GO:0008380	RNA splicing	0.04346	8.04E-09	1.66E-05	104	1.736466	0.220807
	GO:2001020	regulation of response to DNA	0.030924	5.70E-08	8.46E-05	74	1.865224	0.237179

		damage stimulus						
	GO:0010948	negative regulation of cell cycle process	0.031341	6.83E-08	8.46E-05	75	1.848947	0.23511
	GO:0140014	mitotic nuclear division	0.040953	1.09E-07	9.47E-05	98	1.68273	0.213974
	GO:0042770	signal transduction in response to DNA damage	0.020894	1.20E-07	9.47E-05	50	2.125456	0.27027
	GO:0031331	positive regulation of cellular catabolic process	0.040535	1.22E-07	9.47E-05	97	1.683943	0.214128
	GO:2000278	regulation of DNA biosynthetic process	0.015462	1.84E-07	0.000127	37	2.404751	0.305785
	GO:0044772	mitotic cell cycle phase transition	0.041371	2.56E-07	0.000147	99	1.64948	0.209746
	GO:0009060	aerobic respiration	0.02173	2.60E-07	0.000147	52	2.044689	0.26
	GO:0006898	receptor-mediated endocytosis	0.026327	3.23E-07	0.000166	63	1.891007	0.240458
	GO:0018393	internal peptidyl-lysine acetylation	0.018387	5.80E-07	0.000277	44	2.135952	0.271605
	GO:0018394	peptidyl-lysine acetylation	0.019223	6.30E-07	0.000279	46	2.091056	0.265896
	GO:0006475	internal protein amino acid acetylation	0.018387	8.38E-07	0.000345	44	2.109904	0.268293
	GO:0016573	histone acetylation	0.017551	9.22E-07	0.000345	42	2.144778	0.272727
	GO:0034976	response to endoplasmic reticulum stress	0.025909	9.48E-07	0.000345	62	1.846892	0.234848
	GO:0045786	negative regulation of cell cycle	0.035938	1.01E-06	0.000345	86	1.665813	0.211823
	GO:0006261	DNA-templated DNA replication	0.017969	1.06E-06	0.000345	43	2.1135	0.26875
	GO:0018205	peptidyl-lysine modification	0.033849	1.28E-06	0.000396	81	1.685183	0.214286

Table Supplementary 3. List of overlapped dysregulated genes by eIF2B transcriptional signature identified in different groups.

Up regulated genes by eIF2B	
Groups	Gene ID
H358(sh-eIF2B5/PLKO) vs. H358(si-eIF2B5/si-Control)	MAP2, ANKRD35, SELENBP1, MMP13, LRRC10B, ST6GALNAC1, KDR, PLEKHS1, TLE4, CRYM, MUC13, DDIT4L, DAPK2, PIPOX, RND1, HSPA2, SELENOP, RASSF4, CYP2B7P, BHLHE41, NRCAM, ZNF469, ABCA13, ATP6V0A4, THBS4, PIGR, IL6, PRR15L, BMP5, DACH1, KIT, SALL2, BPI, TMOD1, CAVIN2, CDH5, LINC00626, AXIN2, LINC01963, LRRC4, LEF1, HGD, PLIN4, RIPOR2, LOXL4, BASP1-AS1, CXCL17, RCBTB2, CTTNBP2, FOLR1
H358(sh-eIF2B5/PLKO) vs. HCT116(si-eIF2B5/si-Control)	ABCA1, SORCS2 , CEACAM1 , ANK1 , RXRB , RGS2 , NR4A3 , VARS2
H358(sh-eIF2B5/PLKO) vs. HK2-8(si-eIF2B5/si-Control)	FBN1, TAP2
H358(si-eIF2B5/si-Control) vs. HCT116(si-eIF2B5/si-Control)	TRIM22, CD36
HCT116(si-eIF2B5/si-Control) vs. HK2-8(si-eIF2B5/si-Control)	ASMTL
All groups	eIF2B5
Down regulated genes by eIF2B	
Groups	Gene ID
H358(sh-eIF2B5/PLKO) vs. H358(si-eIF2B5/si-Control)	ADAM8, MPZL3, KRT6A, S100A2, CD274, EREG, GJB3, MALL, LETM2, MIR100HG, ARL14EPL, TRIM27, LINC02154, PPP2R3B, MIR31HG, MKX, LINC01088, GCOM1, LOC101929297, RYR1, FAM166B, LINC01338
H358(sh-eIF2B5/PLKO) vs. H358(si-eIF2B5/si-Control) vs. HCT116(si-eIF2B5/si-Control)	RBP1, IL20RB, KRTAP2-3
H358(sh-eIF2B5/PLKO) vs. HCT116(si-eIF2B5/si-Control)	DUSP6, GPT2, KLK10, WWC3, SLC6A9, FUT3
H358(sh-eIF2B5/PLKO) vs. HK2-8(si-eIF2B5/si-Control)	IFI44, DHRS2, FAM241A
H358(si-eIF2B5/si-Control) vs. HCT116(si-eIF2B5/si-Control)	NT5E, CPA4, KLF2, RPPH1, CD22, KDM7A-DT
HCT116(si-eIF2B5/si-Control) vs. HK2-8(si-eIF2B5/si-Control)	CHAC1, PCK2, SLC7A11, TRIB3, PSAT1, STC2, SLC1A4, ULBP1, DDIT4, TSC22D3, ASNS, CSTA
All groups	-

References

1. Doll R, Peto R. The causes of cancer: quantitative estimates of avoidable risks of cancer in the United States today. *JNCI: Journal of the National Cancer Institute*. 1981;66(6):1192-308.
2. Hanahan D, Weinberg RAJ. The hallmarks of cancer review. 2000;100(1):57-70.
3. Lee EY, Muller WJ. Oncogenes and tumor suppressor genes. *Cold Spring Harbor perspectives in biology*. 2010;2(10):a003236.
4. Normanno N, De Luca A, Bianco C, Strizzi L, Mancino M, Maiello MR, et al. Epidermal growth factor receptor (EGFR) signaling in cancer. *Gene*. 2006;366(1):2-16.
5. Sung H, Ferlay J, Siegel RL, Laversanne M, Soerjomataram I, Jemal A, et al. Global Cancer Statistics 2020: GLOBOCAN Estimates of Incidence and Mortality Worldwide for 36 Cancers in 185 Countries. *CA Cancer J Clin*. 2021;71(3):209-49.
6. Latimer KM, Mott TF. Lung cancer: diagnosis, treatment principles, and screening. *American family physician*. 2015;91(4):250-6.
7. Nikolić MZ, Sun D, Rawlins EL. Human lung development: recent progress and new challenges. *Development*. 2018;145(16):dev163485.
8. Testa U, Castelli G, Pelosi E. Lung cancers: molecular characterization, clonal heterogeneity and evolution, and cancer stem cells. *Cancers*. 2018;10(8):248.
9. Lynch TJ, Bell DW, Sordella R, Gurubhagavatula S, Okimoto RA, Brannigan BW, et al. Activating mutations in the epidermal growth factor receptor underlying responsiveness of non–small-cell lung cancer to gefitinib. *New England Journal of Medicine*. 2004;350(21):2129-39.
10. Fukuoka M, Wu Y-L, Thongprasert S, Sunpaweravong P, Leong S-S, Sriuranpong V, et al. Biomarker analyses and final overall survival results from a phase III, randomized, open-label, first-line study of gefitinib versus carboplatin/paclitaxel in clinically selected patients with advanced non–small-cell lung cancer in Asia (IPASS). *Journal of clinical oncology*. 2011;29(21):2866-74.
11. Riely GJ, Kris MG, Rosenbaum D, Marks J, Li A, Chitale DA, et al. Frequency and distinctive spectrum of KRAS mutations in never smokers with lung adenocarcinoma. *Clinical cancer research*. 2008;14(18):5731-4.
12. Marchetti A, Felicioni L, Malatesta S, Grazia Sciarrotta M, Guetti L, Chella A, et al. Clinical features and outcome of patients with non–small-cell lung cancer harboring BRAF mutations. *Journal of clinical oncology*. 2011;29(26):3574-9.
13. Julien SG, Dubé N, Read M, Penney J, Paquet M, Han Y, et al. Protein tyrosine phosphatase 1B deficiency or inhibition delays ErbB2-induced mammary tumorigenesis and protects from lung metastasis. *Nature genetics*. 2007;39(3):338-46.
14. Collisson E, Campbell J, Brooks A, Berger A, Lee W, Chmielecki J, et al. Comprehensive molecular profiling of lung adenocarcinoma: The cancer genome atlas research network. *Nature*. 2014;511(7511):543-50.
15. Lufen Chang MK. Mammalian MAP kinase signalling cascades. *Nature*. 2001;410(6824):37-40.
16. Lavoie H, Therrien M. Regulation of RAF protein kinases in ERK signalling. *Nature reviews Molecular cell biology*. 2015;16(5):281-98.
17. Harvey J. An unidentified virus which causes the rapid production of tumours in mice. *Nature*. 1964;204(4963):1104-5.

18. Kirsten W, Mayer LA. Morphologic responses to a murine erythroblastosis virus. *Journal of the National Cancer Institute*. 1967;39(2):311-35.
19. Scolnick EM, Rands E, Williams D, Parks WP. Studies on the nucleic acid sequences of Kirsten sarcoma virus: a model for formation of a mammalian RNA-containing sarcoma virus. *Journal of virology*. 1973;12(3):458-63.
20. Scolnick EM, Papageorge AG, Shih TY. Guanine nucleotide-binding activity as an assay for src protein of rat-derived murine sarcoma viruses. *Proceedings of the National Academy of Sciences*. 1979;76(10):5355-9.
21. Der CJ, Krontiris TG, Cooper GM. Transforming genes of human bladder and lung carcinoma cell lines are homologous to the ras genes of Harvey and Kirsten sarcoma viruses. *Proceedings of the National Academy of Sciences*. 1982;79(11):3637-40.
22. Zeitouni D, Pylayeva-Gupta Y, Der CJ, Bryant KL. KRAS mutant pancreatic cancer: no lone path to an effective treatment. *Cancers*. 2016;8(4):45.
23. Willingham MC, Pastan I, Shih TY, Scolnick EM. Localization of the src gene product of the Harvey strain of MSV to plasma membrane of transformed cells by electron microscopic immunocytochemistry. *Cell*. 1980;19(4):1005-14.
24. Santos E, Martin-Zanca D, Reddy EP, Pierotti MA, Della Porta G, Barbacid M. Malignant activation of a K-ras oncogene in lung carcinoma but not in normal tissue of the same patient. *Science*. 1984;223(4637):661-4.
25. Guo K, Cui J, Quan M, Xie D, Jia Z, Wei D, et al. The Novel KLF4/MSI2 Signaling Pathway Regulates Growth and Metastasis of Pancreatic Cancer. *Clin Cancer Res*. 2017;23(3):687-96.
26. Grabski IN, Heymach JV, Kehl KL, Kopetz S, Lau KS, Riely GJ, et al. Effects of KRAS genetic interactions on outcomes in cancers of the lung, pancreas, and colorectum. *Cancer Epidemiology, Biomarkers & Prevention*. 2023:OF1-OF12.
27. Kris MG, Johnson BE, Berry LD, Kwiatkowski DJ, Iafrate AJ, Wistuba II, et al. Using multiplexed assays of oncogenic drivers in lung cancers to select targeted drugs. *Jama*. 2014;311(19):1998-2006.
28. Jamal-Hanjani M, Wilson GA, McGranahan N, Birkbak NJ, Watkins TB, Veeriah S, et al. Tracking the evolution of non–small-cell lung cancer. *New England Journal of Medicine*. 2017;376(22):2109-21.
29. Alexandrov LB, Ju YS, Haase K, Van Loo P, Martincorena I, Nik-Zainal S, et al. Mutational signatures associated with tobacco smoking in human cancer. *Science*. 2016;354(6312):618-22.
30. Rodenhuis S, van de Wetering ML, Mooi WJ, Evers SG, van Zandwijk N, Bos JL. Mutational activation of the K-ras oncogene. *New England Journal of Medicine*. 1987;317(15):929-35.
31. Adjei AA, Mauer A, Bruzek L, Marks RS, Hillman S, Geyer S, et al. Phase II study of the farnesyl transferase inhibitor R115777 in patients with advanced non–small-cell lung cancer. *Journal of clinical oncology*. 2003;21(9):1760-6.
32. Riely GJ, Johnson ML, Medina C, Rizvi NA, Miller VA, Kris MG, et al. A phase II trial of Salirasib in patients with lung adenocarcinomas with KRAS mutations. *Journal of Thoracic Oncology*. 2011;6(8):1435-7.
33. Jänne PA, van den Heuvel MM, Barlesi F, Cobo M, Mazieres J, Crinò L, et al. Selumetinib plus docetaxel compared with docetaxel alone and progression-free survival in patients with KRAS-mutant advanced non–small cell lung cancer: the SELECT-1 randomized clinical trial. *Jama*. 2017;317(18):1844-53.

34. Goldman JW, Mazieres J, Barlesi F, Dragnev KH, Koczywas M, Göskel T, et al. A randomized phase III study of abemaciclib versus erlotinib in patients with stage IV non-small cell lung cancer with a detectable KRAS mutation who failed prior platinum-based therapy: JUNIPER. *Frontiers in Oncology*. 2020;10:578756.
35. Drilon A, Schoenfeld AJ, Arbour KC, Litvak A, Ni A, Montecalvo J, et al. Exceptional responders with invasive mucinous adenocarcinomas: a phase 2 trial of bortezomib in patients with KRAS G12D-mutant lung cancers. *Molecular Case Studies*. 2019;5(2):a003665.
36. Ramalingam S, Goss G, Rosell R, Schmid-Bindert G, Zaric B, Andric Z, et al. A randomized phase II study of ganetespib, a heat shock protein 90 inhibitor, in combination with docetaxel in second-line therapy of advanced non-small cell lung cancer (GALAXY-1). *Annals of Oncology*. 2015;26(8):1741-8.
37. Ostrem JM, Peters U, Sos ML, Wells JA, Shokat KM. K-Ras (G12C) inhibitors allosterically control GTP affinity and effector interactions. *Nature*. 2013;503(7477):548-51.
38. Saleh K, Kordahi M, Felefly T, Kourie HR, Khalife N. KRAS-targeted therapies in advanced solid cancers: drug the undruggable? : *Future Medicine*; 2021. p. 587-90.
39. Moore AR, Rosenberg SC, McCormick F, Malek S. RAS-targeted therapies: is the undruggable drugged? *Nature reviews Drug discovery*. 2020;19(8):533-52.
40. Fell JB, Fischer JP, Baer BR, Blake JF, Bouhana K, Briere DM, et al. Identification of the clinical development candidate MRTX849, a covalent KRASG12C inhibitor for the treatment of cancer. *Journal of medicinal chemistry*. 2020;63(13):6679-93.
41. Brachmann SM, Weiss A, Guthy DA, Beyer K, Voshol J, Maira M, et al. Abstract P124: JDQ443, a covalent irreversible inhibitor of KRAS G12C, exhibits a novel binding mode and demonstrates potent anti-tumor activity and favorable pharmacokinetic properties in preclinical models. *Molecular Cancer Therapeutics*. 2021;20(12_Supplement):P124-P.
42. Misale S, Fatherree JP, Cortez E, Li C, Bilton S, Timonina D, et al. KRAS G12C NSCLC models are sensitive to direct targeting of KRAS in combination with PI3K inhibition. *Clinical Cancer Research*. 2019;25(2):796-807.
43. Solanki HS, Welsh EA, Fang B, Izumi V, Darville L, Stone B, et al. Cell type-specific adaptive signaling responses to KRASG12C inhibition. *Clinical Cancer Research*. 2021;27(9):2533-48.
44. Hallin J, Engstrom LD, Hargis L, Calinisan A, Aranda R, Briere DM, et al. The KRASG12C inhibitor MRTX849 provides insight toward therapeutic susceptibility of KRAS-mutant cancers in mouse models and patients. *Cancer discovery*. 2020;10(1):54-71.
45. Lito P, Saborowski A, Yue J, Solomon M, Joseph E, Gadai S, et al. Disruption of CRAF-mediated MEK activation is required for effective MEK inhibition in KRAS mutant tumors. *Cancer cell*. 2014;25(5):697-710.
46. Nazarian R, Shi H, Wang Q, Kong X, Koya RC, Lee H, et al. Melanomas acquire resistance to B-Raf (V600E) inhibition by RTK or N-Ras upregulation. *Nature*. 2010;468(7326):973-7.
47. Awad MM, Liu S, Rybkin II, Arbour KC, Dilly J, Zhu VW, et al. Acquired resistance to KRASG12C inhibition in cancer. *New England Journal of Medicine*. 2021;384(25):2382-93.
48. Tanaka N, Lin JJ, Li C, Ryan MB, Zhang J, Kiedrowski LA, et al. Clinical acquired resistance to KRASG12C inhibition through a novel KRAS switch-II pocket mutation and polyclonal alterations converging on RAS-MAPK reactivation. *Cancer discovery*. 2021;11(8):1913-22.

49. Fox RG, Lytle NK, Jaquish DV, Park FD, Ito T, Bajaj J, et al. Image-based detection and targeting of therapy resistance in pancreatic adenocarcinoma. *Nature*. 2016;534(7607):407-11.
50. Mathews MB, Sonenberg N, Hershey JW. Translational control in biology and medicine. (No Title). 2007.
51. Schwanhäusser B, Busse D, Li N, Dittmar G, Schuchhardt J, Wolf J, et al. Global quantification of mammalian gene expression control. *Nature*. 2011;473(7347):337-42.
52. Buttgereit F, Brand MD. A hierarchy of ATP-consuming processes in mammalian cells. *Biochemical Journal*. 1995;312(1):163-7.
53. Silvera D, Formenti SC, Schneider RJ. Translational control in cancer. *Nature Reviews Cancer*. 2010;10(4):254-66.
54. Hershey JW, Sonenberg N, Mathews MB. Principles of translational control: an overview. *Cold Spring Harbor perspectives in biology*. 2012;4(12):a011528.
55. Sonenberg N, Hinnebusch AG. Regulation of translation initiation in eukaryotes: mechanisms and biological targets. *Cell*. 2009;136(4):731-45.
56. Wek R, Jiang H-Y, Anthony T. Coping with stress: eIF2 kinases and translational control. *Biochemical Society Transactions*. 2006;34(1):7-11.
57. Ma XM, Blenis J. Molecular mechanisms of mTOR-mediated translational control. *Nature reviews Molecular cell biology*. 2009;10(5):307-18.
58. Sriram A, Bohlen J, Teleman AA. Translation acrobatics: how cancer cells exploit alternate modes of translational initiation. *EMBO reports*. 2018;19(10):e45947.
59. Pelletier J, Graff J, Ruggero D, Sonenberg N. Targeting the eIF4F translation initiation complex: a critical nexus for cancer development. *Cancer research*. 2015;75(2):250-63.
60. Hinnebusch AG, Ivanov IP, Sonenberg N. Translational control by 5'-untranslated regions of eukaryotic mRNAs. *Science*. 2016;352(6292):1413-6.
61. Benham AM. Protein secretion and the endoplasmic reticulum. *Cold Spring Harbor perspectives in biology*. 2012;4(8):a012872.
62. Blanchet S, Ranjan N. Translation phases in eukaryotes. *Ribosome Biogenesis: Methods and Protocols*. 2022:217-28.
63. Hinnebusch AG, Ivanov IP, Sonenberg N. Translational control by 5'-untranslated regions of eukaryotic mRNAs. *Science*. 2016;352(6292):1413-6.
64. Koromilas AE. Roles of the translation initiation factor eIF2 α serine 51 phosphorylation in cancer formation and treatment. *Biochim Biophys Acta*. 2015;1849(7):871-80.
65. Costa-Mattioli M, Walter P. The integrated stress response: From mechanism to disease. *Science*. 2020;368(6489):eaat5314.
66. Pakos-Zebrucka K, Koryga I, Mnich K, Lujic M, Samali A, Gorman AM. The integrated stress response. *EMBO Rep*. 2016;17(10):1374-95.
67. Clementi E, Inglin L, Beebe E, Gsell C, Garajova Z, Markkanen E. Persistent DNA damage triggers activation of the integrated stress response to promote cell survival under nutrient restriction. *BMC biology*. 2020;18:1-15.
68. Akman M, Belisario DC, Salaroglio IC, Kopecka J, Donadelli M, De Smaele E, et al. Hypoxia, endoplasmic reticulum stress and chemoresistance: dangerous liaisons. *Journal of Experimental & Clinical Cancer Research*. 2021;40:1-17.

69. Adomavicius T, Guaita M, Zhou Y, Jennings MD, Latif Z, Roseman AM, et al. The structural basis of translational control by eIF2 phosphorylation. *Nature communications*. 2019;10(1):2136.
70. Leppek K, Das R, Barna M. Functional 5' UTR mRNA structures in eukaryotic translation regulation and how to find them. *Nature reviews Molecular cell biology*. 2018;19(3):158-74.
71. Donnelly N, Gorman AM, Gupta S, Samali A. The eIF2 α kinases: their structures and functions. *Cellular and molecular life sciences*. 2013;70:3493-511.
72. Chen J-J. Regulation of protein synthesis by the heme-regulated eIF2 α kinase: relevance to anemias. *blood*. 2007;109(7):2693-9.
73. Guo X, Aviles G, Liu Y, Tian R, Unger BA, Lin Y-HT, et al. Mitochondrial stress is relayed to the cytosol by an OMA1–DELE1–HRI pathway. *Nature*. 2020;579(7799):427-32.
74. Chen J-J. Translational control by heme-regulated eIF2 α kinase during erythropoiesis. *Current opinion in hematology*. 2014;21(3):172.
75. Lemaire PA, Lary J, Cole JL. Mechanism of PKR activation: dimerization and kinase activation in the absence of double-stranded RNA. *Journal of molecular biology*. 2005;345(1):81-90.
76. Garcia M, Meurs E, Esteban M. The dsRNA protein kinase PKR: virus and cell control. *Biochimie*. 2007;89(6-7):799-811.
77. Hetz C, Chevet E, Oakes SA. Proteostasis control by the unfolded protein response. *Nature cell biology*. 2015;17(7):829-38.
78. Harding HP, Zhang Y, Ron D. Protein translation and folding are coupled by an endoplasmic-reticulum-resident kinase. *Nature*. 1999;397(6716):271-4.
79. Han J, Back SH, Hur J, Lin Y-H, Gildersleeve R, Shan J, et al. ER-stress-induced transcriptional regulation increases protein synthesis leading to cell death. *Nature cell biology*. 2013;15(5):481-90.
80. Kopp MC, Larburu N, Durairaj V, Adams CJ, Ali MM. UPR proteins IRE1 and PERK switch BiP from chaperone to ER stress sensor. *Nature structural & molecular biology*. 2019;26(11):1053-62.
81. Inglis AJ, Masson GR, Shao S, Perisic O, McLaughlin SH, Hegde RS, et al. Activation of GCN2 by the ribosomal P-stalk. *Proceedings of the National Academy of Sciences*. 2019;116(11):4946-54.
82. Harding HP, Ordóñez A, Allen F, Parts L, Inglis AJ, Williams RL, et al. The ribosomal P-stalk couples amino acid starvation to GCN2 activation in mammalian cells. *Elife*. 2019;8:e50149.
83. Ishimura R, Nagy G, Dotu I, Chuang JH, Ackerman SL. Activation of GCN2 kinase by ribosome stalling links translation elongation with translation initiation. *Elife*. 2016;5:e14295.
84. Wortel IM, van der Meer LT, Kilberg MS, van Leeuwen FN. Surviving stress: modulation of ATF4-mediated stress responses in normal and malignant cells. *Trends in Endocrinology & Metabolism*. 2017;28(11):794-806.
85. B'chir W, Maurin A-C, Carraro V, Averous J, Jousse C, Muranishi Y, et al. The eIF2 α /ATF4 pathway is essential for stress-induced autophagy gene expression. *Nucleic acids research*. 2013;41(16):7683-99.
86. Pavitt GD. Regulation of translation initiation factor eIF2B at the hub of the integrated stress response. *Wiley Interdisciplinary Reviews: RNA*. 2018;9(6):e1491.
87. Novoa I, Zeng H, Harding HP, Ron D. Feedback inhibition of the unfolded protein response by GADD34-mediated dephosphorylation of eIF2 α . *The Journal of cell biology*. 2001;153(5):1011-22.

88. Jousse C, Oyadomari S, Novoa I, Lu P, Zhang Y, Harding HP, et al. Inhibition of a constitutive translation initiation factor 2 α phosphatase, CREP, promotes survival of stressed cells. *The Journal of cell biology*. 2003;163(4):767-75.
89. Kojima E, Takeuchi A, Haneda M, Yagi F, Hasegawa T, Yamaki K-i, et al. The function of GADD34 is a recovery from a shutoff of protein synthesis induced by ER stress—elucidation by GADD34-deficient mice. *The FASEB Journal*. 2003;17(11):1-18.
90. Fouad YA, Aanei C. Revisiting the hallmarks of cancer. *American journal of cancer research*. 2017;7(5):1016.
91. Hanahan D. Hallmarks of cancer: new dimensions. *Cancer discovery*. 2022;12(1):31-46.
92. Senga SS, Grose RP. Hallmarks of cancer—the new testament. *Open biology*. 2021;11(1):200358.
93. Erin N, Grahovac J, Brozovic A, Efferth T. Tumor microenvironment and epithelial mesenchymal transition as targets to overcome tumor multidrug resistance. *Drug Resistance Updates*. 2020;53:100715.
94. Bhat M, Robichaud N, Hulea L, Sonenberg N, Pelletier J, Topisirovic I. Targeting the translation machinery in cancer. *Nature reviews Drug discovery*. 2015;14(4):261-78.
95. Boussemaert L, Malka-Mahieu H, Girault I, Allard D, Hemmingsson O, Tomasic G, et al. eIF4F is a nexus of resistance to anti-BRAF and anti-MEK cancer therapies. *Nature*. 2014;513(7516):105-9.
96. Dai L, Lin Z, Cao Y, Chen Y, Xu Z, Qin Z. Targeting EIF4F complex in non-small cell lung cancer cells. *Oncotarget*. 2017;8(33):55731.
97. Bitterman PB, Polunovsky VA. eIF4E-mediated translational control of cancer incidence. *Biochimica et Biophysica Acta (BBA)-Gene Regulatory Mechanisms*. 2015;1849(7):774-80.
98. Siddiqui N, Sonenberg N. Signalling to eIF4E in cancer. *Biochemical Society Transactions*. 2015;43(5):763-72.
99. Koromilas AE. M (en) TORship lessons on life and death by the integrated stress response. *Biochimica Et Biophysica Acta (BBA)-General Subjects*. 2019;1863(3):644-9.
100. Corazzari M, Rapino F, Ciccocanti F, Giglio P, Antonioli M, Conti B, et al. Oncogenic BRAF induces chronic ER stress condition resulting in increased basal autophagy and apoptotic resistance of cutaneous melanoma. *Cell Death & Differentiation*. 2015;22(6):946-58.
101. Holcik M, Sonenberg N. Translational control in stress and apoptosis. *Nature reviews Molecular cell biology*. 2005;6(4):318-27.
102. Ye J, Koumenis C. ATF4, an ER stress and hypoxia-inducible transcription factor and its potential role in hypoxia tolerance and tumorigenesis. *Current molecular medicine*. 2009;9(4):411-6.
103. Tameire F, Verginadis II, Leli NM, Polte C, Conn CS, Ojha R, et al. ATF4 couples MYC-dependent translational activity to bioenergetic demands during tumour progression. *Nature cell biology*. 2019;21(7):889-99.
104. Tian X, Zhang S, Zhou L, Seyhan AA, Hernandez Borrero L, Zhang Y, et al. Targeting the integrated stress response in cancer therapy. *Frontiers in Pharmacology*. 2021;12:747837.
105. Stone S, Ho Y, Li X, Jamison S, Harding HP, Ron D, et al. Dual role of the integrated stress response in medulloblastoma tumorigenesis. *Oncotarget*. 2016;7(39):64124.

106. Palam L, Gore J, Craven K, Wilson J, Korc M. Integrated stress response is critical for gemcitabine resistance in pancreatic ductal adenocarcinoma. *Cell death & disease*. 2015;6(10):e1913-e.
107. Zhang Y, Zhou L, Safran H, Borsuk R, Lulla R, Tapinos N, et al. EZH2i EPZ-6438 and HDACi vorinostat synergize with ONC201/TIC10 to activate integrated stress response, DR5, reduce H3K27 methylation, ClpX and promote apoptosis of multiple tumor types including DIPG. *Neoplasia*. 2021;23(8):792-810.
108. Ishizawa J, Kojima K, Chachad D, Ruvolo P, Ruvolo V, Jacamo RO, et al. ATF4 induction through an atypical integrated stress response to ONC201 triggers p53-independent apoptosis in hematological malignancies. *Science signaling*. 2016;9(415):ra17-ra.
109. Koromilas AE. The integrated stress response in the induction of mutant KRAS lung carcinogenesis: Mechanistic insights and therapeutic implications. *BioEssays*. 2022;44(8):2200026.
110. Hamanaka RB, Bobrovnikova-Marjon E, Ji X, Liebhaver SA, Diehl JA. PERK-dependent regulation of IAP translation during ER stress. *Oncogene*. 2009;28(6):910-20.
111. Hu J, Dang N, Menu E, De Bryune E, Xu D, Van Camp B, et al. Activation of ATF4 mediates unwanted Mcl-1 accumulation by proteasome inhibition. *Blood, The Journal of the American Society of Hematology*. 2012;119(3):826-37.
112. Rzymiski T, Harris AL. The unfolded protein response and integrated stress response to anoxia. *Clinical cancer research*. 2007;13(9):2537-40.
113. Chitnis NS, Pytel D, Bobrovnikova-Marjon E, Pant D, Zheng H, Maas NL, et al. miR-211 is a prosurvival microRNA that regulates chop expression in a PERK-dependent manner. *Molecular cell*. 2012;48(3):353-64.
114. Deng J, Lu PD, Zhang Y, Scheuner D, Kaufman RJ, Sonenberg N, et al. Translational repression mediates activation of nuclear factor kappa B by phosphorylated translation initiation factor 2. *Molecular and cellular biology*. 2004;24(23):10161-8.
115. Donzé O, Dostie J, Sonenberg N. Regulatable expression of the interferon-induced double-stranded RNA dependent protein kinase PKR induces apoptosis and fas receptor expression. *Virology*. 1999;256(2):322-9.
116. Burwick N, Aktas BH. The eIF2-alpha kinase HRI: a potential target beyond the red blood cell. *Expert opinion on therapeutic targets*. 2017;21(12):1171-7.
117. Yerlikaya A. Heme-regulated inhibitor: an overlooked eIF2 α kinase in cancer investigations. *Medical Oncology*. 2022;39(7):73.
118. Lee DM, Seo MJ, Lee HJ, Jin HJ, Choi KS. ISRIB plus bortezomib triggers paraptosis in breast cancer cells via enhanced translation and subsequent proteotoxic stress. *Biochemical and Biophysical Research Communications*. 2022;596:56-62.
119. Halliday M, Radford H, Sekine Y, Moreno J, Verity N, Le Quesne J, et al. Partial restoration of protein synthesis rates by the small molecule ISRIB prevents neurodegeneration without pancreatic toxicity. *Cell death & disease*. 2015;6(3):e1672-e.
120. Chou A, Krukowski K, Jopson T, Zhu PJ, Costa-Mattioli M, Walter P, et al. Inhibition of the integrated stress response reverses cognitive deficits after traumatic brain injury. *Proceedings of the National Academy of Sciences*. 2017;114(31):E6420-E6.

121. Rabouw HH, Langereis MA, Anand AA, Visser LJ, de Groot RJ, Walter P, et al. Small molecule ISRIB suppresses the integrated stress response within a defined window of activation. *Proceedings of the National Academy of Sciences*. 2019;116(6):2097-102.
122. Tsai JC, Miller-Vedam LE, Anand AA, Jaishankar P, Nguyen HC, Renslo AR, et al. Structure of the nucleotide exchange factor eIF2B reveals mechanism of memory-enhancing molecule. *Science*. 2018;359(6383):eaag0939.
123. Anand AA, Walter P. Structural insights into ISRIB, a memory-enhancing inhibitor of the integrated stress response. *The FEBS journal*. 2020;287(2):239-45.
124. Kashiwagi K, Takahashi M, Nishimoto M, Hiyama TB, Higo T, Umehara T, et al. Crystal structure of eukaryotic translation initiation factor 2B. *Nature*. 2016;531(7592):122-5.
125. Wortham NC, Martinez M, Gordiyenko Y, Robinson CV, Proud CG. Analysis of the subunit organization of the eIF2B complex reveals new insights into its structure and regulation. *The FASEB Journal*. 2014;28(5):2225-37.
126. Zhu PJ, Khatiwada S, Cui Y, Reineke LC, Dooling SW, Kim JJ, et al. Activation of the ISR mediates the behavioral and neurophysiological abnormalities in Down syndrome. *Science*. 2019;366(6467):843-9.
127. Oliveira MM, Lourenco MV, Longo F, Kasica NP, Yang W, Ureta G, et al. Correction of eIF2-dependent defects in brain protein synthesis, synaptic plasticity, and memory in mouse models of Alzheimer's disease. *Science signaling*. 2021;14(668):eabc5429.
128. Abbink TE, Wisse LE, Jaku E, Thiecke MJ, Voltolini-González D, Fritsen H, et al. Vanishing white matter: deregulated integrated stress response as therapy target. *Annals of clinical and translational neurology*. 2019;6(8):1407-22.
129. Gordiyenko Y, Schmidt C, Jennings MD, Matak-Vinkovic D, Pavitt GD, Robinson CV. eIF2B is a decameric guanine nucleotide exchange factor with a γ 2 ϵ 2 tetrameric core. *Nature communications*. 2014;5(1):3902.
130. Schoof M, Boone M, Wang L, Lawrence R, Frost A, Walter P. eIF2B conformation and assembly state regulate the integrated stress response. *Elife*. 2021;10:e65703.
131. Kuhle B, Eulig NK, Ficner R. Architecture of the eIF2B regulatory subcomplex and its implications for the regulation of guanine nucleotide exchange on eIF2. *Nucleic acids research*. 2015;43(20):9994-10014.
132. Kenner LR, Anand AA, Nguyen HC, Myasnikov AG, Klose CJ, McGeever LA, et al. eIF2B-catalyzed nucleotide exchange and phosphoregulation by the integrated stress response. *Science*. 2019;364(6439):491-5.
133. Gordiyenko Y, Ll  cer JL, Ramakrishnan V. Structural basis for the inhibition of translation through eIF2 α phosphorylation. *Nature communications*. 2019;10(1):2640.
134. Dev K, Qiu H, Dong J, Zhang F, Barthlme D, Hinnebusch AG. The β /Gcd7 subunit of eukaryotic translation initiation factor 2B (eIF2B), a guanine nucleotide exchange factor, is crucial for binding eIF2 in vivo. *Molecular and cellular biology*. 2010;30(21):5218-33.
135. Krishnamoorthy T, Pavitt GD, Zhang F, Dever TE, Hinnebusch AG. Tight binding of the phosphorylated α subunit of initiation factor 2 (eIF2 α) to the regulatory subunits of guanine nucleotide exchange factor eIF2B is required for inhibition of translation initiation. *Molecular and cellular biology*. 2001;21(15):5018-30.

136. Sidrauski C, Acosta-Alvear D, Khoutorsky A, Vedantham P, Hearn BR, Li H, et al. Pharmacological brake-release of mRNA translation enhances cognitive memory. *elife*. 2013;2:e00498.
137. Sidrauski C, Tsai JC, Kampmann M, Hearn BR, Vedantham P, Jaishankar P, et al. Pharmacological dimerization and activation of the exchange factor eIF2B antagonizes the integrated stress response. *elife*. 2015;4:e07314.
138. Sekine Y, Zyryanova A, Crespillo-Casado A, Fischer PM, Harding HP, Ron D. Mutations in a translation initiation factor identify the target of a memory-enhancing compound. *Science*. 2015;348(6238):1027-30.
139. Zyryanova AF, Weis F, Faille A, Alard AA, Crespillo-Casado A, Sekine Y, et al. Binding of ISRIB reveals a regulatory site in the nucleotide exchange factor eIF2B. *Science*. 2018;359(6383):1533-6.
140. Brady LK, Wang H, Radens CM, Bi Y, Radovich M, Maity A, et al. Transcriptome analysis of hypoxic cancer cells uncovers intron retention in EIF2B5 as a mechanism to inhibit translation. *PLoS biology*. 2017;15(9):e2002623.
141. Leegwater PA, Vermeulen G, Könst AA, Naidu S, Mulders J, Visser A, et al. Subunits of the translation initiation factor eIF2B are mutant in leukoencephalopathy with vanishing white matter. *Nature genetics*. 2001;29(4):383-8.
142. Ghaddar N, Wang S, Woodvine B, Krishnamoorthy J, van Hoef V, Darini C, et al. The integrated stress response is tumorigenic and constitutes a therapeutic liability in KRAS-driven lung cancer. *Nature Communications*. 2021;12(1):4651.
143. Nguyen HG, Conn CS, Kye Y, Xue L, Forester CM, Cowan JE, et al. Development of a stress response therapy targeting aggressive prostate cancer. *Science translational medicine*. 2018;10(439):eaar2036.
144. Gallagher JW, Kubica N, Kimball SR, Jefferson LS. Reduced eukaryotic initiation factor 2B ϵ -subunit expression suppresses the transformed phenotype of cells overexpressing the protein. *Cancer research*. 2008;68(21):8752-60.
145. Békés M, Langley DR, Crews CM. PROTAC targeted protein degraders: the past is prologue. *Nature Reviews Drug Discovery*. 2022;21(3):181-200.
146. Nieto-Jiménez C, Morafrail EC, Alonso-Moreno C, Ocaña A. Clinical considerations for the design of PROTACs in cancer. *Molecular Cancer*. 2022;21(1):67.
147. Hughes SJ, Ciulli A. Molecular recognition of ternary complexes: a new dimension in the structure-guided design of chemical degraders. *Essays in biochemistry*. 2017;61(5):505-16.
148. Girardini M, Maniaci C, Hughes SJ, Testa A, Ciulli A. Cereblon versus VHL: Hijacking E3 ligases against each other using PROTACs. *Bioorganic & Medicinal Chemistry*. 2019;27(12):2466-79.
149. Mancarella C, Morrión A, Scotlandi K. PROTAC-Based Protein Degradation as a Promising Strategy for Targeted Therapy in Sarcomas. *International Journal of Molecular Sciences*. 2023;24(22):16346.
150. Bond MJ, Chu L, Nalawansa DA, Li K, Crews CM. Targeted Degradation of Oncogenic KRAS(G12C) by VHL-Recruiting PROTACs. *ACS Cent Sci*. 2020;6(8):1367-75.
151. Békés M, Langley DR, Crews CM. PROTAC targeted protein degraders: the past is prologue. 2022;21(3):181-200.

152. Burslem GM, Crews CM. Proteolysis-targeting chimeras as therapeutics and tools for biological discovery. *Cell*. 2020;181(1):102-14.
153. Zhang X, Cao J, Miller SP, Jing H, Lin H. Comparative Nucleotide-Dependent Interactome Analysis Reveals Shared and Differential Properties of KRas4a and KRas4b. *ACS Cent Sci*. 2018;4(1):71-80.
154. Prior IA, Hancock JF, editors. Ras trafficking, localization and compartmentalized signalling. *Seminars in cell & developmental biology*; 2012: Elsevier.
155. Sasaki AT, Carracedo A, Locasale JW, Anastasiou D, Takeuchi K, Kahoud ER, et al. Ubiquitination of K-Ras enhances activation and facilitates binding to select downstream effectors. *Sci Signal*. 2011;4(163):ra13.
156. Kim H, Ghaddar N, Ghahnavieh LE, Wang S, Cho K-J, Sasaki A, et al. Abstract A022: Translation initiation factor 2B (eIF2B) stimulates mutant KRAS function in cancer. *Molecular Cancer Research*. 2023;21(5_Supplement):A022-A.
157. Zyryanova AF, Kashiwagi K, Rato C, Harding HP, Crespillo-Casado A, Perera LA, et al. ISRIB Blunts the Integrated Stress Response by Allosterically Antagonising the Inhibitory Effect of Phosphorylated eIF2 on eIF2B. *Mol Cell*. 2021;81(1):88-103 e6.
158. Hillig RC, Sautier B, Schroeder J, Moosmayer D, Hilpmann A, Stegmann CM, et al. Discovery of potent SOS1 inhibitors that block RAS activation via disruption of the RAS–SOS1 interaction. *Proceedings of the National Academy of Sciences*. 2019;116(7):2551-60.
159. Williams CJ, Headd JJ, Moriarty NW, Prisant MG, Videau LL, Deis LN, et al. MolProbity: More and better reference data for improved all-atom structure validation. *Protein Science*. 2018;27(1):293-315.
160. Kozakov D, Hall DR, Xia B, Porter KA, Padhorny D, Yueh C, et al. The ClusPro web server for protein-protein docking. *Nat Protoc*. 2017;12(2):255-78.
161. DeLano WL. Pymol: An open-source molecular graphics tool. *CCP4 Newsl Protein Crystallogr*. 2002;40(1):82-92.
162. Alioto TS, Buchhalter I, Derdak S, Hutter B, Eldridge MD, Hovig E, et al. A comprehensive assessment of somatic mutation detection in cancer using whole-genome sequencing. *Nature communications*. 2015;6(1):1-13.
163. Puente XS, Pinyol M, Quesada V, Conde L, Ordóñez GR, Villamor N, et al. Whole-genome sequencing identifies recurrent mutations in chronic lymphocytic leukaemia. *Nature*. 2011;475(7354):101-5.
164. Piskol R, Ramaswami G, Li JB. Reliable identification of genomic variants from RNA-seq data. *The American Journal of Human Genetics*. 2013;93(4):641-51.
165. Coudray A, Battenhouse AM, Bucher P, Iyer VR. Detection and benchmarking of somatic mutations in cancer genomes using RNA-seq data. *PeerJ*. 2018;6:e5362.
166. Benjamin D, Sato T, Cibulskis K, Getz G, Stewart C, Lichtenstein L. Calling somatic SNVs and indels with Mutect2. *BioRxiv*. 2019:861054.
167. Kim D, Paggi JM, Park C, Bennett C, Salzberg SL. Graph-based genome alignment and genotyping with HISAT2 and HISAT-genotype. *Nature biotechnology*. 2019;37(8):907-15.
168. Liao Y, Smyth GK, Shi W. featureCounts: an efficient general purpose program for assigning sequence reads to genomic features. *Bioinformatics*. 2014;30(7):923-30.

169. Love MI, Huber W, Anders S. Moderated estimation of fold change and dispersion for RNA-seq data with DESeq2. *Genome biology*. 2014;15(12):1-21.
170. Robinson MD, McCarthy DJ, Smyth GK. edgeR: a Bioconductor package for differential expression analysis of digital gene expression data. *bioinformatics*. 2010;26(1):139-40.
171. Wickham H. ggplot2. *Wiley interdisciplinary reviews: computational statistics*. 2011;3(2):180-5.
172. Yu G, Wang L-G, Han Y, He Q-Y. clusterProfiler: an R package for comparing biological themes among gene clusters. *Omics: a journal of integrative biology*. 2012;16(5):284-7.
173. Liu Y, Li G. Empowering biologists to decode omics data: the Genekitr R package and web server. *BMC bioinformatics*. 2023;24(1):214.
174. Tang Z, Kang B, Li C, Chen T, Zhang Z. GEPIA2: an enhanced web server for large-scale expression profiling and interactive analysis. *Nucleic acids research*. 2019;47(W1):W556-W60.
175. Chen H, Boutros PC. VennDiagram: a package for the generation of highly-customizable Venn and Euler diagrams in R. *BMC bioinformatics*. 2011;12(1):1-7.
176. Zyryanova AF, Kashiwagi K, Rato C, Harding HP, Crespillo-Casado A, Perera LA, et al. ISRIB blunts the integrated stress response by allosterically antagonising the inhibitory effect of phosphorylated eIF2 on eIF2B. *Molecular cell*. 2021;81(1):88-103. e6.
177. Daugherty MD, Malik HS. Rules of engagement: molecular insights from host-virus arms races. *Annual review of genetics*. 2012;46:677-700.
178. Lee H, Deng M, Sun F, Chen T. An integrated approach to the prediction of domain-domain interactions. *BMC bioinformatics*. 2006;7(1):1-15.
179. Yellaboina S, Tasneem A, Zaykin DV, Raghavachari B, Jothi R. DOMINE: a comprehensive collection of known and predicted domain-domain interactions. *Nucleic acids research*. 2011;39(suppl_1):D730-D5.
180. Han W, Li X, Fu X. The macro domain protein family: structure, functions, and their potential therapeutic implications. *Mutation Research/Reviews in Mutation Research*. 2011;727(3):86-103.
181. Vihervaara A, Duarte FM, Lis JT. Molecular mechanisms driving transcriptional stress responses. *Nature Reviews Genetics*. 2018;19(6):385-97.
182. Han H. RNA interference to knock down gene expression. *Disease gene identification: methods and protocols*. 2018:293-302.
183. Schmitt-Graff A, Ertelt V, Allgaier HP, Koelble K, Olschewski M, Nitschke R, et al. Cellular retinol-binding protein-1 in hepatocellular carcinoma correlates with beta-catenin, Ki-67 index, and patient survival. *Hepatology*. 2003;38(2):470-80.
184. Cai Y, Xu G, Wu F, Michelini F, Chan C, Qu X, et al. Genomic Alterations in PIK3CA-Mutated Breast Cancer Result in mTORC1 Activation and Limit the Sensitivity to PI3Kalpha Inhibitors. *Cancer Res*. 2021;81(9):2470-80.
185. Cai S, Guo X, Huang C, Deng Y, Du L, Liu W, et al. Integrative analysis and experiments to explore angiogenesis regulators correlated with poor prognosis, immune infiltration and cancer progression in lung adenocarcinoma. *Journal of Translational Medicine*. 2021;19(1):1-16.
186. Baltanás FC, Zarich N, Rojas-Cabañeros JM, Santos E. SOS GEFs in health and disease. *Biochimica et Biophysica Acta (BBA)-Reviews on Cancer*. 2020;1874(2):188445.

187. Margarit SM, Sondermann H, Hall BE, Nagar B, Hoelz A, Pirruccello M, et al. Structural evidence for feedback activation by Ras· GTP of the Ras-specific nucleotide exchange factor SOS. *Cell*. 2003;112(5):685-95.
188. Webb B, Sali A. Comparative protein structure modeling using MODELLER. *Current protocols in bioinformatics*. 2016;54(1):5.6. 1-5.6. 37.
189. Schwede T, Kopp J, Guex N, Peitsch MC. SWISS-MODEL: an automated protein homology-modeling server. *Nucleic acids research*. 2003;31(13):3381-5.
190. Varadi M, Anyango S, Deshpande M, Nair S, Natassia C, Yordanova G, et al. AlphaFold Protein Structure Database: massively expanding the structural coverage of protein-sequence space with high-accuracy models. *Nucleic acids research*. 2022;50(D1):D439-D44.
191. Balachandran S, Barber GN. Defective translational control facilitates vesicular stomatitis virus oncolysis. *Cancer cell*. 2004;5(1):51-65.
192. Chen W, Li Z, Bai L, Lin Y. NF-kappaB in lung cancer, a carcinogenesis mediator and a prevention and therapy target. *Front Biosci (Landmark Ed)*. 2011;16(3):1172-85.
193. Yang Q, Graham TE, Mody N, Preitner F, Peroni OD, Zabolotny JM, et al. Serum retinol binding protein 4 contributes to insulin resistance in obesity and type 2 diabetes. *Nature*. 2005;436(7049):356-62.
194. Gao L, Wang Q, Ren W, Zheng J, Li S, Dou Z, et al. The RBP1-CKAP4 axis activates oncogenic autophagy and promotes cancer progression in oral squamous cell carcinoma. *Cell Death Dis*. 2020;11(6):488.
195. Esteller M, Guo M, Moreno V, Peinado MA, Capella G, Galm O, et al. Hypermethylation-associated Inactivation of the Cellular Retinol-Binding-Protein 1 Gene in Human Cancer. *Cancer Res*. 2002;62(20):5902-5.
196. Jeronimo C, Henrique R, Oliveira J, Lobo F, Pais I, Teixeira MR, et al. Aberrant cellular retinol binding protein 1 (CRBP1) gene expression and promoter methylation in prostate cancer. *J Clin Pathol*. 2004;57(8):872-6.
197. Toki K, Enokida H, Kawakami K, Chiyomaru T, Tatarano S, Yoshino H, et al. CpG hypermethylation of cellular retinol-binding protein 1 contributes to cell proliferation and migration in bladder cancer. *Int J Oncol*. 2010;37(6):1379-88.
198. Zhu LC, Gao J, Hu ZH, Schwab CL, Zhuang HY, Tan MZ, et al. Membranous expressions of Lewis y and CAM-DR-related markers are independent factors of chemotherapy resistance and poor prognosis in epithelial ovarian cancer. *Am J Cancer Res*. 2015;5(2):830-43.
199. Chou AP, Chowdhury R, Li S, Chen W, Kim AJ, Piccioni DE, et al. Identification of retinol binding protein 1 promoter hypermethylation in isocitrate dehydrogenase 1 and 2 mutant gliomas. *Journal of the National Cancer Institute*. 2012;104(19):1458-69.
200. Peralta R, Valdivia A, Alvarado-Cabrero I, Gallegos F, Apresa T, Hernández D, et al. Correlation between expression of cellular retinol-binding protein 1 and its methylation status in larynx cancer. *Journal of clinical pathology*. 2012;65(1):46-50.
201. Chen Y, Tian T, Mao M-J, Deng W-Y, Li H. CRBP-1 over-expression is associated with poor prognosis in tongue squamous cell carcinoma. *BMC cancer*. 2018;18:1-10.
202. Wang Y, Zhang L, Chen H, Yang J, Cui Y, Wang H. Coronary artery disease-associated immune gene RBP1 and its pan-cancer analysis. *Front Cardiovasc Med*. 2023;10:1091950.

203. Yokoi K, Yamashita K, Ishii S, Tanaka T, Nishizawa N, Tsutsui A, et al. Comprehensive molecular exploration identified promoter DNA methylation of the CRBP1 gene as a determinant of radiation sensitivity in rectal cancer. 2017;116(8):1046-56.
204. Kuppumbatti YS, Bleiweiss IJ, Mandeli JP, Waxman S, Mira YLR. Cellular retinol-binding protein expression and breast cancer. J Natl Cancer Inst. 2000;92(6):475-80.
205. Orlandi A, Ferlosio A, Ciucci A, Francesconi A, Lifschitz-Mercer B, Gabbiani G, et al. Cellular retinol binding protein-1 expression in endometrial hyperplasia and carcinoma: diagnostic and possible therapeutic implications. Mod Pathol. 2006;19(6):797-803.
206. Ferlosio A, Doldo E, Agostinelli S, Costanza G, Centofanti F, Sidoni A, et al. Cellular retinol binding protein 1 transfection reduces proliferation and AKT-related gene expression in H460 non-small lung cancer cells. Mol Biol Rep. 2020;47(9):6879-86.
207. He Y, Luo W, Liu Y, Wang Y, Ma C, Wu Q, et al. IL-20RB mediates tumoral response to osteoclastic niches and promotes bone metastasis of lung cancer. J Clin Invest. 2022;132(20).
208. Takahashi K, Podyma-Inoue KA, Saito M, Sakakitani S, Sugauchi A, Iida K, et al. TGF-beta generates a population of cancer cells residing in G1 phase with high motility and metastatic potential via KRTAP2-3. Cell Rep. 2022;40(13):111411.
209. Prochazka L, Koudelka S, Dong LF, Stursa J, Goodwin J, Neca J, et al. Mitochondrial targeting overcomes ABCA1-dependent resistance of lung carcinoma to alpha-tocopheryl succinate. Apoptosis. 2013;18(3):286-99.
210. Schimanski S, Wild P, Treeck O, Horn F, Sigrüener A, Rudolph C, et al. Expression of the lipid transporters ABCA3 and ABCA1 is diminished in human breast cancer tissue. 2009:102-9.
211. Liu K, Zhang W, Tan J, Ma J, Zhao J. MiR-200b-3p functions as an oncogene by targeting ABCA1 in lung adenocarcinoma. 2019;18:1533033819892590.
212. Wu Q, He L, Luo J, Jin W, Xu Y, Wang C. Long-term remission under Disitamab Vedotin (RC48) in HR-positive/HER2-positive metastatic breast cancer with brain meningeal, and bone marrow involvement: A case report. 2022;24(4):1-8.
213. Laack E, Nikbakht H, Peters A, Kugler C, Jasiewicz Y, Edler L, et al. Expression of CEACAM1 in adenocarcinoma of the lung: a factor of independent prognostic significance. J Clin Oncol. 2002;20(21):4279-84.
214. Dango S, Sienel W, Schreiber M, Stremmel C, Kirschbaum A, Pantel K, et al. Elevated expression of carcinoembryonic antigen-related cell adhesion molecule 1 (CEACAM-1) is associated with increased angiogenic potential in non-small-cell lung cancer. 2008;60(3):426-33.
215. Wu X, Ye Y, Rosell R, Amos CI, Stewart DJ, Hildebrandt MA, et al. Genome-wide association study of survival in non-small cell lung cancer patients receiving platinum-based chemotherapy. J Natl Cancer Inst. 2011;103(10):817-25.
216. Chano T, Kita H, Avnet S, Lemma S, Baldini N. Prominent role of RAB39A-RXRβ axis in cancer development and stemness. Oncotarget. 2018;9(11):9852.
217. Tessema M, Yingling CM, Picchi MA, Wu G, Ryba T, Lin Y, et al. ANK1 Methylation regulates expression of MicroRNA-486-5p and discriminates lung tumors by histology and smoking status. Cancer letters. 2017;410:191-200.

218. Shi J, Wang L, Yin X, Wang L, Bo L, Liu K, et al. Comprehensive characterization of clonality of driver genes revealing their clinical relevance in colorectal cancer. *Journal of Translational Medicine*. 2022;20(1):362.
219. Pathania AS. Crosstalk between Noncoding RNAs and the Epigenetics Machinery in Pediatric Tumors and Their Microenvironment. *Cancers*. 2023;15(10):2833.
220. Agaram NP, Zhang L, Sung Y-S, Singer S, Antonescu CR. Extraskelatal myxoid chondrosarcoma with non-EWSR1-NR4A3 variant fusions correlate with rhabdoid phenotype and high-grade morphology. *Human pathology*. 2014;45(5):1084-91.
221. Broehm CJ, Wu J, Gullapalli RR, Bocklage T. Extraskelatal myxoid chondrosarcoma with at (9;16)(q22; p11. 2) resulting in a NR4A3-FUS fusion. *Cancer Genetics*. 2014;207(6):276-80.
222. Davis EJ, Wu Y-M, Robinson D, Schuetze SM, Baker LH, Athanikar J, et al. Next generation sequencing of extraskelatal myxoid chondrosarcoma. *Oncotarget*. 2017;8(13):21770.
223. Zhao X-G, Hu J-Y, Tang J, Yi W, Zhang M-Y, Deng R, et al. miR-665 expression predicts poor survival and promotes tumor metastasis by targeting NR4A3 in breast cancer. *Cell death & disease*. 2019;10(7):479.
224. Fedorova O, Petukhov A, Daks A, Shuvalov O, Leonova T, Vasileva E, et al. Orphan receptor NR4A3 is a novel target of p53 that contributes to apoptosis. *Oncogene*. 2019;38(12):2108-22.
225. Consortium APG, Consortium APG, André F, Arnedos M, Baras AS, Baselga J, et al. AACR Project GENIE: powering precision medicine through an international consortium. *Cancer discovery*. 2017;7(8):818-31.
226. JA Deutsch A, Angerer H, E Fuchs T, Neumeister P. The nuclear orphan receptors NR4A as therapeutic target in cancer therapy. *Anti-Cancer Agents in Medicinal Chemistry (Formerly Current Medicinal Chemistry-Anti-Cancer Agents)*. 2012;12(9):1001-14.
227. Cho J, Min H-Y, Lee HJ, Hyun SY, Sim JY, Noh M, et al. RGS2-mediated translational control mediates cancer cell dormancy and tumor relapse. *The Journal of clinical investigation*. 2021;131(1).
228. Yin H, Wang Y, Chen W, Zhong S, Liu Z, Zhao J. Drug-resistant CXCR4-positive cells have the molecular characteristics of EMT in NSCLC. *Gene*. 2016;594(1):23-9.
229. Kim Y, Ghil S. Regulators of G-protein signaling, RGS2 and RGS4, inhibit protease-activated receptor 4-mediated signaling by forming a complex with the receptor and Gα in live cells. *Cell Communication and Signaling*. 2020;18:1-13.
230. Nguyen CH, Ming H, Zhao P, Hugendubler L, Gros R, Kimball SR, et al. Translational control by RGS2. *J Cell Biol*. 2009;186(5):755-65.
231. Wang CJ, Chidiac P. RGS2 promotes the translation of stress-associated proteins ATF4 and CHOP via its eIF2B-inhibitory domain. *Cell Signal*. 2019;59:163-70.
232. Li Y, Sundquist K, Zhang N, Wang X, Sundquist J, Memon AA. Mitochondrial related genome-wide Mendelian randomization identifies putatively causal genes for multiple cancer types. *EBioMedicine*. 2023;88.
233. Pasello M, Giudice AM, Scotlandi K, editors. The ABC subfamily A transporters: Multifaceted players with incipient potentialities in cancer. *Seminars in cancer biology*; 2020: Elsevier.
234. Ling Y, Wang J, Wang L, Hou J, Qian P, Xiang-dong W. Roles of CEACAM1 in cell communication and signaling of lung cancer and other diseases. *Cancer Metastasis Rev*. 2015;34(2):347-57.

235. Hamon Y, Broccardo C, Chambenoit O, Luciani MF, Toti F, Chaslin S, et al. ABC1 promotes engulfment of apoptotic cells and transbilayer redistribution of phosphatidylserine. *Nat Cell Biol.* 2000;2(7):399-406.
236. Dankner M, Gray-Owen SD, Huang Y-H, Blumberg RS, Beauchemin NJO. CEACAM1 as a multi-purpose target for cancer immunotherapy. 2017;6(7):e1328336.
237. Pettersson M, Crews CM. PROteolysis TArgeting Chimeras (PROTACs)—past, present and future. *Drug Discovery Today: Technologies.* 2019;31:15-27.